EXTEROCEPTIVE AND INTEROCEPTIVE CUE CONTROL OF HIPPOCAMPAL PLACE CELLS

Raluca Irina Odobescu

Declaration

I, Raluca Irina Odobescu, confirm that the work presented in this thesis is my own. Where information has been derived from other sources, I confirm that this has been indicated in the thesis.

Raluca Irina Odobescu

Acknowledgments

Abstract

Place cells in the hippocampal formation form the cornerstone of the rat's navigational system and together with head direction cells in the postsubiculum and grid cells in the entorhinal cortex are the key elements of what O'Keefe and Nadel (1978) postulate to be a "cognitive map". The hippocampal formation is ideally positioned anatomically to receive highly processed inputs from almost all brain regions. Previous research has focused on the cues that determine and contribute to place cell selectivity. Such cues include information about the external world that the rat perceives through its senses ("exteroceptive cues") as well as cues internal to the body such as proprioception or somatosensation ("interoceptive cues").

This thesis uses a novel experimental paradigm in which the rat runs on a moving-treadmill linear track to investigate the relative contribution of interoceptive and exteroceptive cues for determining place cell spatial selectivity. The major finding is that place fields shift in the direction of the moving treadmill, both when the animal runs along with or against the motion of the treadmill, indicating that self-motion information is a key input to place cells. Furthermore, place fields in the middle of the track shift more than fields closer to the end walls suggesting that exteroceptive information interacts with interoceptive information to assist in accurate navigation. This conclusion is further supported by experiments performed in complete darkness where two populations of cells are observed: the first are cells which become quiescent or remap, presumably under strong exteroceptive control, while the second are cells that maintain similar firing characteristics under both lighting conditions, putatively under the influence of interoceptive inputs.

Table of contents

Index of figures

Index of tables

1 Functional anatomy of the hippocampus

In this chapter I will give a general introduction to the anatomy and in the next I will discuss the physiology of the hippocampal and parahippocampal regions of the rat's brain.

In accordance with the terminology in Witter and Amaral (2004), the hippocampal formation comprises the hippocampus proper, the dentate gyrus (DG) and the subiculum (SUB), while the parahippocampal region incorporates the presubiculum (PRE), the parasubiculum (PARA), the entorhinal cortex (EC), the perirhinal cortex (PER) and the postrhinal cortex (POR).

This chapter will briefly review the anatomy of the hippocampal and parahippocampal formations of the rat in the context of their relevance for the present experimental work. A particular focus is placed on connectivity and the way various inputs from other regions of the brain reach the hippocampus.

1.1   Hippocampal cytoarchitectonics

The hippocampal formation is a bilateral C-shaped structure with a complex 3D architecture, situated in the caudal part of the forebrain, over the diencephalon [see figure 1.1]. For clarity, the long axis of the hippocampus is called the septotemporal axis, while its orthogonal complement is called the transverse axis. In coronal sections, the DG and hippocampus proper form a 2-C shaped interlocking structure.

The distinguishing anatomical feature of the hippocampal formation is its three-layered appearance, which I briefly review below [see figure 1.2 C].

The DG is a C-shaped structure, comprising a cell-sparse molecular layer, a granule cell layer and a polymorphic layer (or hilus) containing mossy cells.

The hippocampus proper is also a C-shaped structure comprising 3 regions: CA1, CA2, CA3 (CA = cornu ammonis), distinguishable by cell size (larger in CA3/CA2) and connectivity (*e.g.* only CA3 cells receive mossy fiber input). The hippocampus proper has 3 cells layers: a molecular cell layer (which in turn can be subdivided in various sublayers: stratum lacunosum-moleculare, stratum radiatum and stratum lucidum (CA3 only)), the pyramidal cell layer and stratum oriens. Briefly, the pyramidal cell layer contains the soma of the pyramidal cells, the principal cells of the hippocampus, the stratum oriens and radiatum contain the CA1-CA3 Schaffer collaterals and the CA3-CA3 associational projections, stratum lucidum is where the mossy fibers from the DG terminate and stratum lacunosum-moleculare is where perforant pathway fibers from EC, along with afferents from other regions (*e.g.* nucleus reuniens) terminate.

The SUB comprises a molecular layer, which can be subdivided into a superficial and deep layer based on the termination of EC and CA1 inputs respectively, and a pyramidal cell layer. The pyramidal cells in the SUB are thought to form 2 distinct populations which, although they exhibit no difference at the morphological level, have different firing (regular spiking cells and intrinsically bursting cells) and neurochemical properties [Amaral and Lavenex (2007)]. I also note that a similar segregation into two populations has been proposed for CA pyramidal neurons based on their staining for calbindin [see Celio (1990)].

Together with the principal cells briefly mentioned in this section, there is a large body of interneurons, whose characteristics are described in detail by Witter and Amaral (2004), Freund and Buzsáki (1996) and Klausberger and Somogyi (2008).
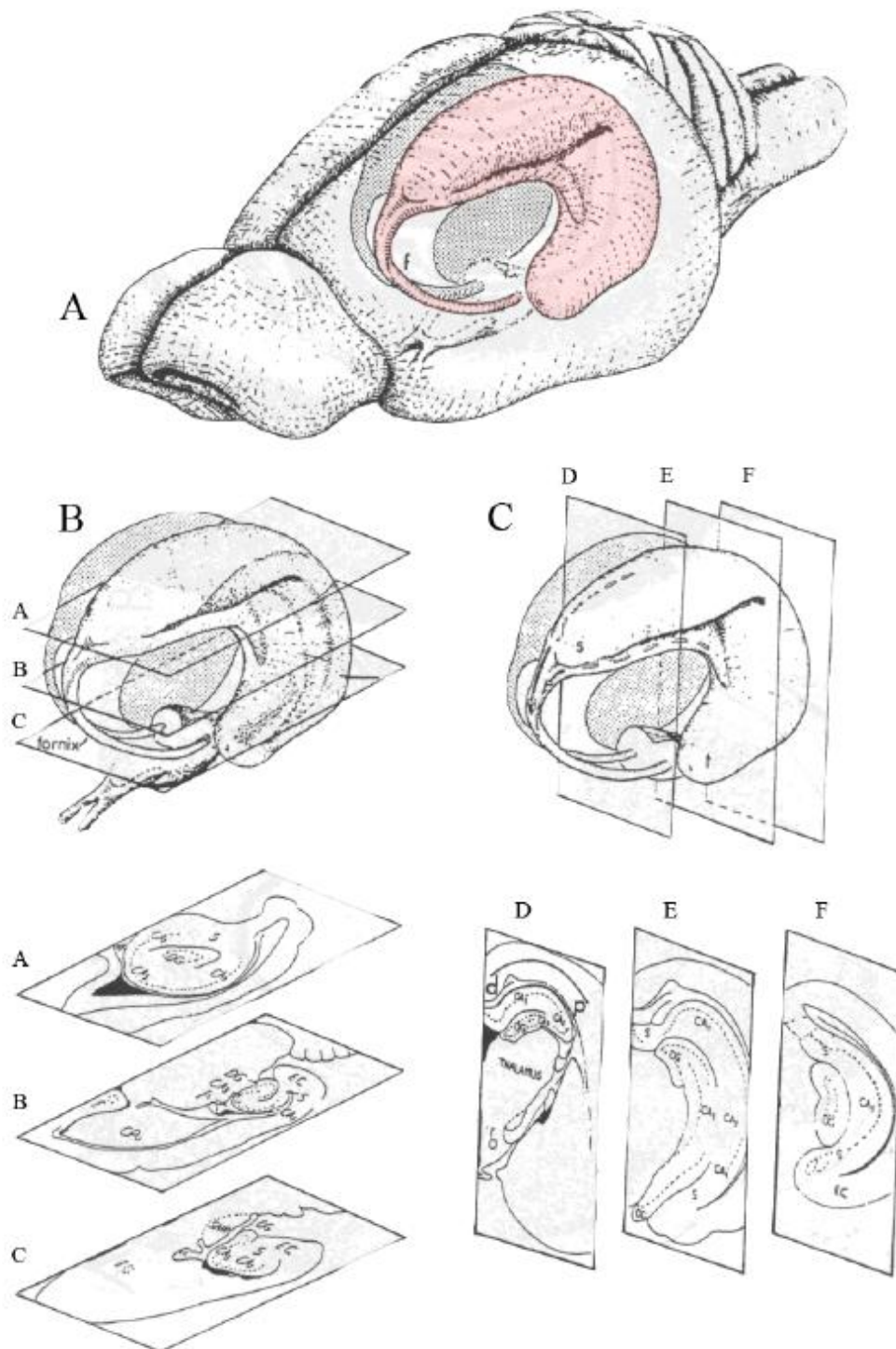
Figure 1.1 Rat hippocampus shown in horizontal and coronal section.

A. The hippocampi are shown in position below the neocortical sheet. Left hippocampus is coloured red. The fornix (f) is indicated descending to its subcortical targets. **B**. Horizontal sections taken at 3 dorso-lateral levels along the hippocampus reveal its differing composition. **C**. Coronal sections taken at 3 rostro-caudal levels. CA1 and CA3, principal fields of hippocampus. CPu, caudate putamen. DG, dentate gyrus. Fi, fimbria. S, subiculum. Adapted from Amaral and Witter (1995), pp 444.
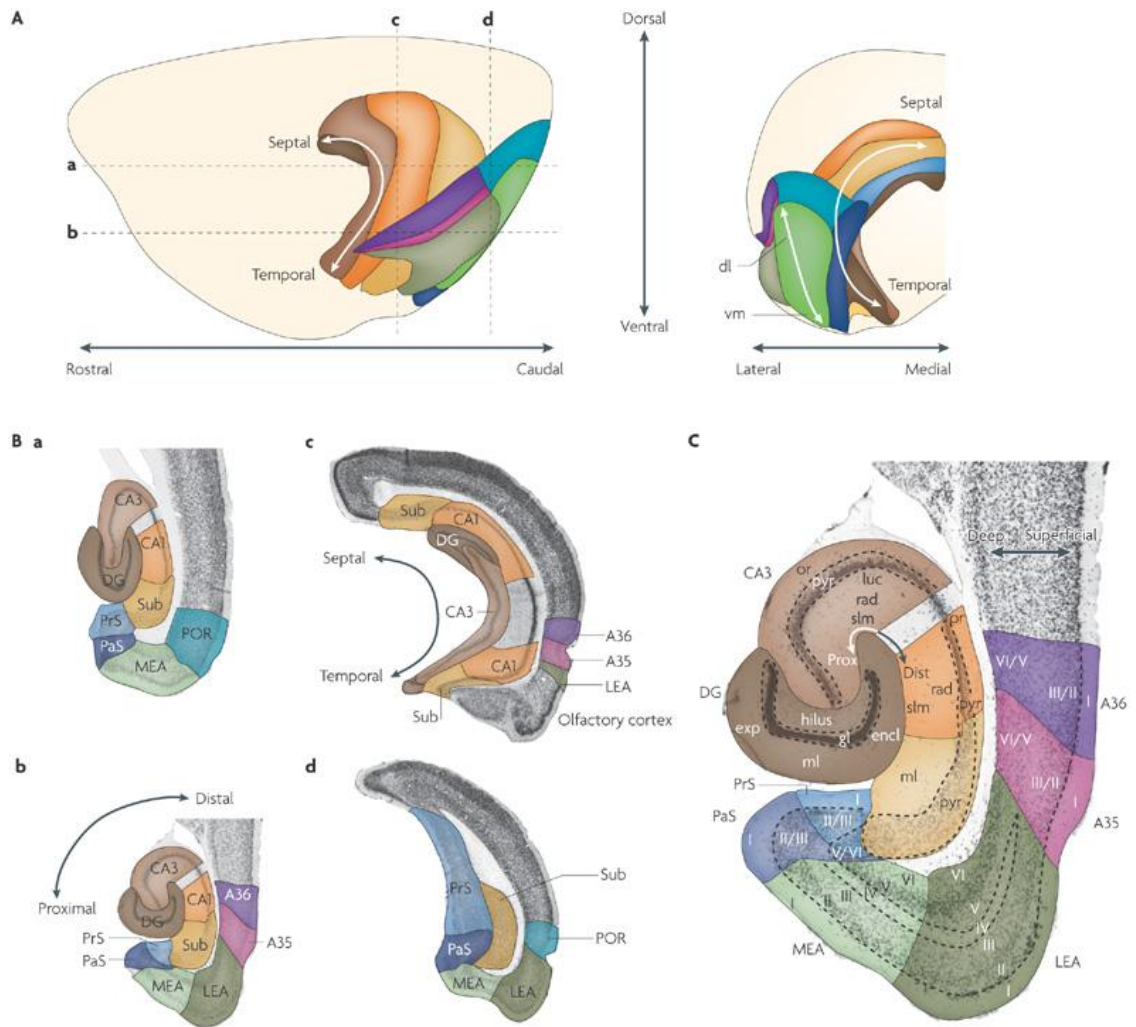
Figure 1.2 Hippocampal and parahippocampal formations in the rat brain. .

A: Lateral (left) and caudal (right) views. **B**: Two horizontal sections (a,b) and two coronal sections (c,d) corresponding to the dashed lines in panel A. **C**: A Nissl-stained horizontal cross section (enlarged from Bb). Regions are colour coded: dentate gyrus (DG; dark brown), CA3 (medium brown), CA2 (not indicated), CA1 (orange), subiculum (Sub; yellow)), presubiculum (PrS; medium blue) and parasubiculum (PaS; dark blue), entorhinal cortex (comprising a lateral (LEA; dark green) and a medial (MEA; light green) area), perirhinal cortex (comprising Brodmann areas (A) 35 (pink) and 36 (purple)) and postrhinal cortex (POR; blue-green). Roman numerals indicate cortical layers. dist, distal; dl, dorsolateral part of the entorhinal cortex; encl, enclosed blade of the DG; exp, exposed blade of the DG; gl, granule cell layer; luc, stratum lucidum; ml, molecular layer; or, stratum oriens; prox, proximal; pyr, pyramidal cell layer; rad, stratum radiatum; slm, stratum lacunosum-moleculare; vm, ventromedial part of the entorhinal cortex. [from van Strien *et al* (2009)]

In contrast to the hippocampal formation, the parahippocampal region exhibits a typical neocortical 6-layer architecture (see figure 1.2 C).

The EC can be divided in two areas, medial entorhinal area (MEA) and lateral entorhinal area (LEA). Briefly, layer I is a cell-poor, fiber-rich molecular layer; layer II contains stellate cells and "islands" of pyramidal cells; layer III contains pyramidal cells; layer IV (lamina dissecans) is a cell-free layer; layer V contains pyramidal cells (based on the packing density of these cells it can be subdivided in a densely packed layer Va and a sparser layer Vb) and layer VI contains a multitude of cell types [see Witter and Amaral (2004) for detailed discussion].

The PRE and PARA exhibit the same 6-layer architecture and their principal cell type is the pyramidal cell [see Witter and Amaral (2004) for discussion].

The PER is divided in two areas: Brodmann area 35 (granular) and area 36 (dysgranular), based on the slightly different neocortical inputs reaching this region. The POR can also be divided into a dorsal and ventral subdivision. The cytoarchitecture of these areas is still very poorly understood.

1.2   Hippocampal fiber bundles

There are three main fiber bundles associated with the hippocampal formation: the angular bundle, the fimbria-fornix pathway and the dorsal and ventral commissures.

The angular bundle comprises the perforant pathway and the alvear pathway, both of which connect the EC with other parts of the hippocampal formation, and it considered the main route of neocortical input. Based on its origin, the perforant pathway can be subdivided into a MEA and LEA projection, with fibers originating in layer II of the EC contacting the DG and CA3 and fibers form layer III of the EC contacting CA1 and SUB. More recently, it has been shown that layers III, V and VI also contribute to this projection. Moreover, LEA and MEA targets of these projections segregate along the

transverse and septotemporal axes of the hippocampal formation. The alvear pathway is also segregated by region of origin (LEA/MEA) and targets CA1 (at more septal levels) and SUB. It originates mainly in layer III of EC, but layers II, V and VI also contribute to this projection. The angular bundle exhibits a topographical organisation in its projections [see van Strien *et al* (2009) and Witter and Amaral (2004) for discussion].

The fimbria-fornix carries input from and to the hippocampus (CA1 and SUB) to the subcortical regions. The dorsal and ventral commissures provide the connection to the contralateral hippocampus.

1.3   Intrinsic connections of the hippocampal formation

The next sections detailing the connectivity of the hippocampal and parahippocampal formation are based on the following sources: Witter and Amaral (2004), Witter (2006), Amaral and Lavenex (2007), van Strien *et al* (2009) and Agster and Burwell (2009). A detailed description of the highly organised topography of these projections is beyond the scope of this chapter.

The granule cells in the DG, via their unmyelinated axons called mossy fibers, target CA3 and the DG polymorphic layer. The polymorphic layer also sends collaterals to the molecular layer, on both the ipsilateral and contralateral sides. There is also an inhibitory network comprised of basket and axo-axonic neurons contacting granule cells in the granule cell and polymorphic layers of the DG.

In CA3/CA2 of the hippocampus proper, there is a strong network of associational connections, and to a much lesser extent there is an associational connection in CA1, DG, although evidence for this is weak [Amaral and Lavenex (2007)] and SUB. CA3 projects via the Schaffer collaterals to the CA1, to all regions of the contralateral hippocampus and also sends a backprojection to the DG. CA1 projects to the SUB, and more recently, back projections to the CA3 have been reported [see van Strien *et al*

(2009) for discussion]. SUB has been reported to send a backprojection to CA1 [see van Strien *et al* (2009) for discussion] but no commissural projections.

1.4   Intrinsic connections of the parahippocampal region

There is a substantial associational network of connections in the EC organized in 3 bands rostrocaudally. Layers II/III project mainly to the superficial layers, whereas layers V/VI project to both deep and superficial layers of EC. Strong commissural projections, in particular to contralateral layers I/II, are also present. EC also projects to PRE and PARA.

PRE and PARA also have strong associational and commissural connections. PRE and PARA are also connected both ipsilaterally and contralatrally. PRE projects bilaterally to layer III (and to a lesser extent layers I, II) of the MEA and also to the LEA, while PARA projects billateraly to layer II of the entire EC. Reciprocal connections with POR and PARA also exist.

PER and POR project to the EC and in the "standard view" the topography of this projection emphasises the PER-to-LEA (from both area 35 and 36) and the POR-to-MEA connections. However, to a lesser extent, PER (mainly area 36) projects to MEA and POR to LEA. The PER-EC connections are much stronger than the POR-EC connections. The EC reciprocates these projections from both its deep and superficial layers. There is a strong interconnectivity between PER and POR, but the POR to PER connection is stronger.

1.5 Hippocampal-parahippocampal connectivity

The CA1 and SUB reciprocate the projections they receive form the EC via the angular bundle. PRE and PARA (all layers) project bilaterally to the SUB, the molecular layer of DG and stratum lacunosum-moleculare of the hippocampus proper (CA1/CA3). CA3 and SUB project to PRE and PARA. The precise topography and layer interactions are summarised by Witter *et al* (2000), see figure 1.3; a detailed discussion is beyond the scope of this chapter. PER and POR also project directly to CA1 and SUB, which reciprocate these projections.
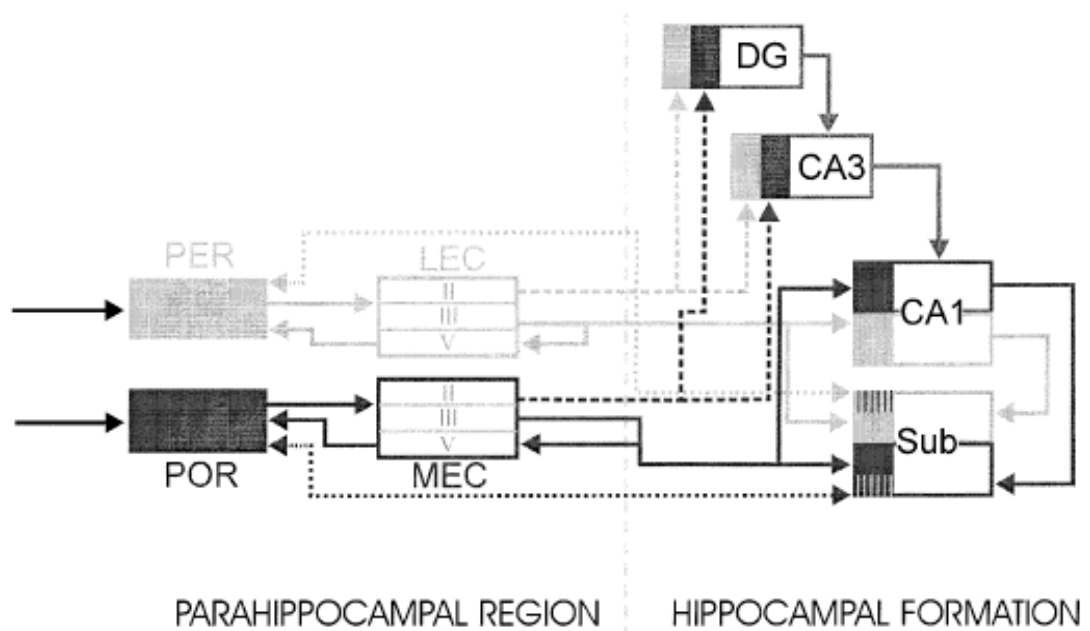
Figure 1.3 Connectivity of the hippocampal region.

PER and POR inputs are grayscale coded. Shaded blocks summarise the precise topographical organisation. Reproduced from Witter *et al* (2000).

1.5.1 A challenge to the hippocampal loop

One of the main features of the hippocampal connectivity is that, unlike in the neocortex, the flow of information is largely unidirectional. In the "standard view", see figure 1.4, that has long dominated our understanding of hippocampal organisation the superficial layers of the EC project to the DG via the perforant pathway, the DG projects to CA3 via the mossy fibers, CA3 contacts CA1 via the Schaffer collaterals (this is historically called the "tri-synaptic loop"). In turn, CA1 projects to the SUB, which projects to PRE and PARA. The separate projections from SUB and CA1 to the deep layers of the EC close the hippocampal loop.

The more recent data indicated in the previous sections, suggest that this connectivity pattern requires substantial revision and also challenges the unidirectionality of the flow [see van Strien *et al* (2009) for review of all 1600 currently known hippocampal-parahippocampal connections].
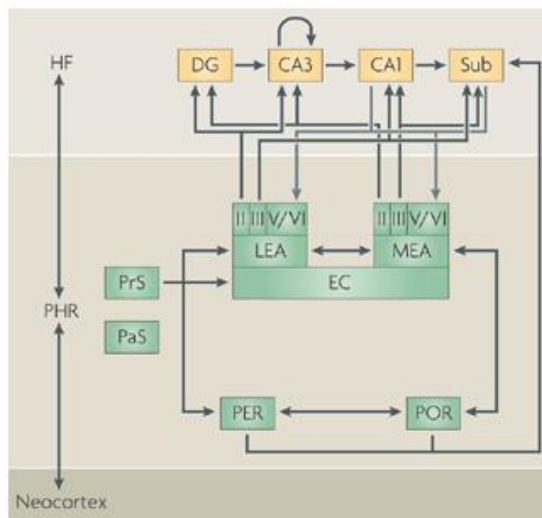
Figure 1.4 The "standard view" of the parahippocampal-hippocampal circuitry.

Dentate gyrus (DG), hippocampal layers (CA1-3), subiculum (Sub), presubiculum (PrS) and parasubiculum (PaS), entorhinal cortex (comprising a lateral (LEA) and a medial (MEA) area), perirhinal cortex (PER) and postrhinal cortex (POR). Roman numerals indicate cortical layers. [from van Strien *et al* (2009)]

1.6 Extrinsic hippocampal connections

This section will summarise the main inputs that the hippocampus receives from other regions of the brain. The hippocampus is one of the few brain regions that receive highly processed, multimodal sensory information from a variety of sources. In an oversimplified view, neocortical inputs reach the hippocampus via PER and POR and subcortical inputs arrive mainly via the fimbria-fornix bundle.

1.6.1 Neocortical connections

The main source of neocortical inputs to the hippocampus is via PER, POR and EC [Burwell and Amaral (1998), Jones and Witter (2007), Witter and Amaral (2004)] and the majority of these inputs are reciprocated [Agster and Burwell (2009)]. The other parts of the hippocampal formation also send efferents to the neocortex.

As seen in figure 1.5, sensory information from all modalities reaches the hippocampal formation. These projections are organised topographically and functionally.

In respect to topography, the EC cortical input is regionally organised in respect to the LEA/MEA subdivisions and also across its superficial/deep layers. Furthermore, only the lateral and caudal parts of the EC are heavily innervated by the neocortex. MEA receives less direct cortical input than LEA and both receive indirect cortical input from PER and POR.

Quantitatively, visual input mainly targets POR while auditory input targets mainly PER. Both regions of the EC receive about 30% of their inputs from the piriform cortex, 20% from temporal cortex and 10% from frontal regions [see Amaral and Lavenex (2007)]. Other major contributors are: insular cortex (20% of LEA input), and cingulate (11%), parietal (9%) and occipital (12%) for MEA.
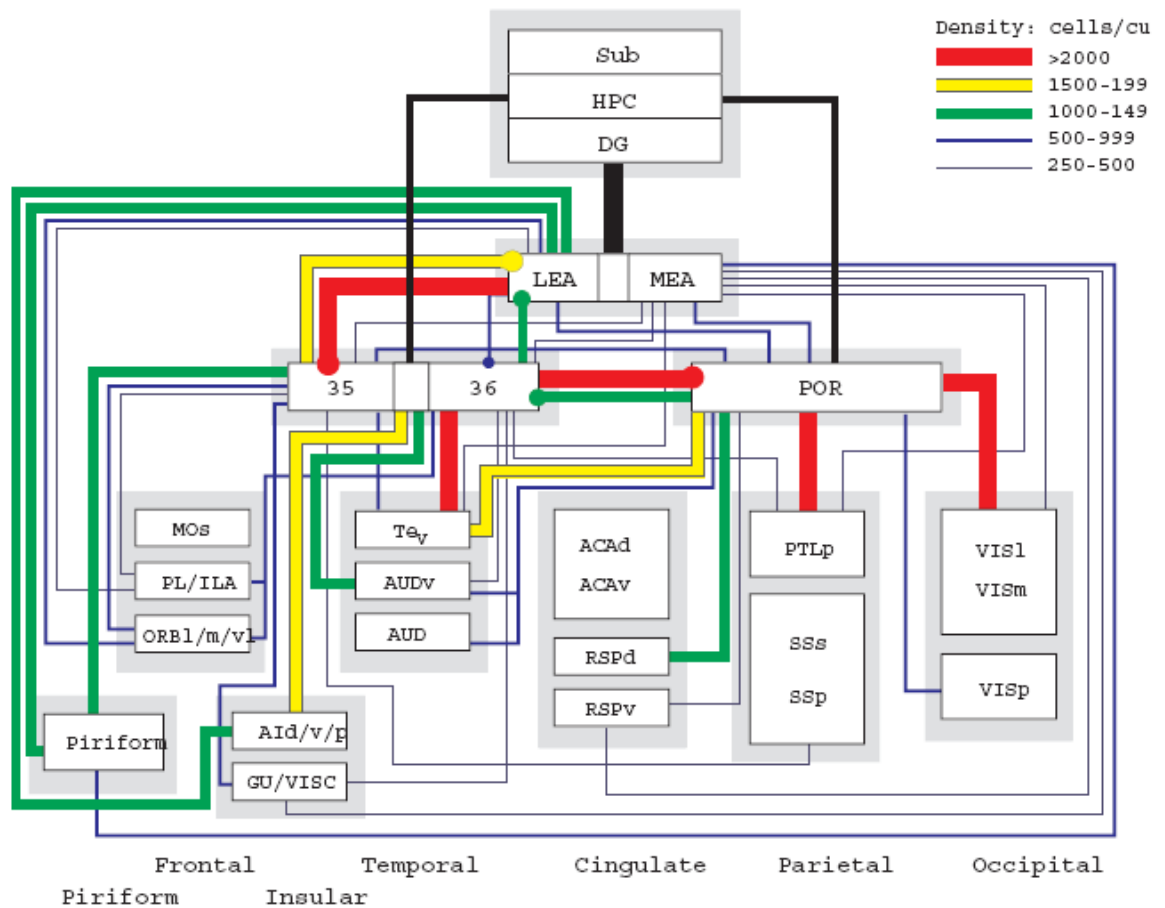
Figure 1.5 Cortical connectivity of the hippocampal and parahippocampal formations of the rat.

Strength of connections are based on densities of retrogradely labeled cells in the afferent region. Some regions were combined and the density of labeling averaged for simplicity. Reciprocal projections shown were also averaged unless dramatically different. Also for simplicity, the weakest connections (250 labeled cells/cu mm) are not shown in the figure. ACAd and ACAv, dorsal and ventral anterior cingulate cortex; AId/ v/p, dorsal, ventral, and posterior agranular insular cortices; AUD, primary auditory cortex; AUDv, auditory association cortex; GU, gustatory granular insular cortex; MOs, secondary motor area; Pir, piriform cortex; PTLp, posterior parietal cortex; RSPd,v, retrosplenial cortex, dorsal and ventral; SSp and SSs, primary and supplementary somatosensory areas; Te$_v$, ventral temporal cortex; VISC, visceral granular insular cortex; VISl and VISm, lateral and medial visualassociation cortex; VISp, primary visual cortex. [from Burwell and Amaral (1998)]

1.6.2   Subcortical afferents

This section describes the subcortical projections to all parts of the hippocampal and parahippocampal formations, as identified in Witter and Amaral (2004). The hippocampal connectivity with the amygdala and the claustrum are beyond the scope of this chapter [see Witter and Amaral (2004) for detailed review]. Figure 1.6 gives an overview of the global extrinsic connectivity of the hippocampal and parahippocampal formations.

While neocortical projections to the hippocampal formation have been the focus of intense anatomical research, the importance of subcortical projections has also been recently reassessed. Quantitative studies by Furtak *et al* (2007) and Kerr *et al* (2007) have shown that the EC and PER area 36 receive about 30% (PER area 35 receives as much as 50% and POR as little 15%) of their input from subcortical afferents.

The **septum**, in particular the medial septal nucleus and the nucleus of the diagonal band of Broca, sends mainly cholinergic and GABAergic projections to all areas of the hippocampal and parahippocampal formation [see Witter and Amaral (2004) and also Furtak *et al* (2007) for projections to POR/PER].

Various nuclei of the **hypothalamus** send projections to the hippocampus: the suprammilary nucleus [to DG, CA2, CA1/3 (very weakly), SUB, EC, PRE]; tuberomammilary nucleus [to CA2, EC]; premammilary nucleus [to SUB]; lateral hypothalamic area [to EC] and posterior nucleus [to PER].

Thalamic input to the hippocampal formation arrives from: separate populations of nucleus reuniens cells to CA1 and SUB and paraventricular, paratenial, rhomboid nuclei, anteromedial and anteroventral nuclei to SUB. Thalamic projections from various nuclei to EC [Kerr *et al* (2007)], PER/POR [Furtak *et al* (2007)] and PRE/PARA [Witter and Amaral (2004)] have also been documented. In particular, the reciprocal connections of PRE/PARA with the anterodorsal, anterolateral and laterodorsal nuclei, together with the PARA to DG connection, have been postulated to form the main route of thalamic input to the hippocampal formation [Witter and Amaral (2004)].
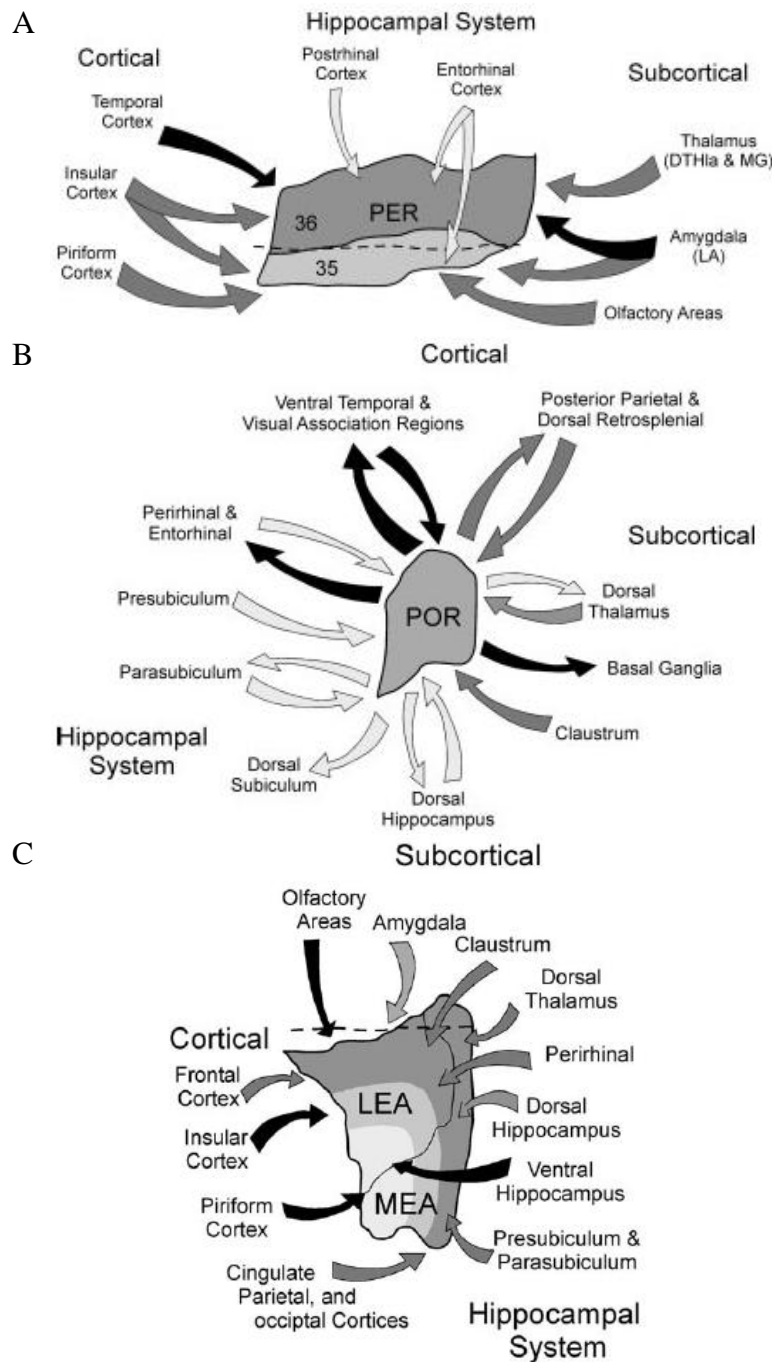
Figure 1.6 Afferent connections of the parahippocampal formation

A. PER, **B**. POR and **C**. EC Strength and direction of connections are denoted by colour-coded arrows (black - strong, dark grey - moderate connections, light grey - weak).

A & B: from Furtak *et al* (2007)
C: from Kerr *et al* (2007)

Brainstem inputs from the pontine nucleus locus coeruleus (noradrenergic), ventral tegmental area (dopaminergic) and raphe nuclei (serotonergic) target various parts of the hippocampal and parahippocampal formations [see Witter and Amaral (2004) for detailed discussion]. The EC also receives projections from nucleus incertus and pontine projections from the parabrachial nucleus, dorsal tegmental nucleus and nucleus subcoeruleus.

Weak **basal ganglia** input to EC [Kerr *et al* (2007)] and POR/PER [Furtak *et al* (2007)] has been documented. In contrast, the hippocampal formation (CA1, SUB) and

the parahippocampal formation project very strongly to the basal ganglia (in particular to the caudate putamen and nucleus accumbens).

1.7   Functional implications

One of the greatest challenges imposed by this intricate connectivity is uncovering its functional role. This section will give a brief, and necessarily oversimplified, insight into this. Its main purpose is to identify how sensory information reaches the hippocampus and what inputs are integrated by place cells in order to achieve spatial selectivity.

1.7.1   Cortical information is relayed to the hippocampus by two parallel streams

Information from all sensory modalities reaches the hippocampus via various cortical afferents, mainly through PER, POR and EC. The current view is that such information is split into two parallel streams [Witter *et al* (2000), see also sections 1.4-5 for connectivity details and figure 1.3 for a diagram]. The first one, PER→LEA, carries nonspatial information about discrete stimuli (objects, odours, sounds), while the second, POR→ MEA, transmits information about location and context. Recent evidence suggests that these streams are not segregated and integration might occur as early as in the cingulate cortex [Jones and Witter (2007)]. It is clear however that integration also occurs at the PER/POR level and, since the PER to POR projection is stronger, Agster and Burwell (2009) propose that PER "informs" POR about the context of the discrete stimuli. Integration also occurs in the EC, via its prominent associational connectivity.

POR, based on its cortical and thalamic connections, has a clear bias towards visual information processing and has been implicated in visuospatial orienting [Furtak *et al*

(2007)]. PER, in turn, is the site of convergence of unimodal and polymodal sensory information and is believed to be the site of perceptual processing of complex (but not simple) stimuli and memory of objects [see Murray *et al* (2007) for a review].

1.7.2   *Cortical sites involved in spatial navigation*

The posterior parietal cortex (PTL) [see Palomero-Gallagher and Zilles (2004) and Whitlock *et al* (2008) for a detailed discussion of anatomy], a complex multisensory region, has recently been implicated in spatial navigation. Cells in this region are capable of representing routes through space and, more broadly put, process sensory information in register with the different coordinate systems of the eye, head and body in order to support accurate animal movements to targets [see Nitz (2009) and Witlock *et al* (2008) for recent reviews]. Interestingly, PTL projects most heavily to POR and very weakly to LEA and PER area 36, and it receives strong inputs from all of these areas, as well as PER area 35 [Burwell and Amaral (1998), Agster and Burwell (2009)]. There are no direct projections to or from the hippocampal formation.

The retrosplenial cortex (RS) has also been involved in spatial navigation and the current view is that it may play a role in transforming allocentric (view-point independent/world centred, medial temporal lobe-mediated) into egocentric (view-point dependent/self centred, PTL-mediated) frames of reference and vice versa [see Vann *et al* (2009) for a review]. RS sends projections to the hippocampus, specifically PER, PARA, POR and MEA [Jones and Witter (2007)], as well as a wide range of cortical [most notably primary and secondary motor areas, Shibata *et al* (2004)] and subcortical structures [noted reciprocal connections include: anterior thalamic nuclei and lateral dorsal thalamic nucleus and mammilary bodies, *cf.* Harker and Whishaw (2004)]. Lesion studies show that the RS is involved in a range of both allothetic and idiothetic spatial navigation tasks [see Harker and Whishaw (2004) for review], while electrophysiological studies have found head direction cells in the RS along with cells that respond to angular velocity, running speed or location [Cho and Sharp (2001)]. Based on these findings, Harker and Whishaw (2004) posit that the RS is responsible

for integrating and transmitting movement-related and visuospatial information between the cortex and the hippocampus.

1.7.3   Beyond the cortex: Thalamic functionality

Compared to the intense efforts dedicated to studying cortico-hippocampal functional interaction, subcortical inputs are often overlooked, despite the substantial amount of inputs that the hippocampus receives from these structures [see section 1.7.2].

At the global functional level, the thalamus is the relay and modulator of information flow to the cortex [Groenewegen and Witter (2004)]. Despite its very important role, the precise nature and mechanism of its functionality are still poorly understood. At a broad level, the thalamic nuclei can be grouped functionally into sensory, motor and associational relays and "non-specific" nuclei, believed to be involved in arousal and attention mediation.

A very telling point in case are the projections from the nucleus reuniens and the rhomboidal nucleus, which are the major source of thalamic input to the hippocampal formation and the EC [Vertes *et al* (2006)], and whose functional relevance has only recently come into focus [Vertes *et al* (2007), Davoodi *et al* (2009)]. These "non-specific" nuclei are believed to be part of a circuit involved in polymodal sensory awareness [Groenewegen and Witter (2004), Vertes *et al* (2007)].

Other midline/intralaminar thalamic nuclei project to various parts of the (para)hippocampal formation [Furtak *et al* (2007), Kerr *et al* (2007)], but their role has not been studied in detail. They are generally implicated in visceral functions, awareness and arousal [Van der Werf *et al* (2002)]. However, recently demonstrated connections with a large array of brainstem nuclei [Krout *et al* (2002)] indicate that they might provide a more direct route for sensorymotor input to the hippocampus.

1.7.4   The anatomy of the head direction system: contribution of motor and vestibular inputs

The anterior thalamic nuclei (anterodorsal, anteroventral and anteromedial and also laterodorsal) form part of a circuit reciprocally connected to the SUB, PRE/PARA (and also PER/POR) and the cingulate cortex (both anterior and posterior) and receiving input from the mammilary bodies (and possibly their afferent input from the dorsal tegmental nuclei). This circuit is involved in spatial orientation, spatial memory and attentional processes [Groenewegen and Witter (2004)]. Head direction cells can be found in all anterior nuclei, but mostly in the anterodorsal and laterodorsal nuclei, as well as upstream in the lateral mammilary nucleus and the dorsal tegmental nucleus [Taube (2007)]. Thus, it is possible that the directional signal reaches the hippocampus via this circuit.

Recent work of Taube and colleagues [Taube (2007), Clark *et al* (2009)] has focused on identifying the origin of the head direction signal [which they posit to be the dorsal tegmental nuclei and the lateral mammilary nuclei circuitry] and the mechanism by which vestibular and motor inputs reach this site. They propose that a pathway originating in the medial vestibular nucleus and continuing through the nucleus prepositus/supragenual nucleus to the dorsal tegmental nuclei and the lateral mammilary nuclei relays vestibular information.

The picture about the contribution of the motor signal is less clear. Clark *et al* (2009) provide recent evidence that such a signal might be relayed to the dorsal tegmental nucleus from the interpeduncular nucleus (IPN). This, in turn, receives inputs from the lateral habenula [Andres *et al* (1999)], via the entopeduncular nucleus (the rat equivalent of the primate globus pallidus), which is considered a major output path of the basal ganglia [Gerfen (2004)]. In support of this, they elegantly demonstrate that head direction cells in anterodorsal nucleus of IPN-lesioned versus control rats increase their directional firing range, are less influenced by visual landmarks and less stable in the dark or when rats locomote from a familiar environment to a novel one. Corroborating evidence comes from Sharp *et al* (2006) who found movement related neurons in IPN (running speed) and lateral habenula (running speed, angular head velocity). Moreover, IPN lesioned rats are impaired in the hidden platform spatial

variant of the Morris water maze task [Clark and Taube (2009)] and the same holds for habenula lesions [see Lecourtier and Kelly (2007) for review].

An alternative hypothesis about where motor/proprioceptive inputs are integrated points to the vestibular nuclei. These integrate optokinetic visual information from the retina and proprioceptive and somatosensory information from the spinal cord [Vidal and Sans (2004), Smith *et al* (1997), Smith *et al* (2010)]. This signal is relayed to various thalamic nuclei [Shiroyama *et al* (1999), Krout el al (2002)] from where it reaches the hippocampus through a direct or indirect route [via the parietal cortex cf Smith *et al* (1997)].

Supporting evidence for the involvement of this pathway in relaying self-motion signals comes from work in primates. In a recent study, Marlinski and McCrea (2009) recorded from vestibular sensitive neurons in the thalamus of the squirrel monkey and found they encoded translations and rotations of the head and/or trunk. Interestingly, they found a small population of neurons that receive vestibular but not neck proprioceptive input, and responded only to involuntary head movements. The authors propose that the vestibular input to these neurons during voluntary movement of the head is cancelled by a motor efference copy. Furthermore, they found neurons that responded to rotation of the trunk, irrespective of whether the trunk moved alone or simultaneously with the head. Thus, they propose that vestibulothalamic neurons build a somatokinetic signal of the movement of the trunk in space, by integrating both vestibular and neck proprioceptive input.

1.7.5   Corollary discharge and locomotion

The nervous system is able to disambiguate between sensory input created by one's own movements ("reafference") and those imposed from the outside world ("exafference"), even though at the level of sensory inputs they are indistinguishable. This can be achieved by sending copies of motor commands to the sensory structures, via a signal termed corollary discharge or efference copy [see Crapse and Sommer (2008) and Sommer and Wurtz (2008) for discussion and review]. There is no specific level within the ascending pathways carrying sensory information and the descending motor pathways at which corollary discharge occurs. More likely, corollary discharge affects sensory integration at multiple levels.

Of particular interest for this thesis is the motor efference copy arising from locomotion and how this signal might reach the hippocampal formation. Unfortunately, little is know about this particular signal, and this stems from our still limited understanding of locomotion [see Dickinson *et al* (2000), Kiehn (2006), Goulding (2009) for reviews].

A clear view has emerged about how locomotion is generated at the level of the spinal cord via the central pattern generators that govern the timing and pattern of complex, rhythmic and coordinated muscle activities [Kiehn (2006)] and about how sensory and motor inputs interact at this level [Rossignol *et al* (2006)].

At the supraspinal level the picture is still unclear. An important role in controlling locomotion is ascribed to the mesencephalic locomotor region (MLR), which is a functional rather than anatomical construct and involves various brainstem nuclei depending on behavioural context [Jordan (1998)]. This lax definition, as the area of the brainstem from which it is possible to elicit locomotion by electrical stimulation in decerebrate animals, makes it difficult to identify functional circuits, although it is generally agreed that it receives inputs from the basal ganglia and the hypothalamus and, together with the cerebellum, acts upon locomotor reticulospinal cells directly. As to where sensory inputs are integrated with motor ones at supraspinal levels, Rossignol *et al* (2006) review evidence of phasic [in this context this refers to the step cycle] modulation of responses to sensory inputs from limb movement in the motor and

somatomotor cortices, dorsal column nuclei and thalamus. Ahissar (2008) describes a system for motor modulation of sensory processing in the rat vibrissal system. Of particular interest to this sensory and motor input integration is the observation that in the rat there is a region of overlap between the primary somatosensory (SI) and the motor cortex, superimposed on the representation of the limbs.

While little is presently understood about the circuitry of motor efference copy, direct evidence that it plays an important role in locomotion comes from studies in insects and humans. Wittlinger *et al* (2006) showed that ants with elongated/shortened legs take longer/shorter strides respectively and misjudge travelled distances as a result. Dominici *et al* (2009) describe the case of an achondroplastic child that, after surgical limb elongation, kept the same stride length as before but systematically stopped short of a goal location when trying to reach it with his eyes closed. The same results were replicated in volunteers walking on stilts. Mittelstaedt and Mittelstaedt (2001) showed through a series of experiments that, for humans, path estimation when walking in the dark varies not only as a function of velocity but also step length and step rate.

Conjectural evidence that information about stance and locomotion is available to the hippocampus comes from a human fMRI study of Jahn *et al* (2009) who found that subjects imagining prior experience in standing/walking/running training show activation of the hippocampus. Standing was associated with hippocampal and locomotion to parahippocampal activity. Moreover, vestibular-loss patients showed reduced activity in the anterior parahippocampal region while blind subjects showed reduced activity in the posterior parahippocampal gyrus. The authors conjecture that, in humans, visually guided locomotion involves the posterior hippocampal formation while vestibular signals are relayed via the entorhinal cortex and the anterior hippocampal formation.

1.8   Hippocampal LFP and the theta rhythm

It has long been known that the local field potential (LFP) present throughout the hippocampus as the rat engages in its daily activities oscillates with a frequency ranging from 1 to 200 Hz [see Buzsáki (2005) for a historical perspective]. Various LFP patterns can be observed in the freely moving rat, including: theta (6-12Hz), beta (12-30Hz), gamma (30-100Hz) and ripples (140-200Hz) oscillations, as well as small and large irregular amplitude activity (SIA/LIA).

The behavioural correlates of various LFP rhythms, in particular the theta oscillation, are still not fully elucidated [see Buzsáki (1996), Buzsáki (2005) and O'Keefe (2007) for detailed discussion]. The currently accepted consensus, however, is that theta is associated with "voluntary" locomotion/exploration and REM sleep.

Two types of theta activity have been identified, based on their behavioural correlates and pharmacological properties. Type I theta occurs during periods of immobility associated with arousal or attention and co-occurs with type II theta during movement. Atropine antagonists abolish type I theta, therefore it has been termed atropine-sensitive. Type II theta is atropine-resistant and occurs during translational movement [O'Keefe (2007), Buzsáki (2002), Bland and Oddie (2001)].

At the anatomical level, theta generation depends on a circuit originating in the brainstem and reaching the hippocampus via the medial septum [see Vertes and Kocsis (1997), Bland and Oddie (1998) for reviews]. Theta is initiated in the brainstem, in the rostal pons region [nucleus reticularis pontis oralis], which is modulated by cholinergic inputs from the pedunculopontine tegmental nucleus. Tonic input from this nuclei is relayed either directly or indirectly via the nucleus incertus [Teruel-Marti *et al* (2008)] to the supramammilary area (SuM), which has been implicated in theta frequency generation [see Pan and McNaughton (2004) for detailed discussion]. Another pathway is via the posterior hypothalamic nucleus [PH], whose cells discharge tonically with the theta rhythm [Vertes and Kocsis (1997)] and which has recently been implicated in generating Type I, movement-related theta [Bland *et al* (2006)]. SuM/PH project to the medial septum/diagonal band of Broca, which has been termed

the "pacemaker" of the hippocampus (as well as that of the EC and posterior cingulate cortex [Rislod (2004)]), in the sense that phasic firing in the hippocampus follows that of the septum and has the same frequency. GABAergic and cholinergic septal inputs synchronize hippocampal neurons while serotonergic inputs have been shown to desynchronise theta LFP. It is also worth noting that both SuM and PH input reaches the (para)hippocampal formation through routes other that via the medial septum, either directly or indirectly [Vertes and Kocsis (1997), Bland and Oddie (1998)].

Lesions and pharmacological studies show that both types of theta recorded in the hippocampus proper are dependent on the medial sepal nucleus and the nucleus of the diagonal band of Broca, but atropine resistant theta also requires an intact EC [see O'Keefe (2007) for detailed discussion].

At the level of the hippocampus, theta current generation is also influenced by the cells' intrinsic oscillatory properties and network properties of the hippocampal formation [Buzsáki (1996), Buzsáki (2002), Sirota and Buzsáki (2005)]. Theta waves in the awake rat show a gradual phase reversal in the dorsoventral axis, from CA1 stratum oriens to the hippocampal fissure and to a lesser extent in DG and CA3. The standard view is that theta oscillations are synchronized within each layer across the entire extent of the hippocampus, but recent evidence from Lubenov and Siapas (2009) suggests that, at least in CA1, they are travelling waves that propagate along the septotemporal axis.

As to the functional relevance of the theta rhythm, a great number of hypotheses have been put forward, both from a computational point of view relating to how information is processed in the brain [Buzsáki and Draguhn (2004), Sirota and Buzsáki (2005)] as well as a mechanism related to sensorymotor integration [Bland and Oddie (2001), Hallworth and Bland (2004)]. The latter model proposes that sensory and movement related inputs, possibly in two parallel streams, reach the hippocampus via the ascending brainstem synchronising pathways. The hippocampus relays these inputs to motor structures in the basal ganglia, possibly via its projections to the nucleus accumbens, which initiate and maintain voluntary motor behaviour as well as providing feedback about this to the hippocampus. While the authors are primarily interested in this model as demonstrating the hippocampal capacity of "providing

voluntary motor systems with continually updated feedback on their performance relative to changing environmental conditions", I note that it fits very nicely with the above discussion about the circuitry of motor efference copy and might provide a route by which this signal reaches the hippocampus.

1.8.1   Ripples and the hippocampus

During LIA, sharp waves occur in the hippocampal LFP, in particular during sleep and periods of quiet sitting [O'Keefe (2007)]. Among these a high frequency (140-200 Hz) oscillation (termed ripples) can be observed, whose peak amplitude occurs in the CA1 layer is associated with a large number of neurons discharging simultaneously [Csicsvari *et al* (1999), Csicsvari *et al* (2000)].

During sleep, place cells fire synchronously in sequences that have been correlated with the rat's previous activity [Lee and Wilson (2002), Louie and Wilson (2001), Nádasdy *et al* (1999)]. Place cell reactivation has also been demonstrated during ripple events that occur transiently during exploratory behaviour or in periods of waking immobility [O'Neill *et al* (2006)]. Interestingly, the place selective activity of cells is maintained when ripples occur during brief pauses in exploration. In contrast, when ripples are associated with longer periods of immobility, the pattern of waking place cells activation is "replayed" in both forward and reverse-order [Foster and Wilson (2006), Csicsvari *et al* (2007), Diba and Buzsáki (2007), Davidson *et al* (2009)].

This replay phenomenon associated with the occurrence of ripples in the hippocampal LFP has been postulated to play a role in synaptic potentiation and the transfer of information from the hippocampus to the neocortex [see O'Keefe (2007) for discussion]. In support of this interpretation, O'Neill *et al* (2008) have recently shown that firing of CA1 cells during sleep epochs follows a Hebbian learning rule.

In the context of this thesis, their relevance is limited to constituting an important electrophysiological marker that allows electrode positioning within the CA1 layer [Csicsvari *et al* (1999)].

2 Hippocampal neurophysiology

Since their discovery by O'Keefe and Dostrovsky (1971), hippocampal place cells have been the object of intense study. The remarkable feature of these cells is that they are almost completely silent while the rat explores a given environment with the notable exception of a specific region called "the place field". No specific sensory stimuli other than the (abstract) concept of space can be shown to be responsible for the firing selectivity of place cells.

The purpose of this thesis is to investigate the sensory information that place cells use in order to encode the animal's location in the environment. A large variety of sensory inputs, of all modalities, is available to the hippocampus, as reviewed below. The rat can use a combination of these inputs to establish were it is. The classical manipulation relies on putting such information in conflict, in order to uncover which one has primary influence over the control of place fields.

This chapter summarises our current knowledge of how place fields are governed by exteroceptive (visual, auditory, olfactory, tactile) and idiothetic (*e.g.* vestibular, ambulatory *etc*) inputs. It then looks at how the availability of such information influences the rat's choice of navigational strategy (whether based on exteroceptive cues or the integration of its own motion). Lastly, it exposes the rationale for the experiments performed in this thesis, designed to further our understanding of the combination of sensory information that the place cells use in order to encode location in an environment.

2.1   Place cells and spatial selectivity

At any given location in space, a subset of place cells will be active thus forming a distributed representation of the environment [Wilson and McNaughton (1993), Fenton *et al* (2008)]. However, unlike in other cortical regions, anatomically proximal cells will not have adjacent place fields in physical space [Redish *et al* (2001)].

Only a subset (up to about 33%) of anatomically proximal pyramidal cells have place fields in a given environment, even though all cells are similarly active during short-wave sleep and antidromic stimulation [Thompson and Best (1989), Henze *et al* (2000)]. Even fewer cells have fields in 2 (14%) or 3 environments (1%). However, if place cells are active in a given environment, their activity is stable over an extended period. Thompson and Best (1990) recorded from the same cell in the same environment for up to 153 days.

2.2   Place cells: space coding

It is now understood that place cells use two coding strategies in order to represent spatial location.

The first is their firing rate. This is measured by the number of spikes a cell fires in a given region of the environment divided by the time the animal has spent in that location. Hippocampal pyramidal neurons fire both simple spikes and complex spike bursts, a series of 2-6 spikes, separated by short (up to 6ms) intervals at decreasing extracellular amplitude [Ranck *et al* (1973), Harris *et al* (2001)]. The profile of the firing rate roughly follows a Gaussian curve [but see section 2.3.3] thus rendering this code imprecise. Because of its symmetrical nature, this code cannot disambiguate whether the rat is at the beginning or the end of the place field.

The second is a temporal code, taken with respect to the LFP theta rhythm in the hippocampal region. During locomotion, the local field potential (LFP) oscillates with a frequency of 4-12Hz [see section 1.8]. O'Keefe and Recce (1993) discovered that, as the rat traverses the place field of a given cell, the phase of each spike (measured relative to the theta oscillation) precesses, *i.e.* the cell fires on progressively earlier phases of successive theta cycles. The maximum amount of precession is approximately 360 degrees. The phenomenon can be explained by the rhythmical firing of place cells at a frequency slightly higher than theta, as originally proposed by O'Keefe and Recce (1993). The increase in place cell oscillation frequency might be modulated by the rat's locomotion speed [McNaughton *et al*. (1983), Maurer *et al* (2005), Geisler *et al* (2007)].

There is a good correlation between the phase of firing and an animal's location in the environment and, thus, phase precession constitutes a temporal code. Moreover, the phase code, unlike the rate (which is a symmetrical Gaussian curve), is a linear one. Thus, it has been proposed that it might encode the proportion of the field that the rat has traversed [Huxter *et al* (2000), Skaggs *et al* (1996), Huxter *et al* (2008)], which cannot be achieved by the symmetrical rate code.

An important open question is whether these two codes convey information about location alone or also encode other variables. Experimental evidence indicates that there is "excess firing variance" on individual passes that the rat makes through the place field [Muller and Kubie (1987), Fenton and Muller (1998), Olypher *et al* (2002)], suggesting that place cells carry information in addition to position. Several candidates have been proposed, such as keeping track of multiple reference frames [Olypher *et al* (2002)], speed encoding [Huxter *et al* (2003), Geisler *et al* (2007)] or task relevance [Wiener *et al* (1989), Hok *et al* (2007)].

2.3 Basic properties of place cells

I review here the basic properties of place cells that are relevant for this thesis. For extensive reviews, see Best *et al* (2001) and O'Keefe (2007).

2.3.1 Directionality

In open enclosures (as opposed to narrow mazes/tracks), place cells are omnidirectional [Muller *et al* (1994)], *i.e.* they fire irrespective of the direction in which the animal traverses the place field, suggesting that they are not bound to an egocentric (self-centred) frame of reference, but to an allocentric one (established by visual or other available cues). This hypothesis is further supported by experiments that rotate the experimental enclosure or the set of available cues and result in a proportionate rotation of the place fields [O'Keefe and Conway (1978), Muller *et al* (1987), Fenton *et al* (2000)].

In contrast, in experiments on narrow mazes or tracks, where the trajectories of the rat exhibit a high degree of stereotypy, place cells become highly unidirectional [McNaughton *et al*. (1983), but see Redish *et al* (2000)]. In addition, even in an open environment, if the animal is trained to run on a stereotypical path, the place cells become directional [Markus *et al* (1995)]. Moreover, enriching a narrow track with local cues [Battaglia *et al* (2004)] causes a significant proportion of the place cells to become bi-directional. Note, however, that local cues are not necessary in open fields for the cells to be omnidirectional.

Therefore, it has been postulated that the major difference between directionality and omnidirectionality is the influence on the firing of the place cells of the trajectory of the path in the stereotypical paradigms [O'Keefe (2007]. Experiments where the animal had to traverse the same region of the apparatus as part of 2 different paths, *e.g.* after choosing a particular arm of a T/Y maze and then returning to the start arm [Wood *et al* (2000), Frank *et al* (2000), Cheng and Frank (2008)] have shown that place cell

activity depends on the animal's chosen route. However, it is possible that these results are due to sampling different end points of the track, to a particular motor behaviour (*i.e.* the way the rat has to turn) or to the different sequence of place fields being traversed (depending on what arm was visited).

2.3.2   Place field stability versus remapping

Place fields are remarkably stable under a wide range of experimental manipulations such as removing cues [O'Keefe and Conway (1978)], changing rewards, turning off the lights [Quirk *et al* (1990)], changing the colour of the enclosure [but see Letugeb *et al* (2007) for rate remapping in CA3] and, when the animal is inexperienced, even the shape of the environment [Lever *et al* (2002)]. It takes a drastic change in experimental environment characteristics and/or a large amount of experience, so that the animal learns that 2 environments are different [Bostock *et al* (1991), Wilson and McNaughton (1993), Wills *et al* (2005)], in order for the place cells to alter the position and configuration of their firing fields and perform what is know as "remapping".

2.3.3   Place cells may become asymmetric with experience

Mehta *et al* (1997) found that as the rat runs along a linear track, the place field of a given cell expands and its centre of mass moves backward, opposite to the direction of movement, on successive individual runs through the place field. Mehta *et al* (2000) further expanded on this paradigm and showed that, on successive runs, the Gaussian profile of the firing rate becomes negatively skewed, independent of the location of the field on the track. It is important to note that the skew effect resets overnight. They proposed that this phenomenon is dependent on the amount of experience the rat has had on a given day in a given environment. However, other studies fail to fully corroborate this finding, showing that individual cells can be skewed either forward or not at all, as well as backward [Schmidt *et al* (2009), Lee and Knierim (2007)].

2.4   Components of a cognitive map

Shortly after the discovery of place cells in the hippocampus, O'Keefe and Nadel (1978) postulated that they are part of a *cognitive map* that allows the animal to navigate in space. Since then, spatially selective cells have been found in other brain regions, notably the subiculum, presubiculum, parasubiculum [see O'Keefe (2007) for detailed review].

The subsequent discovery of two more types of spatially selective cells supports this hypothesis. Ranck (1984) and Taube *et al* (1990) found head direction cells in the dorsal presubiculum. These cells are tuned to the head direction of the animal in the yaw axis, but not in the pitch and roll ones, irrespective of its location in the environment. Subsequently, head direction cells and their additional sensory correlates (such as angular head velocity, neck proprioception, location, *etc*) have been identified in several other brain areas [see Taube (2007) for a comprehensive review].

Hafting *et al* (2005) identified grid cells in the layer II of the dorso-lateral medial entorhinal cortex. These fire in a regular, grid-like pattern, with repeated fields arranged on the vertices of an equilateral triangle. Their firing is omnidirectional. Sargolini *et al* (2006) subsequently found directionally modulated grid cells in the deep layers (III, V, VI) of the entorhinal cortex.

Due to their highly regular pattern, grid cells can be characterised by three variables: *orientation*, defined as their angle with respect to an arbitrary axis; *offset*, *i.e.* the position of the grid in space and *spacing*, representing the distance between adjacent peaks. While grid cells in the same animal appear to have the same orientation [Sargolini *et al* (2006)], their spacing is topographically organised, with more dorsally positioned grid cells exhibiting a finer spatial representation and their offset appearing randomly distributed.

Taken together, place cells, head direction cells and grid cells can form the basis of a spatial navigation system. The grid cells can be the basis for computing Euclidian distance, head direction cells provide the orientation in space, and place cells bind together this information to signal specific locations, thus constructing a map.

2.5   Map navigation: allocentric vs. egocentric frameworks

If space is represented in the hippocampus in a map-like fashion, the question arises as to how exactly does the animal determine its location and uses it to navigate. The earliest suggestion, and to this date the most accurate, is that of O'Keefe (1976) who highlighted two sources of information:

"Each cell receives two sources of inputs, one conveying information about the large number of environmental stimuli or events, and the other from the navigational system which calculates where an animal is in an environment independently of the stimuli impinging on it at the moment. The input from the navigational system gates the environmental input, allowing only those stimuli occurring when the animal is in a particular place to excite a particular cell"

Thus, two strategies of navigation are available: one based on exteroceptive information, such as visual/olfactory/auditory or tactile cues, and one based on self-movement, integrating proprioceptive and vestibular information, termed path-integration or dead reckoning [Mittelstaedt and Mittelstaedt (1980), Mittelstaedt (2000)]. These two strategies are not mutually exclusive, and it is highly probable that rats would use both, depending on circumstances [see Etienne *et al* (1996), Etienne and Jeffrey (2004) for reviews].

The exact interplay between these two navigational strategies and place cell activity has not yet been fully determined [reviewed in Etienne and Jeffrey (2004) and McNaughton *et al* (2006)]. Evidence will be summarised in this chapter while discussing the input that place cells receive from various sensory modalities.

2.6 Sensory input and its influence on place cells

The hippocampus receives highly processed sensory input via the entorhinal cortex (see section 1.6.1). Consequently, one of the major foci of place cell research has been the relative influence that various sensory modalities play on determining spatial selective activity. This section summarises current experimental evidence about how place cell integrate sensory inputs.

Exteroceptive senses

2.6.1 Visual input: evidence from darkness and blindness

The simplest way to test the importance of visual stimuli is to run experiments in the dark [(O'Keefe (1976), Quirk *et al* (1990), Markus *et al* (1994), Gothard *et al* (2001), Puryear *et al* (2006)].

Quirk *et al* (1990) ran experiments in an open cylinder with the lights off, and found that the majority of the place fields are unaffected. This does however depend on whether the rat was placed in the enclosure with the lights on (LDL) or off (DL). They identified 3 types of cells: "persistent/nonpersistent" (which were unaffected by the LDL condition, but fired differently in the DL condition; 11 out of 28 cells), "always persistent" (unaffected by either condition; 8 cells), "never persistent" (showed altered firing patterns in both dark conditions; 3 cells). Only 4 cells ceased to fire completely in the dark, illustrating a small proportion of cells that crucially depend on visual information.

In contrast, fewer cells retain a field in the dark on a radial maze, as opposed to an open-field apparatus. A study by Markus *et al* (1994) found that only 29/87 cells have a field in both light and dark conditions. Additionally, 45/87 cells became quiescent in the dark and 13/87 only had a field in this condition. The authors described fields in the dark to be "less specific and less reliable". Although they do not describe it in these

terms, this is equivalent to some cells having larger fields and/or remapping [see also Puryear *et al* (2006)]. Furthermore, they note that fields with higher information content and selectivity (*i.e.* smaller/tighter fields) are the ones that are most affected by the darkness trials.

Thus, it appears that place fields are more visually influenced in restrictive environments that constrain the rat to a linear path. In support of this conclusion, Gothard *et al* (2001) found that the influence of landmarks (a moving start box from which the rat initiated runs on a linear track) is significantly more persistent in the dark. In their study, the cells were aligned with the start box for a considerably longer span of the track than they were under normal light conditions, when the rat can use a multitude of visual cues for orienting itself. Unfortunately, this study does not compare individual cells across light and dark conditions.

Evidence that visual information is not crucial for place cell activity comes from rats that are blind from birth [Save *et al* (1998), see also Poucet *et al* (2003) for a review of relevant behaviour literature]. Save and colleagues found fully functional place cells which, rather than firing when the rat is first introduced in the environment, required the rat to first make contact with one of the objects therein. In order to reliably establish the position of place fields away from landmarks, rats had to use motion-related information and, since this strategy is prone to cumulative errors, they were forced to make more contact with landmark objects as compared with sighted rats in order to recalibrate their positional information. Remarkably, the place fields did not cluster around the landmarks, but covered the environment in a similar fashion to that seen in sighted rats.

Paz-Villagrán *et al* (2002) found functional place cells in rats with visual cortex lesions, but unlike in normal or early blind rats, these cells made less efficient use of objects placed in the environment as anchors for their place fields. Unlike in normal rats, a rotation of the objects placed inside the environment, along its borders, almost always failed to induce a matching rotation in the place fields. Instead, place fields in the lesioned rats remained stable in the room frame, indicating that the rats were able to use other cues, possibly olfactory or auditory ones to maintain their reference.

2.6.2   Cue Control

A crucial determinant for classifying place cells as spatially selective has been the observation that they are governed by a large and varied selection of environmental landmarks/cues. The rat experiences these cues via a variety of senses comprising vision, audition, touch and smell. These landmarks/cues can belong to the environment and thus can be directly explored by the rat (local cues) or they can be part of the larger reference frame of the experimental room (distal cues). The relative influence that such cues have over place cell activity is briefly summarised in this section.

In a classic experiment, O'Keefe and Conway (1978) trained animals in a T-maze enclosed by curtains in which they placed 4 objects to serve as orientation landmarks. This type of environment gives the experimenter control over the availability of visual cues. The animal was trained to choose one arm of the maze to obtain a reward. When the position of the objects was rigidly rotated, place fields followed these cues. Removal of some combination of the cues did not alter the location of the place fields, and established that 2 cues were sufficient for a correct representation of the environment.

This seminal article established several avenues in investigating cue control over place cell activity: distal versus local cues, cue rotation, cue removal, and cue mismatch (*i.e.* creating a conflict between 2 particular sets of cues by, for instance, double rotation or scrambling).

It is now generally accepted that rotating a salient cue (such as a polarising card) causes all simultaneously recorded place and head direction cells to follow this rotation [Muller and Kubie (1987), Knierim *et al* (1995), Hetherington and Shapiro (1997), Fenton *et al* (2000)]. This holds provided that the rat has not learned that such cues are unstable, either due to seeing the cue card being moved or provided that the cue rotation was not too large [Knierim *et al* (1995), Jeffrey (1997), Jeffrey and O'Keefe (1999), Rotenberg and Muller (1997), Bures *et al* (1997), Goodridge and Taube (1995)]. However, removal of this salient cue card does not disrupt place field activity, indicative of the fact that place cells are highly flexible in their use of cues and/or navigational strategies.

Furthermore, the influence of cues on place fields is task dependent. Markus *et al* (1995) have shown that when the rat performs two tasks in the same environment (random foraging and directed searching for food), place fields remap and become more directional between the two types of behaviour. Zinyuk *et al* (2000) also showed that putting in conflict distal versus local cues is very disruptive for the spatial firing of place cells in the case of rats trained to randomly forage for food but has little effect on rats that are solving a place-preference navigational task. Lenck-Santini *et al* (2002) expanded this experiment to several navigational tasks and combined it with hidden and visible rotations of cues. The authors found a strong interaction between task type and the responses of place cells to cue rotations.

Cressant and colleagues [Cressant *et al* (1997), Cressant *et al* (1999)] investigated the importance of cue position within the environment. They found this to be the case provided the objects where placed by the side of the environment rather than towards the centre. A possible interpretation for this is that, when in the middle of the environment, objects can be perceived in a multitude of configurations based on the relative position of the rat, and thus are deemed "too computationally expensive" to be used as orientation landmarks. In contrast, objects on the periphery of the environment generally maintain their relative locations within the visual field of the rat, irrespective of its position.

Another avenue for investigating the influence of various cues on place field spatial selectivity relies on disturbing the absolute spatial relationship between landmarks. Fenton *et al* (2000) moved two salient cue cards located within the environment closer together or further apart, causing a topological distortion of the place cell representation of the environment. Shapiro *et al* (1997), Tanila *et al* (1997), Knierim (2002) and Renaudineau *et al* (2007) distorted by rotation, scrambling, or removal the relationship between "proximal cues" (located in the environmental enclosure) and "distal cues" (located outside it, usually on the curtains). This line of studies showed that individual cells could respond to either type of cues by either becoming silent, rotating with the distal cues, rotating with the proximal cues, remaining fixed in the laboratory frame or remapping the environment. Importantly, simultaneously recorded cells responded discordantly to the manipulations [but see Fenton *et al* (2000)].

A translation of the experimental enclosure within the recording room [Knierim and Rao (2003), Siegel *et al* (2007)] reveals that place cells maintain their firing with respect to the enclosure, ignoring the distal landmarks (although rotation of distal landmarks causes place field to rotate, showing that they are not necessarily ignored by the rat).

In conclusion, place cells are able to encode both the relative configuration of local and distal cues as well as their individual characteristics in a flexible manner that can best be described as "opportunistic". Current evidence has not provided a definite answer to the question of whether there is a hierarchical use of environmental cues (*e.g.* configuration>distal>local). Furthermore, it appears that experience and behaviour (*i.e.* the task that the rat is performing) also play an important role in determining how the rat uses available sensory information for navigation [Etienne *et al* (1993), Markus *et al* (1995), Zinyuk *et al* (2000), Lenck-Santini *et al* (2002)].

2.6.3   Environment geometry and frame of reference

O'Keefe and Burgess (1996) used a box of changing shape and size (*i.e.* 2 squares, one double the size of the other, and 2 rectangles with the small side equal to the side of the small rectangle and the large side equal to the side of the large rectangle) to test the effect that environment geometry has on place fields. They found that the field size and location was influenced by its distance from two or more walls of the box but also to the walls of the room, rather than by the shape of the box [see also Muller and Kubie (1987), Lever *et al* (2002), Huxter *et al* (2003), Fenton *et al* (2008)]. Their results were supported by those of Gothard *et al* (1996b), who also found cells anchored to the laboratory framework in a task in which the rat shuttled from an ever-moving start box to two goal objects.

Further experiments by Gothard and colleagues [Gothard *et al* (1996a), Gothard *et al* (2001), see also Redish *et al* (2000), Rosenweig *et al* (2003)] showed that place cells can have different preferred frames of reference. The rat was trained to run on a linear

track between 2 reward locations: one in an ever-moving start box and another one fixed at the end of the track. They found that place fields closer to the box shifted in constant relation to it (*i.e.* there were tied to it) and place cells with fields at the fixed end stayed fixed with respect to the room and the goal location. A number of cells were influenced by both, proportionally to the distance of their place field from each goal location.

This result can be interpreted in several ways. The authors propose that the environment is viewed in two frameworks, one related to the box and one to the room. Alternatively, there could be a single map in which two landmarks (box and fixed goal location) both exert an influence proportional to their distance from the place field. Conceptually, these interpretations fall under the discussion of the previous section that investigated the relative influence of different cues on place cell activity. A different interpretation is that the animal is using both a path integration strategy, which would account for the place fields that maintain a constant relationship to the box, and an external sensory strategy which permits the correction between the mismatch of the start location and fixed goal one, thus accounting for the cells that maintain a constant relationship to the laboratory framework [see also Etienne *et al* (2004) for a behaviour study supporting this idea]. Section 2.6.8 will discuss at length this interplay of path integration-based and exteroceptive cue based navigation.

2.6.4   Olfactory, tactile and auditory cues

The input to place cells from sensory modalities other than the visual has not been studied as extensively [see Wiener (1996) for a review].

Evidence that olfactory and tactile cues can be used to establish place fields comes from the blind rat study of Save *et al* (1998) discussed before. The rats had to use olfactory and tactile cues placed in the environment in order to orient themselves. These could then be integrated with interoceptive cues, resulting in a completely normal place map. Save *et al* (2000) also found that, in a cue-deprived environment,

cleaning of the apparatus floor, which results in a neutralization of olfactory cues, causes place field instability under both light and dark conditions.

A large body of behavioural studies showed that rats can use a range olfactory cues [their own, conspecific or another scent (vanilla, almond *etc*)] to guide navigation both in light and dark conditions [Lavenex and Schenk (1995), Lavenex and Schenk (1998), Maaswinkel and Whishaw (1999), Wallace *et al* (2002)]. Interestingly, it appears that olfaction is dominant in young rats but is gradually superseded by vision and other sensory modalities in adult rats [Rossier and Schenk (2003), Maaswinkel and Whishaw (1999)].

Auditory and tactile were also shown to be able to influence place cells but their precise role and individual importance has been even less investigated [Rossier *et al* (2000), Sakurai (1994), O'Keefe and Conway (1978) also used a buzzer/fan, which can be considered auditory cues, as part of their cues in the study]. Thus rats deprived of both vision and audition during adulthood [Hill and Best (1981)], which are forced to use only local cues (olfactory and tactile), possess normal place fields. Rossier *et al* (2000) found that, while auditory cues are not sufficient on their own to guide navigation, they can support it in conjunction with other sensory modalities.

Idiothetic cues

2.6.5 Vestibular input

The vestibular system is responsible for registering acceleration due to gravitational and inertial forces due to movement. However, this system is "multisensory" since, as early as the level of the second synapse, its inputs converge with the optokinetic and proprioceptive ones. Thus, pure behaviour experiments fail to reveal the exact interplay of stimuli that elicit vestibular responses and their relative influence on place cell activity [see Wiener *et al* (2002), Wallace *et al* (2008) for reviews]. This section will review the work on the postulated vestibular inputs to place cell activity.

Sharp and colleagues [Sharp *et al* (1995): place cells, Blair and Sharp (1996), Zugaro *et al* (2000), Zugaro *et al* (2002): head direction cells; see also Wiener *et al* (1995), Jeffery *et al* (1997), Jeffrey and O'Keefe (1999)] rotated either the walls or the floor of the enclosure independently at a fast or low speed (*i.e.* either above or below the acceleration threshold detectable by the vestibular system) in light and dark. Slow rotations result in the fields rotating with the enclosure relative to the laboratory frame, consistent with the rat being unaware that it was displaced. In contrast, fields retained their position relative to the laboratory frame during fast rotations, suggesting that the vestibular input was sufficient for signalling that the environment did not change and updating the rat's position relative to it. In these experiments, however, the rat is free to move, thus the effect of motor signals or optic flow cannot be separated.

Another line of evidence comes from lesion studies. Bilateral labyrinthectomised rats are unable to locate the correct reward arm (whose position was fixed in room coordinates, but otherwise unmarked) in a radial maze following random apparatus rotations [Matthews *et al* (1989)]. Their performance is only moderately improved by the addition of visual cues. At the level of place cells, such lesions result, in the long term, in severe disruption of location-specific firing [Russell *et al* (2003), see also Stackman *et al* (2002) for transient lesions], namely place fields become larger, less coherent and unstable even over periods of few minutes. Furthermore, they disrupt the rhythmicity and lower the frequency of the hippocampal theta rhythm [Russell *et al* (2006)]. Similar effects are observed in head direction cells in various brain areas [see Taube (2007) for a review].

Conversely, electrical stimulation of the medial vestibular nucleus results in increased CA1 cells firing rates in a current intensity dependent manner in urethane-anaesthetized rats [Horii *et al* (2004)]. There is also evidence that vestibular lesions/stimulation have neurochemical effects on the hippocampus [Zheng *et al* (2001), Horii *et al* (1994)].

2.6.6 Optic flow

Lu and Bilkey (2009) allowed the rat to shuttle on a linear track whose walls were decorated with either horizontal or vertical gratings, the latter allowing for enhanced optic flow stimulation. They found that increased optic flow in the vertical grating condition resulted in smaller place fields but similar firing rates. In a converse experiment (also discussed at length in the following section), Terrazas *et al* (2005), found that reduced rates of optic flow resulted in place field increases.

In the study discussed in section 2.6.5, Sharp *et al* (1995) found that rapidly moving the vertically grated walls of their environment, while the rat was within it, did not cause the place fields to rotate accordingly (with one exception), *i.e.* visual motion alone was not sufficient to convince the animal it had moved. However, in conjunction with corroborating vestibular input (floor rotation in the same direction) it was very effective in causing the place cells to remap.

Taken together, this small body of evidence suggests that while optic flow input is available to the hippocampus, its role is in itself insufficient for remapping and/or can be overshadowed by other sensory modalities.

2.6.7 Self motion signals

Few studies have investigated the effect of locomotion on place cell activity. This is because impairing locomotion usually results in silencing place fields.

Foster *et al* (1989) have shown that tightly restraining the rat in a towel while passively translating it resulted in the silencing of place cells. In contrast, light restrain did not seem to disrupt place cell activity. Gavrilov *et al* (1998) and Dayawansa *et al* (2006) used robots to passively translate restrained rats and observed reduced but spatially selective place cell activity. The latter study also allowed the rat to selectively locomote on a treadmill, whilst being restrained by a harness and translated, and found that a large proportion of the place cells were only active during locomotion.

Lu and Bilkey (2009) showed that lightly restraining a rat on a cart while shuttling him back and forth on a linear track caused 60-75% of the cells to become silent and generally shift their firing location (results not quantified). They also found that the residual out-of-field firing rate and sparsity of cells was higher, while information content was lower, than during active locomotion. In a similar experiment on a circular track, Song *et al* (2005) also found that 80% of place cells partially remapped during passive translation (while the remaining 20% maintained their spatial firing across passive translation/active locomotion session) and that their information content was reduced. Theta LFP features were preserved in this experiment.

Passive translation on a cart also severely disrupts the activity of head direction cells in the postsubiculum and anterodorsal thalamic nucleus in both light and dark conditions [Stackman *et al* (2003)]. When the rat was allowed to locomote to a novel environment via a connecting tunnel, the orientation of head direction cells varied, on average, by 17 degs (lights on) and 30 degs (lights off). In contrast, after passive translation through the tunnel, cells shifted by about 70 degs in both lighting conditions. Furthermore, active locomotion, as opposed to passive rotation, increases firing rates in the anterodorsal thalamic head direction cells [Zugaro *et al* (2001)].

Terrazas *et al* (2005) performed an experiment in which the rat was passively driven around in a car on a circular track or was stationary and the environment was rotated around it in order to simulate pseudo-motion. The first condition is designed to eliminate ambulatory signals and the latter further eliminates vestibular self-motion signals. In each condition, the place cell firing rates were reduced, place field sizes increased and consequently information contents [Skaggs *et al* (1993)] were also reduced by about ~0.5 bits in each condition, while phase precession slopes were proportionally shallower. Furthermore, they observed remapping when the movement condition was changed. These results were interpreted as indicative of the fact that the hippocampus is strongly driven by path integration and that self-motion signals are the principal determinant of the scale at which the hippocampal activity changes with location.

Behavioural experiments, the majority of which have been carried out in invertebrates, corroborate the importance of proprioception in path-integration based navigation

[reviewed by Wallace *et al* (2008)]. Interestingly, altering the length of the leg of the Saharan desert ant [Wittlinger *et al* (2006)] results in misestimating the distance to the nest. However, direct evidence that step-counting is an essential part of distance estimation has not to date been replicated in rats, due to experimental difficulties.

"Space clamping experiments", where the rat was kept in one place in relation to the room reference framework and which were designed to minimize visual motion, translational movement and vestibular acceleration, revealed robust and spatially selective place cell firing [Bures *et al* (1997), Czurkó *et al* (1999), Hirase *et al* (1999)]. However, a caveat in these experiments is that the rat could demonstrably make use of distal room cues [cells were directional in the running wheel and its rotation caused a change in firing rate in Czurkó *et al* (1999), Hirase *et al* (1999)].

Taken together, the above results provide a strong indication that self-motion is an important component of place cell's spatial selectivity and that the proprioceptive system and motor command play a more vital role than visual or vestibular sensory information. The major drawback of these studies is that, in order to control for sensory inputs, they severely restrain the rat's behaviour.

2.6.8   *Idiothetic versus exteroceptive cues: which is preferred?*

As the conjoint influence of exteroceptive and idiothetic cues over place cell activity gains experimental support, one question that arises is which of the two is dominant.

One line of enquiry is based on constructing connected visually identical enclosures, which the rat could only distinguish based on self-motion information. Sharp *et al* (1990) have shown that most place cells maintain the same firing field when an asymmetrical environment (*i.e.* a cylinder with a cue card) is made symmetrical (by introducing another cue card 180 degs away from the initial one), although a very small percentage did remap. The authors suggest that rats make use self-motion signals to disambiguate their location in the modified environment which presents two identical views, one facing each cue card.

Skaggs and McNaughton (1998), Tanila *et al* (1999), Fuhs *et al* (2005) and Paz-Villagrán *et al* (2006) have expanded on this idea by using cleverly designed connected, identical environments that were only distinguishable if the rat kept track of its movements, but obtained somewhat different results. To reconcile the results of these studies several factors need to be accounted for, such as the site of recording [Tanila *et al* (1999) recorded mainly from CA3], experience in the environment, whether the rat is free to explore both enclosures and light/cue availability. Skaggs and McNaughton (1998) found partial remapping in 50% of the cells in naïve rats that were only rewarded in one enclosure at a time. Using the same type of apparatus, Fuhs *et al* (2005) found no remapping across enclosures in rats that had 16-23 days of experience and were confined to one box (using a door). However, if the two boxes were pitted 180 degs against each other, by rotating each one by 90 degs, complete remapping ensued. Based on this manipulation, Fuhs and colleagues concluded that it is the angular and not the linear component of path integration that supports accurate discrimination between identical enclosures. These results were confirmed by Paz-Villagrán *et al* (2006) in a circular environment divided into 3 communicating but not simultaneously observable sectors, two of which were identical and a 3rd, distinct one, provided the only means of disambiguation. The authors found that almost all the cells were either unique to one sector or, if they had several fields, these were completely remapped across sectors. In addition, as a control, rotation of the enclosure resulted in a coherent and matching rotation of the fields, indicating that distal cues were not used for disambiguation.

To summarise, self-motion information is sufficient to signal to the rat that it is in a different environmental enclosure, even if this is not visually distinguishable from other enclosures. Consequently, place cells remap across enclosures.

Bures *et al* (1997) found that "space clamping", achieved by a counterbalancing movement of the environment so that the rat was always confined to the same location in the laboratory framework, causes place fields to disappear and not return for up to 1 hour or more. This is indication that the place cells cannot reconcile severe conflict between exteroceptive and idiothetic inputs.

In a less extreme paradigm, Knierim *et al* (1998) have shown that when the mismatch between two sources of information (cue card and/or apparatus rotation) was small (45 degs) both place and head direction cells followed the visual landmarks, while during large mismatches (180 degs), place cells remapped while head direction cells usually followed the idiothetic input.

The results of experiments based on creating a conflict between visual and vestibular inputs (generally derived from rotating the rat) are not in perfect agreement [see Knierim *et al* (1998) for detailed discussion]. However, this can be explained by methodological factors concerning the salience and learned stability of the cues, and experience in the environment [see section 2.6.2]. A tentative conclusion is a generalization of previous findings, namely that, place cells make a flexible and opportunistic use of available information, not only across various exteroceptive sources but also across idiothetic vs. exteroceptive sources. This is supported by behavioural experiments showing that hamsters can be conditioned to rely on idiothetic information [Etienne *et al* (1993)] and that mice have an hierarchical preference for various navigational strategies, based on both types of cues [Alyan and Jander (1994)]. This latter study indicates a preference for distal visual cues, path integration and directional orientation to the source of light and proximal cues, in this order, as navigational references. Furthermore, it shows that such preferences are relative and their usage is highly adaptive depending on their reliability.

2.6.9 Conclusion of section

The previous section summarized the effects of sensory modalities on place cells spatial selectivity. Multiple factors, both exteroceptive and interoceptive, have been show to affect place cells and their spatial selectivity. However, little of the evidence presented so far can provide a definite answer as to what combination of the two navigational strategies (landmark control and path integration) the place cells use in the face of the multiple inputs they can choose from.

2.7   LFP and theta rhythm

The experimental evidence investigating the relationship between place cell activity and the theta rhythm [see section 1.8], in particular the phenomenon of phase precession, is briefly summarised below. It is beyond the scope of this chapter to investigate the functional relevance of this mechanism to memory consolidation [see Buzsáki (2005) for a detailed discussion of this topic] and the importance of theta to place cell activity during sleep.

2.7.1   Phase precession

O'Keefe and Recce (1993) first observed, in a linear track task, that as the rat entered the place field, the first spike of CA1/CA3 principal neurons always occurred near the positive peak of the local theta LFP, and that bursts of subsequent spikes tended to occur at progressively earlier phases of subsequent theta cycles.

Several other observations were made about the nature of phase precession. First, the amount of precession varied across cells but never exceeded 360 degs. Second, the first spike always seemed to occur at the same phase of the theta cycle, indicating a preferred onset firing phase. Third, the phase of firing correlated better with position than with any other variable, such as time since entry into the field.

Skaggs *et al* (1996) and Huxter *et al* (2008) extended these findings to 2D environments and confirmed that they are not a result of stereotyped behaviour associated with the linear track. Recent studies [Maurer *et al* (2006), Ego-Stengel and Wilson (2007)] showed that some CA1 inhibitory interneurons also exhibit phase precession.

Skaggs *et al* (1996) and Yamaguchi *et al* (2002) also noted that phase precession appears to accelerate in the later portions of the field and that there is also much more variability in the firing phase as the rat exits the field, suggesting that there is a nonlinear relationship between phase and position.

Harris *et al* (2002) showed that phase precession characterises both spatial and nonspatial tasks (running-wheel and REM sleep) and that there is a significant linear correlation between firing rate and the phase of firing (*n.b.* this might be the result of both firing rate and phase correlating with position on the linear track). Based on this, they suggested that the two variables were not independent but the result of the same phenomenon (membrane depolarisation). Mehta *et al* (2002) reported similar results and also noticed a difference in the correlation of firing phase with distance for spikes occurring early and late in the theta cycle.

In contrast with these results, Huxter *et al* (2003) demonstrated that the rate and phase codes are independent and that firing rate codes for additional variables, such as speed.

Zugaro *et al* (2005) temporary silenced pyramidal neurons and reset the hippocampal theta phase via an electric shock to the fibers of the ventral hippocampal commissure. When the place cells resumed firing they did so at the correct (reset) theta phase, *i.e.* precession continued as if nothing had happened. This result suggests that the precession effect might by determined by the input to the place cells, presumably from the entorhinal cortex, where grid cells have also been shown to phase precess [Hafting *et al* (2008)] rather than their internal dynamics [see also Maurer *et al* (2005), Geisler *et al* (2007)].

Several computational models have been proposed to account for the origin and the functional relevance of phase precession [see Maurer and McNaughton (2007) for a recent review]. One of the major setbacks for these models has been that replicating 360 degrees phase precession is not computationally straightforward [*i.e.* it is rarely an emergent property of the model, rather it requires several constraints to be imposed in order to be achieved, if at all]. Recently, Schmidt *et al* (2009) have shed some light on the issue by showing that phase precession on any given run through the field is usually less than 360 deg (most frequently ~180 deg, but showing a large degree of variability which they could not account for by taking into account single-trial properties such as speed or firing rate). The full 360 deg of precession appears to be the result of pooling individual trials.

2.7.2   *Other correlates of theta*

The frequency and amplitude of theta have been shown to correlate with the animal's speed of movement [McNaughton *et al* (1983), Czurkó *et al* (1999), Maurer *et al* (2005), Terrazas *et al* (2005)]. This relationship also holds for theta power in CA1 [Montgomery *et al* (2009)]. However, recent studies have shown that this relationship is secondary to the correlation of theta power and frequency with the behavioural task that the rat is performing [see Montgomery *et al* (2009) and Jeewajee *et al* (2007) for discussion].

2.8   Rationale for experimental design

This thesis investigates the effects of self-motion on place cell activity. For this, we use a linear track with a movable treadmill as a floor. This treadmill can be moved at varying speeds as the rat shuttles back and forth between the ends of the linear track for a food reward. The effect of the moving treadmill is that the rat is unable to reliably keep track of the distance it has travelled relative to the laboratory frame based solely on self-motion information. If the rat is running with the treadmill, it will arrive at the end of the track faster than it expects, while if it is running against the treadmill, it will have to run longer to get to the end. The rat will also experience faster/slower optic flow.

If motor efference copy or optic flow provide a direct input for place cells to use in spatial coding, it is expected that the place fields will be shifted with the direction of the moving treadmill.

This paradigm is a novel way of directly targeting the self-motion inputs that the hippocampus might integrate with less disruption to behaviour than in previous studies (which involved restraining and passive translations). The behavioural regime involved in this experiment is highly similar to that of freely moving rats, thus allowing the disambiguation of possible confounders (*i.e.* the influence of locomotion on theta, the influence of restrain on vestibular inputs, *etc*). By using a linear track set-up in which

the animal is constrained to almost one-dimensional trajectories and in which place cells are unidirectional, angular movement contribution to vestibular input is also minimised.

To test the extent to which specific place cells are affected by external visual cues we preformed the simple manipulation of switching off the lights, while keeping everything else constant. If place cells are particularly visual, their fields should be substantially disrupted by darkness. If they are controlled by other sensory modalities, there should be no change. Assuming that cells which persist in the darkness condition are able to perform path integration, there should be a slight shift in their position relative to the lights on condition the further their fields are away from a local cue, such as the end walls, as this is a navigational strategy prone to cumulative error.

The behaviour of the cells in the dark can be used as a predictor for their response during the moving treadmill experiments. If a cell is deemed to be very visual, it is unlikely that the moving treadmill will have a great effect on it, or that the magnitude of this effect will be as great as the magnitude of the effect in a cell which is "less visual".

To avoid confounding factors, such as olfactory cues or some mechanical variable related to the treadmill's movement, the treadmill is very slowly moving in all the baseline trials with a speed of 0.2-0.3 m/min. This ensures that the floor of the environment travels markedly during the course of the recording session, thus displacing any olfactory cues. Although I was unable to find literature pertaining to the lowest speed that the rat might perceive, such low speeds are probably below its detection threshold (based on comparing training stationary and baseline moving trials and finding no obvious difference in the animal's behaviour).

While auditory cues cannot be removed, the noise level in the recording room was large enough to be perceived as similar along the entire track. The air conditioning machine, situated along and above the track, was left on during all experiments. The recording system, which is also noisy, is situated at the west end of the track. In case that it had a noticeable effect during darkness trials, this should result in west end proximal fields being more spatially accurate than east end proximal ones.

3 General Methods

3.1 Subjects

Ten adults male Lister Hooded rats are included in this study. Prior to training and between experimental sessions, rats were individually housed in a holding room where lights were set to a 12h/12h light/dark cycle that started with lights on at 12:00. Water and food were provided ad lib prior to surgery. After recovery from surgery, rats were food restricted to up to 85% of their free-feeding weight and their weight and health was monitored daily. All rats were allowed to gain a minimum of 3 grams per week as time progressed and as they acquired the experimental task.

3.2 Experimental room

All training and experiments were carried out in a room measuring 4.81 x 2.35 meters. The room was air-conditioned and its temperature was controlled to match that of the animal housing room.

Room lights were kept on while the animal was inside but not performing any task. During training and experiments, the room lights were switched off and illumination was provided by a 25 watt lamp directed towards the ceiling, situated on a shelf in the North-East corner of the room. During dark trials, all light sources were removed, including switching off the recording equipment monitors and obscuring equipment indicator lights. During such trials, the rat was observed using an infrared monocular scope [Yukon Advanced Optics].

The experimental apparatus consisted of a linear track [length: 254 cm, width: 10cm, floor height 70cm] set within an elongated grey wooden rectangular enclosure 14cm wide, 25cm high and 200cm long. The floor of the track consisted of a motorized grey suede leather treadmill that could move in both directions at various speeds. In front of each end wall of the enclosure, a piece of slightly darker grey cardboard was wedged to create an acute corner and was fixed in place with surgical tape. The cardboard end walls were wedged either left or right during training on the task, and their position was altered randomly and frequently during each training trial (one change approximately every 2.5 minutes). The purpose of this was to reduce the rat's bias towards turning in the same direction at the end of the track. Once the task was acquired the wedge walls were fixed in place and their position was not changed. While this design was only partly successful, it did contribute to training the rat not to turn 100% in the same direction during future experiments.

Food cups [blue Eppendorf 50ml tube lids], used when the animal was rewarded, were attached to each cardboard wall with Bluetack.

The linear track was placed in the middle of the room, directly below an infrared tracking camera. It was oriented along the long axis of the room from East to West (see Figure 3.1).

The room contained numerous salient visual cues and no attempt was made to obscure any of these cues from the rat's view. However, as walls bordered the track, objects below the level of these walls were invisible to the rat while it ran along the track, unless it stopped and peered over the walls.
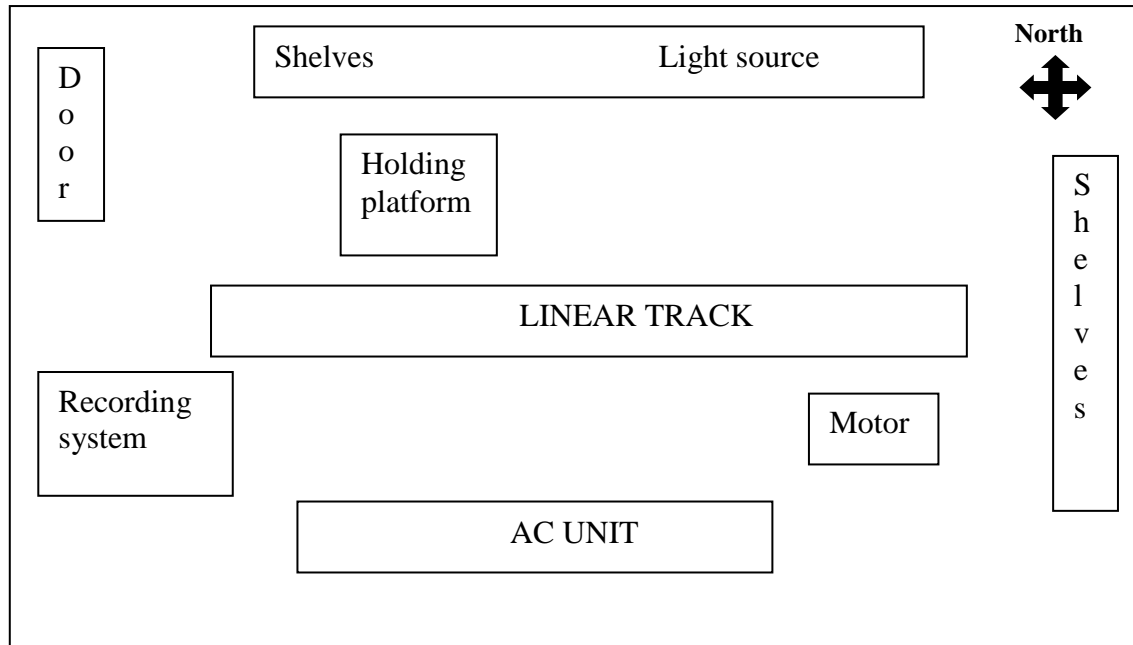
Figure 3.1 Schema of the experimental room.

The recording equipment was situated at the West end of the linear track, and the audio sound monitor of the recording system was left on at all times. During experiments, the same oscilloscope channel was kept on. This was necessary in order to insure that nothing went wrong with the recording, such as spurious DC noise or hardware malfunctioning. The recording equipment also generated audible white noise. The air conditioning unit, which was situated up on the wall along the South side of the track generated audible noise, and hence was kept on at all times. The treadmill motor, which did not generate any audible noise, was placed on the floor at the East end of the linear track.

A day of training, screening or recording always commenced with the animal being placed in the room on a holding platform, situated next to the experimental apparatus (on the North side, next to its middle). The holding platform consisted of a 40 x 40 box with 2 cm high walls, positioned on a high bar stool and covered in sawdust. The animal was connected to the recording system via a long flexible lead and allowed to rest for 30 minutes before any manipulation commenced. Its behaviour was not restricted in any way. The same holding platform was used to allow the animal to rest between manipulations.

3.3 Implant and recording equipment

Extracellular electrophysial activity was recorded using a "poor lady" 16 channel microdrive which allowed accurate electrode positioning within the brain [see figure 3.2].
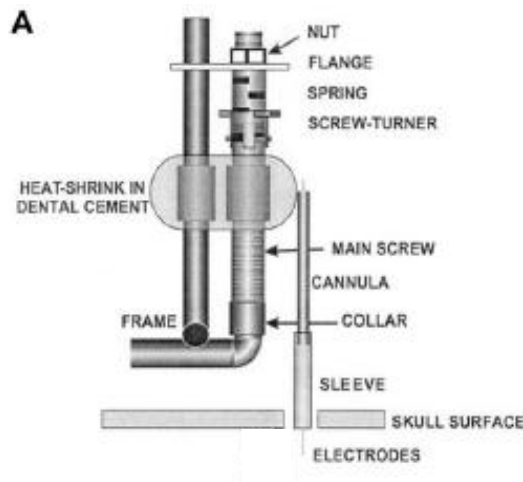
Figure 3.2 Schema of a poor lady microdrive.

Recording electrodes were made out of 17 μM diameter, H-ML insulated, platinum-iridium fine wire [California Fine Wire]. Four strands of wire were twisted together at a pitch of 3 turns/mm to form a tetrode. The upper ends of the strands remained untwisted, were stripped of insulation and then wrapped to the microdrive posts, each electrode being connected to a single recording channel. Silver paint was used to generate good electrical contact and the whole set-up was then fixed in position using commercially available nail varnish. The twisted part of the tetrode was loaded into the microdrive canula and cut to size, so that it protruded no more than 7 mm below the drive. These protruding ends of the tetrodes were glued together with Superglue for added strength and to ensure that the tips will span, as much as possible, the hippocampal medio-lateral axis at the same depth level. The tips of the tetrodes were re-cut with precision surgical scissors to ensure their ends followed a rhomboidal pattern separated by no more than the diameter of the wire. This allows, in general, for all the 4 electrodes to record a similar signal but with different amplitudes. This can be used to isolate single cells via a process similar to telecommunication triangulation.

Before implantation, the tips of the electrodes were plated with platinum solution [Merrill and Ainsworth (1972)] in order to deposit platinum black onto them and reduce their electrical resistance to 300-500 kOhms. This process also allowed to verify that no short-circuits occurred across electrodes.

Each microdrive was loaded with 3 tetrodes, resulting in 12 recording channels.

Additionally, a similar but less twisted tetrode was made out of 100 μM diameter, H-ML insulated, stainless steel wire [California Fine Wire]. At one end, this tetrode was stripped of insulation and, at the other, the tips of the electrodes were cut 300 μM apart in depth [*i.e.* spanning 1.2 mm] using fine precision surgical scissors and fixed in place with Superglue. This tetrode was used for LFP recording from the contralateral hippocampus and was not loaded into the microdrive. Its free ends were only connected to the microdrive once it had been implanted. For clarity, these will be referred to as the LFP electrodes.

After implant, the electrodes were connected to op-amp headstages, providing 16 channels of unity gain buffered amplification [which increases current drive without affecting voltage] for the electrical brain activity picked up by both the tetrodes and the LFP electrodes. The headstage was connected with lightweight hearing wire (3 m long) to a 100x gain preamplifier, which was in turn connected with ribbon cable to the recording equipment. Additionally, the headstage included tracking LEDs, which were attached to the head of the rat using a fixed plastic screw and a crocodile clip and were used for position tracking.

3.4   Recording techniques

The recording system allowed for simultaneous recording of extracellular action potentials (spikes) from individual neurons (units), local field potential (LFP) and 2D animal position. Each of these measures is individually time stamped, at different rates, but they were recombined offline on a PC workstation.

3.4.1 Position tracking

Two clusters of infrared LEDs are mounted on a copper wire frame that is part of the headstage. There are 2 clusters, a big 4 white LED one, positioned in front of the rat (above the level of its eyes) and a small 2 blue LED one, positioned behind the rat's head (above its neck). Their position was adjusted at the beginning of each recording day so that the clusters are aligned to the rat's body axis and the large cluster is located above and between its eyes. The distance between the two lights clusters was 5 cm. The design of this lights set-up allows the system to distinguish accurately between the two lights clusters and use this information to infer the head direction of the rat in space.

An infrared camera attached to the ceiling of the room, positioned above the middle of the linear track, was used to monitor the position of the two LED clusters. This allows tracking of the rat's position at a rate of 50 Hz. The camera resolution was 768 x 547 pixels and the optical zoom was adjusted to cover the entire length of the linear track. This resulted in a tracking resolution of 300 pixels/metre.

3.4.2 Unit recording

For each implant, there were 12 independent extracellular electrophysiological recording channels. Unit data was recorded differentially, *i.e.* for each individual channel from each tetrode, a single channel from a different tetrode was used as a reference channel, and its signal was subtracted from the active one. This allows for the removal of common noise (usually generated by the animal moving, chewing or other artefacts). The reference channel was generally selected as a channel that had little activity to avoid spurious addition of unit activity to the original channel.

Signals from the channels were digitalised at 48 kHz, bandpass filtered at 500-6700kHz, and digitally amplified 10000-40000x, resulting in an amplitude trace of +/-95-200 microvolts. A threshold rule was used to determine the occurrence of a spike, with the threshold usually set to 60-80% of the maximum signal amplitude. When the

threshold was exceeded on any channel of a tetrode, a spike was recorded as a 1ms voltage trace (0.2 ms before and 0.8 ms after the trigger) from all 4 channels of a tetrode simultaneously. This typically captures the entire waveform of a pyramidal spike. Furthermore, digital noise rejection based on template matching to a square wave was used to reject artefacts, which were redirected to a separate file.

3.4.3 LFP recording

The LFP signal was digitalised at 250 kHz, and lowpass filtered at 500 Hz and additionally notch filtered at 50 Hz [to minimize 50Hz mains interference]. This signal was digitally amplified 4000-15000 times resulting in amplitudes of +/-350-900 microvolts.

Four LFP signals were available, one from each LFP electrode implanted in the contralateral hippocampus. As the LFP electrodes were positioned 300 μM in depth apart, their theta profile was used to accurately determine their depth based on the particular properties of the hippocampal LFP. The hippocampal LFP theta phase undergoes a 180 degs inversion from the level of CA1 to that of the fissure. Based on this and the relative positions of the 4 LFP wires, the channel that was deemed closest in depth to the fissure was selected for recording.

Furthermore, a local LFP from each tetrode was used to determine the depth of the electrodes in the CA1 layer by observing the relationship between the LFP amplitude and coincident ripples while the animal was quietly sitting on the holding platform. However, as the 17 μM wire generally records a very noisy and low amplitude local field potential signal, due to its small diameter, this signal was not used for LFP analysis.

3.5   Surgery

Rats were anaesthetised with Isoflurane/N_2O/O_2 and given injections of an antibiotic 2.5% solution of enrofloxacin, 0.25 ml, subcutaneous] and an analgesic [0.3 mg/ml Buprenorphine hydrochloride, 0.01 ml, intramuscular]. The top of their head was shaven. When breathing was stable under anaesthetic [usually within 20 mins] the rat was placed in the stereotax framework and its head was disinfected with a topical antiseptic (Betadine). An incision was made along the midline of the skull, and the skin and muscles removed to expose the skull. A small burr drill was used to tap 6 holes in the skull in which stainless steel screws were inserted [one screw was attached to a piece of insulated wire and would subsequently serve as an electrical ground].

A trephine drill was used to make 2 trepanations, one above each hippocampus at the following implant coordinates with respect to bregma: 3.3-3.8 mm posterior, 2.7-3.3 mm lateral right for the tetrodes implant and 3.8-4.2 mm posterior, 2.5-2.8 mm lateral left for the LFP electrode implants. The dura and pia were removed from both implant sites and the surface of the brain was kept moist with sterile saline solution until the implant was completed.

The LFP electrodes were implanted at a depth of 3mm using a micromanipulator. Care was taken to ensure that all electrodes were placed perpendicular to brain surface and went in without bending. Once the electrodes were in place, the brain was covered with sterile Vaseline and a layer of dental cement was used to set them permanently in place. After the LFP implant was stable, the microdrive was implanted in the contralateral site and the electrodes were lowered to a depth of 1.5 mm inside the brain, their protective sleeve was lowered to the level of the brain and covered with sterile Vaseline. The feet and the sleeve of the microdrive were attached to the stainless steel screws with dental cement and the edges of the wound were further sealed with cement.

With the microdrive implant firmly in place, the loose ends of the LFP electrodes were wired to the microdrive posts, the ground wire was soldered to the microdrive and protective plastic screws were set in cement around both implants for protection.

The rat was then taken off anaesthetic, the implant site was further cleaned with Betadine and topical powered antibiotic mixture was applied [2% chlortetracycline hydrochloride + 1% benzocaine]. A piece of surgical tape was placed around the implant to prevent the animal from scratching it and promote fast healing. The rat received a further 0.01 ml injection of 0.3 mg/ml Buprenorphine hydrochloride intramuscularly and was placed in heated cage to recover.

Once the rat fully recovered [usually within 15-30 minutes], it was placed back in its home cage where food and water were provided ad lib. The rat was allowed to recover for 1 week after surgery, and received further doses of the antibiotic [0.5% of 2.5% solution of enrofloxacin with its drinking water for 5 days post surgery] and 0.1 ml of 0.3 mg/ml Buprenorphine hydrochloride mixed with jelly was provided daily for at least 3 days after surgery.

3.6   Cell screening

Cell screening is the process by which the tetrodes are lowered dorsoventarlly from their initial implant position to the CA1 layer, in search of place cells. This process preceded all experimental manipulations.

Over the first few days of screening, the electrodes were lowered up to 200 μM a day until hippocampal electrophysiological markers were observed. The first marker was the 200 Hz ripple oscillations in the unit recording trace, which are present in the CA1 layer while the animal is sleeping or standing still. Once these were observed, the advancement of the electrode was slowed to 25 μM steps and usually not more than 50 μM per day, until place cell unit activity was found. Upon finding place cells, the rat was returned to its home cage until the following day to ensure that the tetrodes were stable, as it is quite common for the electrodes to keep travelling through the brain after being moved due to tissue drag. Recordings only commenced once the tetrodes were deemed stable (*i.e.* recorded activity was similar across successive days). No recordings were made on days that the electrodes were moved.

Place cells were identified by their characteristic burst firing (complex spiking) and by the presence of a place field on the holding platform. No cell waveform criteria were used at this stage. If a cell did not exhibit bursting or appear to have a clearly defined place field on the platform (*i.e.* it was firing at a very high rate consistently across the platform environment) it was deemed to be an interneuron.

Because place cells are not always active across different environments, the rat was placed on the linear track and cells were further checked for place fields. If no cells with fields on the track were found, the electrodes were advanced.

Electrode movement was halted once all tetrodes passed the CA1 layer. This is identifiable by the relationship between ripples and the local LFP recorded from each tetrode (even if the quality of the signal is poor). Once ripples coincide with a large off- scale, negative deflection in the local LFP, the "bottom" of the CA1 pyramidal layer has been reached. In a few cases, the electrodes were lowered up to a further 1 mm in an attempt to reach CA3. However, limited data were recorded from this region and CA3 cells are not analysed in this thesis.

3.7   Training

Once the animal recovered after surgery, the rat was gradually food deprived up to 85% of its full weight and cell screening and training began concomitantly. The animal was taken from its home cage to the recording room and placed on the holding platform. It was connected to the recording equipment and allowed to rest on the platform for 30 minutes before any manipulation was carried out.

The first behavioural task consisted of the rat learning to shuttle back and forth between the ends of the linear track, where it was rewarded with a small grain of boiled rice to which commercial sweetener had been added. On the first two days of training, the rat was placed in the track and allowed to explore freely for a few 10-15 minutes sessions (the exact amount dependent on the rat). These sessions were interspersed with similar duration resting sessions on the holding platform. During the

first day of training, the moving treadmill was stationary. Starting on the 2nd day, the treadmill was set to move at very low speed (0.33 cm/sec). Such trials will be referred to as baselines. No behavioural effects associated with stress or fear were observed as a result of the treadmill moving at this speed. Rather, the rat's performance in the shuttling task improved, consistent with it having already experienced this environment. Therefore, this treadmill speed was considered "undetectable" for the rat and suitable as a baseline condition.

As the rat acquired the shuttling task on the linear track, this was expanded to include moving treadmill trials. This was introduced gradually over several days (usually 1 week) with speeds usually being increased 0.5 m/min between successive 10 minutes trials. This was necessary as the rat had to learn to adjust its position when it reached the end walls. In particular, it took time for the rat to learn to step backwards constantly when it reached the end towards which the treadmill was moving. The amount of training varied each day, depending on the rat's performance.

To balance training experience, the moving treadmill training was performed in both directions (treadmill moving eastwards and westwards) and was interspersed with baseline trials. The experimenter ensured that, during training, the rat was exposed to equal amounts of baselines, track moving eastward and track moving westward trials.

As the rat acquired the behavioural task in all conditions, its running speed increased and so did the frequency of runs (shuttles form one end to the other of the track). As discussed previously, rats tend to have a very strong turning bias on this task. To alleviate this, during training, the wedged cardboard end walls were turned left and right randomly and frequently (at a rate of one turn approximately every 2.5 minutes). This created an acute angle to the adjacent lateral wall which pointed left or right respectively. To a certain extent, this induced the rat to explore the acute angle and vary its turning behaviour at the end of the track. As the rat acquired the full task and maximum treadmill speeds reached the desired level, the end wedged walls were fixed in place and remained so during all subsequent trials.

However, the success of this manipulation was limited in forcing the rat to adopt a balanced turning pattern and a strong bias remained. Because of this, the duration of

the trials was reduced to 7.5 minutes, which ensured that even if a rat had a very strong turning bias, the wires that attached the headstage to the recording equipment could take the twist while allowing the rat to span the entire length of the linear track comfortably. After or during any training trial, if the headstage wires had twisted too much, the rat was first returned to the holding platform and slowly "untwisted" by the experimenter.

Training was considered complete when the rat learned to shuttle consistently between the ends of the track, and the moving treadmill could be set to a speed as high as 10cm/sec in each direction. Cell screening was adjusted so that placement of the electrodes in CA1 coincided with this point and, if it lagged behind, the rat was subjected to 1-2 more days of "mini" training which consisted of 2 baselines and 2 moving treadmill at 10 cm/s (one in each direction) trials until screening was complete.

As rats acquired the task at different efficiencies, it was not possible to ensure that all rats had received the same amount of training. Typical training lasted 7-10 days for all rats.

3.8   Recording sessions

Once the rat had acquired the task and place cells were found on the linear track the recording session began.

Each recording day began with the rat being placed on the holding platform and allowed to rest for 30 minutes. Afterwards a baseline trial was carried out to allow the experimenter to adjust channel gains optimally for future analysis and to ensure that the rat's behaviour was adequate. These baseline trials were not used for any further analysis.

A recording day consisted of baselines alternating with probe trials. All trials lasted 7.5 minutes and were separated by 12.5 minutes inter-trial intervals, during which the rat was "untwisted", if necessary, and allowed to rest on the holding platform. To ensure

the stability of the recording, at no point was the headstage unhooked and the rat reconnected.

During the inter-trial intervals, the experimenter set up the next trial and no attempt was made to mask any preparations from the view of the rat. These consisted of washing the walls of the linear track with water and adjusting the speed of the moving treadmill. All trials (except the dark probe) were carried out with the room lights off and a small desk lamp on (see section 3.2). During all rest intervals, the room lights were switched on.

All baselines consisted of the treadmill moving at 0.33 cm/sec in a randomly chosen eastward or westward direction. The purposes of this were: 1) to ensure that no olfactory cues associated with the treadmill (which was suede leather and as such unwashable, as there was no cleaning product that the rat would not find noxious) remained stable; 2) to preserve cues that might be generated by the treadmill moving (possible noise from the motor, treadmill vibrations *etc*) across all trials.

The probe trials were: treadmill moving slow (5 cm/sec) in an eastward (es, short for East Slow) or westward (ws) direction, treadmill moving fast (10 cm/sec) in an eastward (ef, short for East Fast) or westward (wf) direction; dark trials (dk), where the room was completely darkened and the track was moving at baseline speeds. The sequence of probe trials was altered in a semi-random fashion across days. Generally, slow or fast trials in the same moving treadmill direction followed each other (separated by an intervening baseline), as it was observed during training that the rat finds this pattern less disruptive. The dark trial was usually performed as a last probe as it was the most complicated to set up.

A typical recording day would follow the pattern: test baseline, baseline, probe es, baseline, probe ef, baseline, probe ws, baseline, probe wf, (baseline), probe dk and baseline. Due to the large number of trials, the rat would sometimes get too satiated or tired and thus lose its determination to shuttle back and forth across the track. If this was the case, the baseline before the dark trial was omitted to ensure comparable behaviour across all trials. The order of the trials was always varied across successive days.

At the beginning of the trial, the rat was placed in the middle of the track, facing eastwards or westwards in a random order, and allowed to shuttle for a few seconds (*i.e.* until it performed at least one run in each direction) before the recording began. This allowed the rat to gauge the speed at which the treadmill was moving and adjust its behaviour accordingly.

For darkness trials, the rat was allowed to shuttle for up to one minute with the room lights on, and for another few runs in complete darkness while the experimenter set-up the recording system. This was done with the purpose of ensuring that the rat was not confused about its location, which might induce cells to remap because of the rat thinking it is in a different environment [see section 2.6.1. for discussion].

Once a full set of manipulations was obtained from a given cell population, the tetrodes were advanced until a new set of place cells [*i.e.* as indicated by the signal from all channels and location of the fields on the track being different from the previous day] was found or until no more place cells could be identified.

3.9   Experimental design

The purpose of the experiment was to assess the influence of the moving treadmill on place cell activity. As place cells on the linear track exhibit directional fields, it was necessary to design the probes so that different treadmill directions are sampled (*i.e.* ones when the treadmill was moving in the preferred direction of cell firing and ones when it moves against this).

To account for any effect that the speed of the treadmill might have, slow (5 cm/sec) and fast (10 cm/sec) probes were added. These speeds were selected based on the observed behaviour of the animal so that any rat could learn to perform the task comfortably. The speeds of the track are small compared with the rat's shuttling speed on the track used here, which can reach up to 2 m/sec. However, the moving treadmill task has proven quite disruptive for rat behaviour as it takes time to learn to move

backwards when reaching the end wall. This is apparent in the length of time it takes the rat to acquire the moving treadmill task at 10 cm/sec. It takes usually about 2-3 days of training for the rat to learn to shuttle back and forth on the linear track at its full running speed and up to a further week to get gradually accustomed to the moving treadmill.

Dark trials were added to disambiguate the effects of visual cues versus moving treadmill on place cell activity. Unfortunately, it was not possible to include a moving treadmill variant of the dark trials, as this was found too disruptive of the rat's behaviour. Thus, all dark trials were conducted at baseline speed.

3.10 Off-line preliminary analysis

Once the data had been acquired, off-line analysis was necessary to identify place cells via spike clustering and to characterise the local LFP recordings. This preliminary analysis was only used during screening to determine the position of the electrodes and whether cells were suitable for inclusion in the present study. Custom designed software available in the O'Keefe laboratory, TINT (Tetrode Interface, Axona) was used for spike clustering, combining position, unit and LFP data, and to calculate momentary speed and direction, as well as basic cell properties.

3.10.1 Position related measures

Position samples were averaged using a boxcar 400ms sliding window. Missing points (due to unusual rat posturing or the headstage cable obscuring the LEDs) were corrected using interpolation between existing samples. Positions were computed based on the tracked locations of the two LED clusters using a weighted average (the rat's position was taken to be a factor of 0.3 from the large cluster situated above and between the eyes of the rat, on the segment uniting the large and small LED clusters).

As place cells on the linear track exhibit directional firing, data were filtered by the direction of rat heading. This was computed from the relative positions of the large and small LED clusters, and interpolated accordingly in the case of missing data points.

Momentary rat speed was estimated from position samples as the distance travelled between two consecutive data points divided by the time interval that separates them. Speeds over 4 m/sec were considered artefactual and positions samples were adjusted accordingly by interpolation. Such artefacts occur when the LED's inadvertently reflect off shiny surfaces, for instance when they touch the walls of the track.

3.10.2 Spike clustering

Spikes from each tetrode were analysed separately using peak-to-peak amplitude plots on each of the 4 electrodes. Given the close proximity of the 4 electrodes tips in each tetrode, spikes from a single cell will be picked up with a similar waveform but different amplitude on each wire. Comparing the relative amplitude of each spike across all 4 electrodes performs, in essence, triangulation of the signal in space, if we assume that the extracellular medium is homogeneous.

Thus, in a scatter plot of multi-cell spike amplitude across any two channels, spikes from the same cell will form distinctive clusters. TINT was used to manually assign cell spikes into single cell cluster, by drawing ellipsoid-approximating polygons disjunctive across all 6 possible projections around each cluster. Further refinement was achieved by using voltage versus amplitude projections. For instance, a particular voltage was chosen where the peak-to-peak amplitude plot on a channel revealed the waveforms were very similar, usually on the ascending phase of the spike. A cross plot of this voltage and the amplitude on the same channel should also follow a cluster pattern, while any stray spikes diverge from the average waveform of the cell. Using clustering based on these 2 types of projections ultimately results in a form of template matching unit isolation.

Once cells were assigned to clusters, a temporal autocorrelation was performed for each cell. A cell was retained if this autocorrelation showed a clear 2 ms refractory period.

During screening and the test trial that initiated each recording day, this clustering procedure was used to adjust channel gains to achieve optimal cluster separation.

3.10.3 Place cell identification

For each cell, firing rate maps were constructed to determine whether the cell had a place field on the linear track. Tracking coordinates were scaled down by a factor of 0.7 to ensure the tracking camera coordinates will fit in TINT's pre-designed 512 x 512 pixels window. This window was then divided into a 64 x 64 grid of bins, each measuring 8 x 8 pixels. Given the tracking resolution of 300 pixels/meter and the 0.7 scaling for TINT, each bin spanned 3.8 x 3.8 cm of the linear track.

For each bin, the cells' firing rate was defined as the number of spikes divided by dwell time. This measure was then boxcar smoothed in a block of 5 x 5 bins centred on the given bin and excluding unvisited bins. As place cells exhibit directional firing on the linear track, separate maps (directional map) were constructed for the rat facing each cardinal direction with a tolerance of +/- 45 degrees. The peak rate of a cell was defined as the rate of the bin with maximal firing. For the purpose of plotting, the rates were autoscaled and colour coded in 5 levels. The bins with maximal firing appear in red, those with 60-80% of peak firing appear yellow, 40-60% green, 20-60% light blue, and less than 20% dark blue. Thus, at this stage the field was defined as a group of contiguous bins with firing rate greater than 20% of the peak rate. Unvisited bins appear white.

Place cells were identified as suitable for further analysis if: 1) they exhibited a clear place field in one or both of the east or west directional maps, 2) their peak firing rate exceeded 1Hz, 3) they fired more than 40 spikes during the entire trial. No further data filtering was used at this stage.

The cell population was considered suitable for recording if at least three place cells with fields on the track fulfilling the above criteria could be identified. If no suitable cells were identified, the electrodes were moved and screening continued.

3.11 Data extraction and analysis

Custom Matlab software was used for analysing the data, except for spike clustering, which was done with TINT (as described above).

3.11.1 Position

Tracking data from the linear track is fraught with environment specific problems. Firstly, as the track is very narrow, it is impossible to avoid a degree of light reflection off the track walls, even though the wall material was selected to be as matte as possible. These problems are apparent when the rat turns at the end of the track and the lights touch the wall. This effect restrains the size of the LED clusters that can be used. Therefore, only 4 LEDs were used for the large cluster. To achieve reliable cluster separation, the small cluster was limited to 2 LEDs. This resulted in the small cluster not being tracked during 5-10% of the trial duration, mainly due to the rat's unusual positioning while eating, turning or rearing.

To achieve an accurate measure of the rat's position in the environment during the entire duration of the trial, the position data was amended as follows. Only the large LED cluster was considered for position indication, as it is reliably tracked during 99% of the duration of the trial. Care was taken to swap back all the confusion points between the large and the small cluster (this was based on interpolating positions and the size of the tracked clusters). Position samples were collapsed on the x-axis, to discount any effect that shining off the track side walls might have played, particularly

when the rat was at the end of the track. Position samples were boxcar averaged in a 400 ms sliding window and missing points were interpolated.

Position samples were scaled by a factor of 0.7 to fit into a 512 x 512 pixels window. This resulted in a resolution of 210 pixels/meter.

3.11.2 Speed

Speed was inferred from the distance between every 3rd adjacent position sample divided by the inter-sample time. This was preferred to every adjacent position sample as it yields a more reliable inter-sample time interval. The sign of speed was positive if the rat was moving eastwards (increasing x values) and negative if the rat was moving westwards (decreasing x values).

As the moving treadmill was in constant motion, the speed data was adjusted to reflect the speed of the rat relative to the moving treadmill. For example, if the treadmill moved eastwards at 10 cm/sec, the tracking camera would overestimate the rat's speed by 10 cm/sec if the rat is moving with the treadmill and would underestimate it by the same amount if the rat is moving against the treadmill. Once speed adjustment took place, speed was converted to absolute values, *i.e.* always positive. All future references to speed will be to the rat's actual speed in absolute spatial coordinates.

3.11.3 Direction

Direction was computed from position data. Namely, as the rat runs on the track in a linear fashion, direction was inferred based on displacement in the x dimension. Direction was only estimated when the rat ran in a linear fashion at a speed greater than 10 cm/sec. This stringent criterion was imposed so that no head turning without rat displacement could be mistakenly considered as forward movement. For simplicity, directional data was only assigned to east or west directions and positions that did not match this criterion were excluded.

3.11.4 Theta rhythm analysis

LFP voltage was bandpass filtered between 4-12 Hz with a Blackman windowed, 125 tap, finite impulse response filter. The Hilbert transform was then used to assign a phase angle to each spike, with 0 degrees phase corresponding to the positive to negative crossing of the theta oscillation. As the LFP is recorded at a 250 Hz sampling rate and position only at 50 Hz, position was 5 times up-sampled before it was matched to a theta phase.

3.11.5 Behavioural data filtering

For further analysis, only data when the rat ran eastward or westward at a speed greater than 10 cm/sec for more than 0.2 seconds were included.

3.11.6 Definition of place fields

Once good behaviour data had been selected, rate maps were constructed by dividing the track into a 128 x 128 bins grid. Each bin measured 4 x 4 pixels or 1.9x1.9 cm. Eastward and westward firing rate maps were constructed as previously described. Peak firing rate was defined as the maximal firing rate.

A place field was defined as a row of contiguous bins in which the firing rate exceeded 20% of the peak firing rate. This criterion was relaxed if there was a single bin where the firing rate dipped below 20% but remained above 10% of peak firing rate and then it exceeded 20% in adjacent bins. One bin-long fields were deemed artefactual and excluded from analysis. All the spikes fired by the cell but not deemed to be part of its field were excluded from further analysis.

In the few cases where a cell had multiple fields in one direction, only the field where maximal firing occurred was used in the analysis, provided that such field was clearly isolated across all trials.

3.11.7 Field measures

For each field the following measures were defined.

The peak firing rate was defined previously and the peak bin was taken to be the bin associated with the peak rate. The size of the field was defined as the number of contiguous bins spanned by the field.

The field centroid (centre of mass) was defined as a function of the dwell time weighted spike distribution. Namely, each position bin belonging to a field was replicated 100 times per 1 Hz of firing rate occurring in this bin, and the mean of this distribution (expressed in bin number) was taken to be the centroid of the field. This measure was used in all subsequent analyses, as it is more robust than the peak bin.

The robust skew of this distribution, defined as (Q(3)+Q(1)-2Q(2))/(Q(3)-Q(1)), where Q(i) stands for ith quantile, was taken to be the field's skew. Unlike the classical definition of skewness, this measure is not only robust to outliers but is also scaled on the [-1,1] interval, where 1 represents extreme right skewness and -1 represents extreme left skewness, which allows meaningful comparison across fields of different cells.

The field size was defined to be the number of bins included in each field, and since positions were collapsed to the x-axis, this is equivalent to the field's length.

Information was computed for each field in terms of bits per spike and bits per second as proposed by Skaggs *et al* (1993):

$$I = \int_x \lambda(x) \log_2 (\lambda(x)/\lambda) \, p(x) \, dx$$

where I is the information rate of the cell in bits per second, x is the spatial location, $p(x)$ is the probability density function of the rat being at location x, $\lambda(x)$ is the mean firing rate when the rat is at location x, and

$$\lambda = \int_x \lambda(x)\, p(x)\, dx$$

is the overall mean firing rate of the cell. Bits per spike information is computed as

I/λ.

The first measure is an indication of the rate at which the cell discharges. The second reflects the spatial specificity of the cell and can be seen as giving an indication of how "grandmother-ish" this is. As such, bits per spike information is related to field size and bits per second information is related to the firing rate of the cell.

For each field, in-field average speed was computed as the average of momentary speeds that the cell exhibited whilst traversing the field. This was calculated after the data was filtered by speed and direction. Such a measure is useful for comparing "behaviour" across different manipulations.

Phase precession was characterised by using a linear-circular plot between the momentary position of the rat (the linear variable) and the phase at which each spike occurred (the circular variable, 0-359 deg range). A method similar to that proposed by Fisher (1993) was used to relate the two variables by a linear relationship, based on the cos distance. Namely, instead of the classical least square fitting, a quantity based on the cos of the residuals was minimised using numerical methods (Matlab fminbind function). The slope of the best fitting line was searched for in an interval of [-360, -0.1 degs/field size]. To ensure that the numerical results don't converge to a local minimum, the procedure was subsequently repeated by dividing the search interval in 4 equal parts. The slope that gave the best fit was then chosen to describe the phase precession relationship. The amount of precession was defined, based on the best fit line, as the difference in phase traversed between the two field edges.

A linear correlation coefficient was computed once phase angles were unwrapped around the best fit line [*i.e.* if the linear distance from the line to any point was greater than +/- 180 degs, the phase of that point was corrected by -/+ 360 degs respectively]. The regression line that fits the unwrapped angles does not always yield a slope similar to that found by the circular-linear fit, and in some cases the fit is so bad that a positive correlation is found [usually for cells that exhibit a strongly nonlinear phase-position relationship, see Yamaguci (2002)].

To ensure that any results reported in this thesis are not spuriously induced by the constraints imposed on the linear-circular fit used to define the precession line, all analyses were also performed with the minimising procedure extended to a search interval of [-720, -0.1 degs/field size]. No difference in results was observed, indicating that precession does not indeed surpass 360 degress.

3.12 Analysis of response to manipulations

For each probe trial, the preceding and subsequent baselines were considered. The effects of probe trials on place field characteristics are quantified by comparing them against those of the adjacent baselines.

Five probe trials were used in this study. Four concern the moving treadmill, which can move either east or west at a slow or fast speed. The fifth manipulation is the darkness probe. These probes will be abbreviated as: ef = eastward fast, es = eastward slow, wf = westward fast, ws = westward slow, dk = darkness.

3.12.1 Data selection criteria

This section describes the criteria used in selecting suitable place fields. These include the standard minimal firing requirements and impose additional constraints regarding place field stability. This latter part stems from the fact that this study is concerned with assessing shifts in the place fields induced by the moving treadmill probes. If a

place field does not behave in a similar fashion across successive baselines, we cannot ascertain whether any observed shift is the predicted effect of the treadmill's action or the consequence of a remapping phenomenon.

Good baseline cells were defined based on minimal firing and stability criteria. Each cell had to fire at least 50 spikes and have a peak rate greater than 1 Hz during all but one baseline recorded during successive trials in one day. Furthermore, its field centroid had to be stable across baselines, namely all pair-wise differences of baseline centroids had to be less than 20 bins (38 cm). This criterion is not met by cells that remap to a different position on the track [*e.g.* the field jumps from one end wall to the other and this is consistent across several trials]. In such cases, baseline centroids were assigned to 2 clusters based on the same distance criterion within cluster [if this was not possible, the field was deemed unstable and excluded from further analysis]. Probes were then only considered within clusters, *i.e.* only if the previous and following baseline were stable [belonged to the same cluster].

For each probe, cells were accepted if their place field was stable across both previous and subsequent baseline trials. As cells tended to fire less during probes, the selection criteria for firing during probes were relaxed and a cell was considered if it fired a minimum of 30 spikes during the probe trial.

3.12.2 General analysis format

Place cells are unidirectional on the linear track and in the rare cases where they fire in both directions the fields are almost never overlapping [Battaglia *et al* (2004)]. Therefore the analysis is done on individual place fields. If a cell fired both when the rat moves eastward and westward, each directional field was separately assigned to the corresponding eastward/westward data set. Results will also sometimes be reported for all fields taken together, irrespective of the cell's preferred direction of firing.

Tables take the general form shown below. The number of fields is the same within column. There are usually 3 tables, one for eastward fields, one for westward fields and one when the previous two sets are merged (all cells). Fields are pooled across rats

and recording days, and care was taken that if a cell was recorded over successive days it was only considered once [on the first day that it was recorded].

Probe type/ Data set	ef	es	wf	ws	dk
Previous baseline	Size "a"	Size "b"	…	…	…
Probe	Size "a"	Size "b"	…	…	…
Following baseline	Size "a"	Size "b"	…	…	…

In general, changes during probes are assessed by taking the difference from the previous baseline (delta probe) and comparing this to the difference between the previous and subsequent baseline trials (delta baselines) as a control. This should distinguish probe-induced effects from inter-baseline variability.

3.13 Histology

Following experimentation, rats were killed by sodium pentobarbitone overdose (Euthatal™, 1ml, i.p.) and immediately perfused. The brains were removed, quick frozen, cut into 40 microns thick sections, stained using cresyl violet, and mounted for inspection. Typical histological results are presented in figure 3.3.
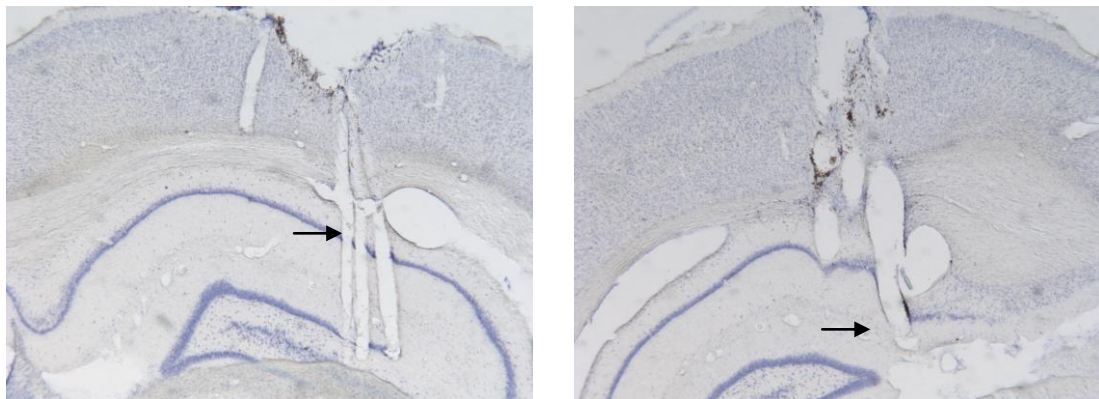
Figure 3.3 Histology results
Tetrode location (left) and LFP electrodes location (right) in two cresyl violet stained sections from one rat. Recording sites are indicated by arrows.

4 Results

This chapter presents the results of the thesis in two sections. The first describes the properties of place fields on the linear track and the second part covers the analysis of the results of the moving treadmill and darkness manipulations.

For each probe trial, the preceding and subsequent trials were used as baselines, as described in chapter 3. The effects of probe trials on place field characteristics are quantified by comparing them against those of the adjacent baselines. As a reminder, 5 probe types are used in this study and they are referred to as follows: moving treadmill probes (ef = eastward fast, es = eastward slow, wf = westward fast, ws = westward slow) and darkness probe (dk).

4.1   Basic field properties

In this section I will describe the basic properties of fields on the linear track during the baseline trials. Data in this section includes all valid eastward and westward fields recorded during baselines, which means a cell generated a data point every time it was included in a probe analysis [*i.e.* an eastward firing cell that was included in both the eastward fast and westward slow analysis will generate 2 points]. Data from each baseline trial prior to probes as well as the probes themselves, shown separately, are provided in chapter 6 [Supplementary Material].

We will see that the field centroids are not distributed evenly on the track, but follow a trimodal distribution. In compensation, the field sizes in the middle of the track are larger than those at the end. This also bears a relationship to the way the rat runs on the

track, with lower speeds at the start and the end of the run and higher speeds in the middle.

4.1.1 Distribution of fields on the linear track

Figure 4.1 shows the centroids of the fields in the eastward and westward direction. Note that the fields are not evenly distributed but their numbers tend to increase towards each end of the track and in the middle.
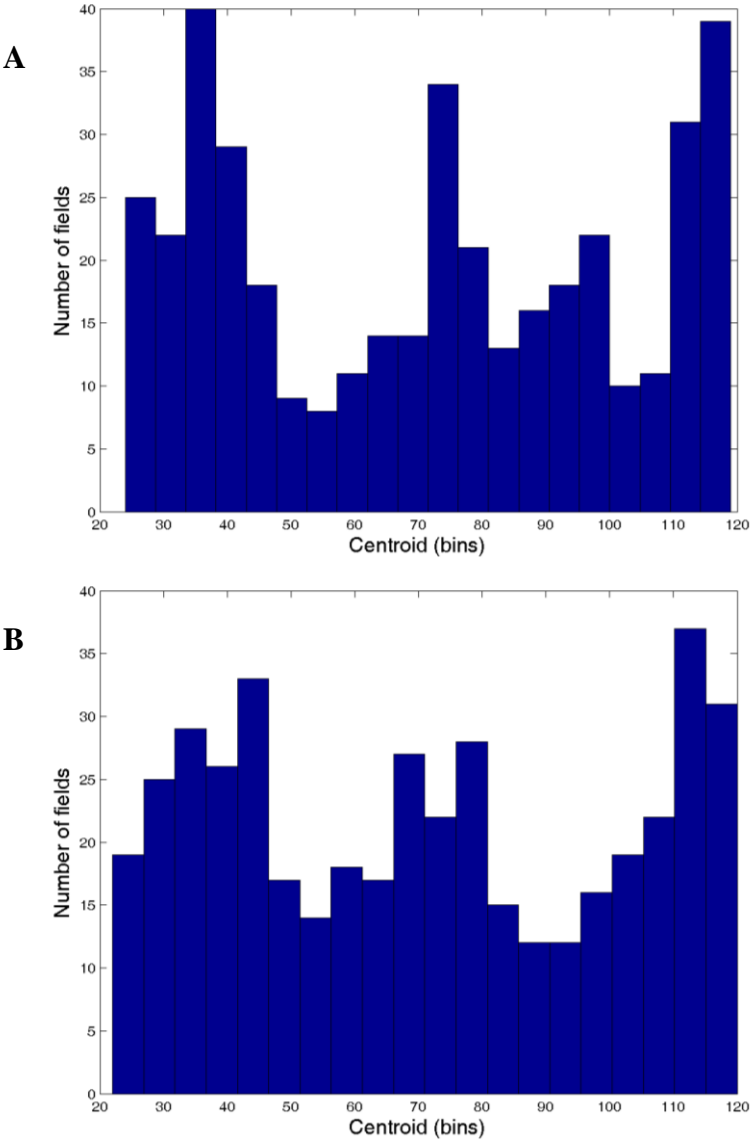
Figure 4.1 Distribution of the fields on the track during baseline trials

for eastward (A) and westward (B) firing cells. Note that for eastward firing cells the rat moves left to right and for westward firing cells the rat moves right to left. The x-axis indicates the centroid of the field, measured in bins. One bin equals 1.9cm. Note that the track spanned bins from 16-124. The y-axis indicates the number of fields.

4.1.2 Comparison and interrelatedness of place field characteristics

Due to the nature of the linear track, a 1-D environment through which the rat runs in a highly stereotypical fashion, various place cell measures that are not mathematically related can exhibit a large degree of correlation. This stands in contrast to open environments, where the rat forages randomly and can generally enter a place field from any direction and at various speeds. Thus, in an open environment, the speed at which the field is traversed bares no relationship with the location of the field in the environment. In contrast, on the linear track, the rat's speed is larger in the middle of the environment and so is field size, inducing a relationship between these two field measures.

4.1.3 Field centroid

As can be seen from Figure 4.2 there is a strong convex relationship between the location of place fields, as represented by their centroids, and their size, with fields in the middle of the track being many times larger than those closer to the end walls [R^2=0.56, F statistic=258.75, $p<10^{-15}$ (eastward firing cells), R^2=0.60, F statistic=327.24, $p<10^{-15}$ (westward firing cells); *n.b.* R^2 values are obtained from quadratic fits and all reported F statistics test the null hypothesis that all regression coefficients other than the constant term are zero]. Furthermore, as shown in Supplementary Table 6.1, the same relationship between **centroid and field size** can be seen regardless of trial type.

As expected, there is also a strong convex relationship between **in-field average speed and centroid**, as the rat runs faster in the middle of the track [R^2=0.56, F statistic=254.80, $p<10^{-15}$ (eastward firing cells), R^2=0.59, F statistic=319.70, $p<10^{-15}$ (westward firing cells)]. Figure 4.3 shows in-field speed plotted versus centroids for baselines. Supplementary Table 6.2 shows that the same relationship holds independently of trial type, but indicates that the strength (*i.e.* R^2) of the quadratic fit is reduced during probe trials (however the relationship remains significant).

The precise differences in running speed between baselines and probes are analysed in detail in Supplementary section 6.1. It is clear that animals run more slowly during probes, but in a similar pattern to baselines. The differences in speed might reflect a greater caution on the moving treadmill during probe trials.

A

B
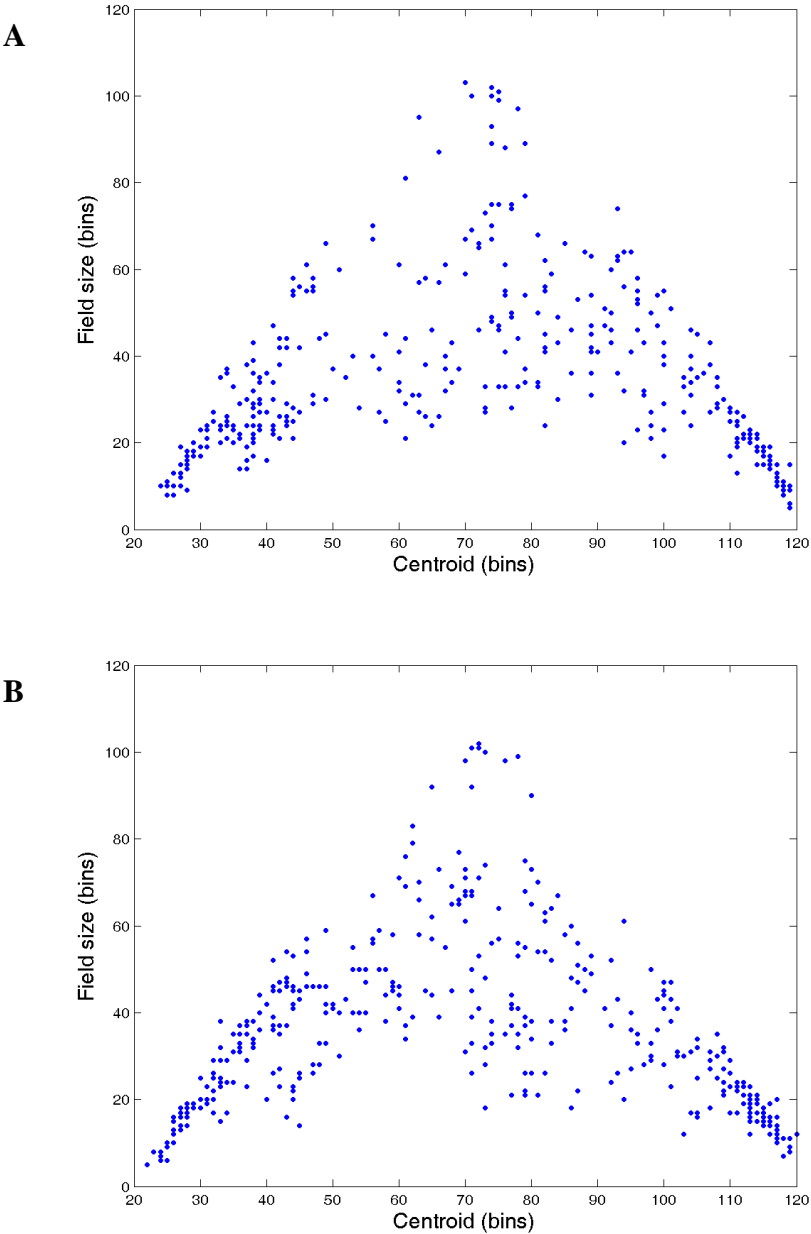
Figure 4.2 Field size vs. field's location on the track in baseline trials

for eastward (A) and westward (B) firing cells. The x-axis indicates the centroid of the field and the y-axis indicates field size, both measured in bins (1 bin= 1.9 cm).
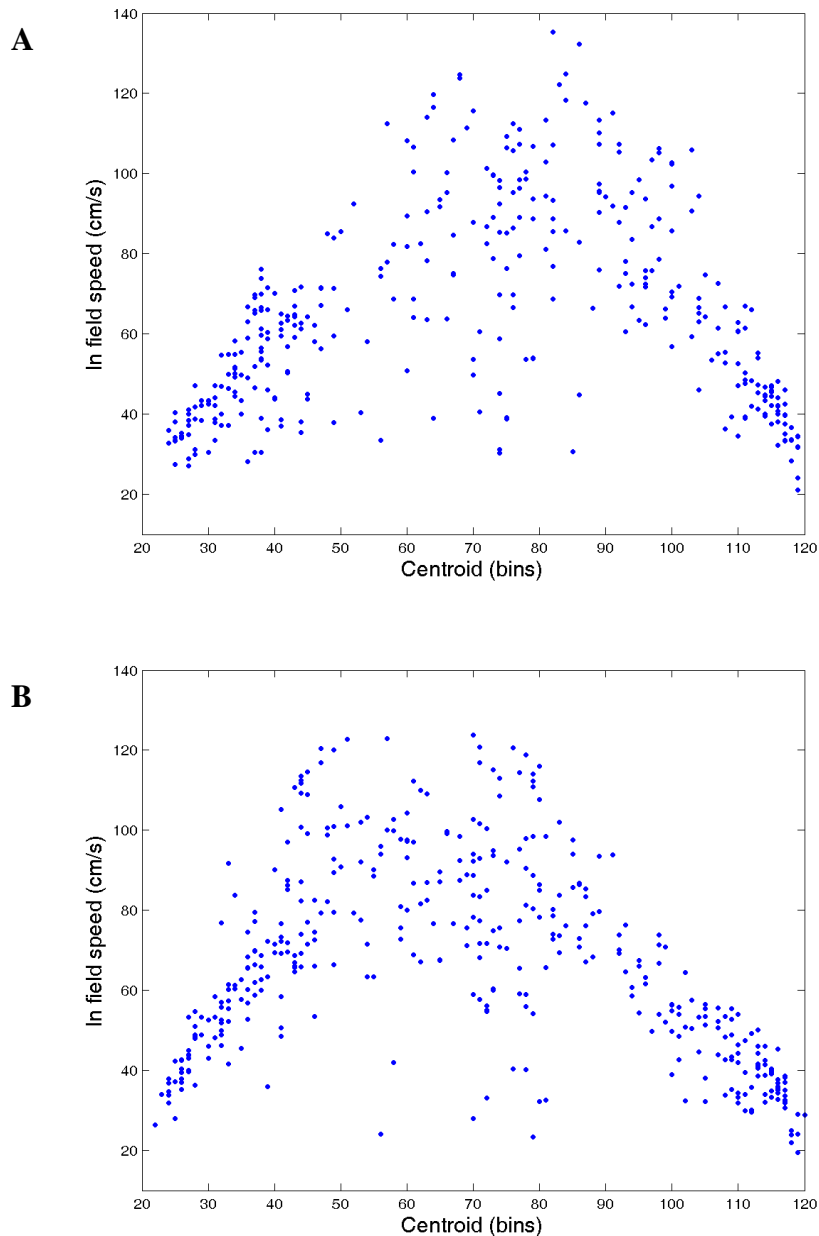
Figure 4.3 In-field average speed vs. field's location on the track during baseline trials for eastward (A) and westward (B) firing cells. The x-axis indicates the centroid of the field, measured in bins. The y-axis indicates the in-field speed, measured in cm/s.

There is also a convex relationship between **centroid and the slope of phase precession** [R^2=0.14, F statistic=32.49 (eastward firing cells), R^2=0.29, F statistic=89.16 (westward firing cells), all $p<10^{-15}$], with cells in the middle of the track exhibiting shallower precession slopes [see figure 4.4]. Supplementary Table 6.3 shows that the same relationship holds independent of trial type.

As will be shown in the next section, this relationship stems from the fact that there is a strong relationship between field size and the slope of phase precession.
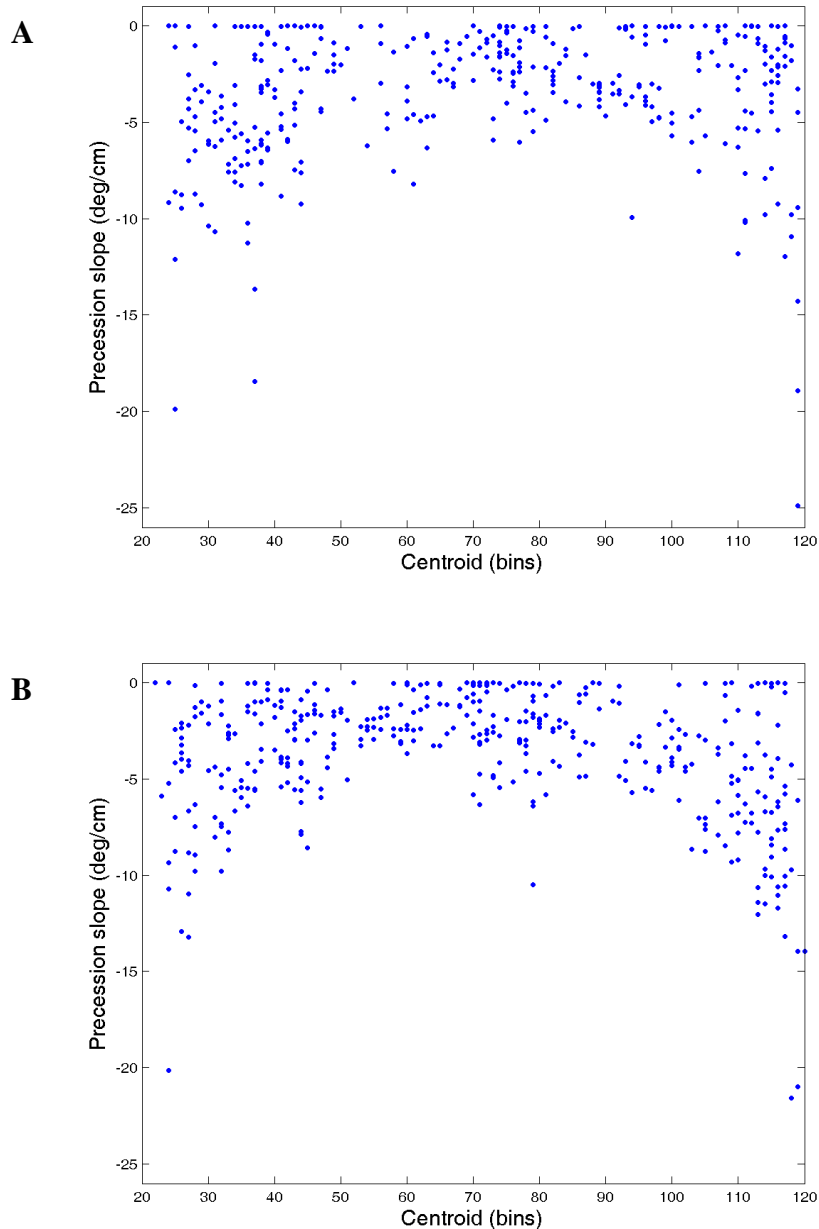
Figure 4.4 Slope of phase precession vs. field's location on the track during baseline trials for eastward (A) and westward (B) firing cells. The x-axis indicates the centroid of the field, measured in bins. The y-axis indicates the slope of the phase precession line, measured in deg/cm.

Field skew and centroid are linearly related [R= -0.39 (eastward firing cells), R= -0.38 (westward firing cells), all p<10^{-15}, see also Supplementary Table 6.4]. Fields closer to the end walls are skewed towards the middle of the track [fields closest to the east end wall are skewed negative and fields closest to the west end wall are skewed positive], while fields in the middle of the track exhibit very little skew, *i.e.* they are symmetrical, as shown in figure 4.5.
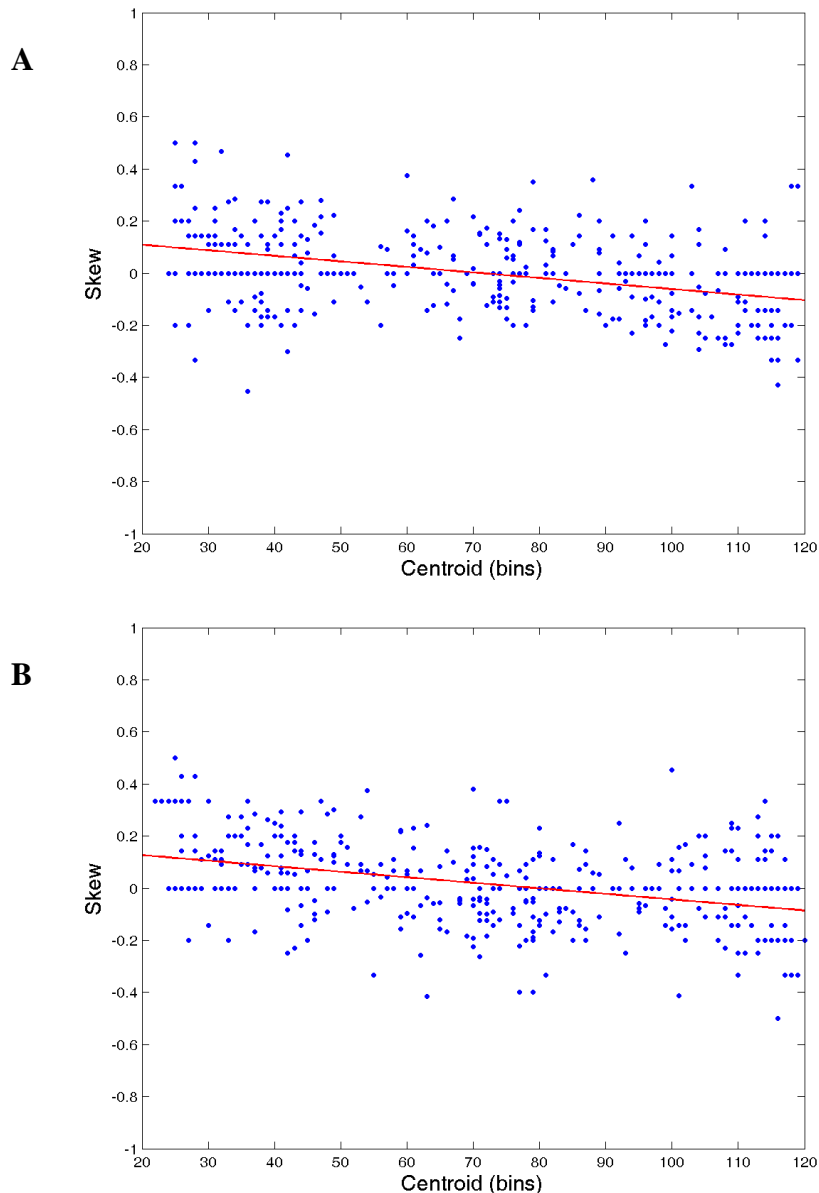
Figure 4.5 Field skew vs. field's location on the track during baseline trials for eastward (A) and westward (B) firing cells. Red line: linear regression line. The x-axis indicates the centroid of the field, measured in bins. The y-axis indicates the skew value, which spans a possible [-1,1] range as discussed in chapter 3.

There is a strong concave relationship between **centroid and bits per spike information** [see Supplementary Table 6.5]. Cells with fields in the middle of the track convey less information than those of cells closer to the end walls. As information in bits per spike is a measure of a cell's spatial specificity, it can be said that cells close to the end walls of the track are more "grandmother-ish". This relationship stems from the computational relationship between bits per spike information and field size and is in good agreement with the fact that fields are larger in the middle of the track.

There was no significant correlation between centroid and peak rate, bits per second information or amount of precession, for either baselines or probes (all p>0.1).

In conclusion, there is a relationship between field position and its size, the speed at which it is traversed, the rate at which it encodes spatial information, and the amount of phase precession it exhibits, as well as its skew. Fields in the middle of the track are larger, are traversed at a higher speed, encode less information, are less skewed and show shallower precession slopes.

4.1.4   Field size

Since both **field size and in-field speed** are related to field centroid ($R^2 > 0.5$), one might expect them to correlate with each other. They do, but with a lower coefficient [R=0.32 (eastward firing cells), R=0.36 (westward firing cells), all $p<10^{-15}$]. These surprisingly low values [see also Supplementary Table 6.6] are due to large fields in the centre of the track, for which the linear relationship breaks down. This stems from the fact that there is an upper limit for the rat's speed, meaning that it is impossible for speed to scale up with the field size indefinitely [see figure 4.6].
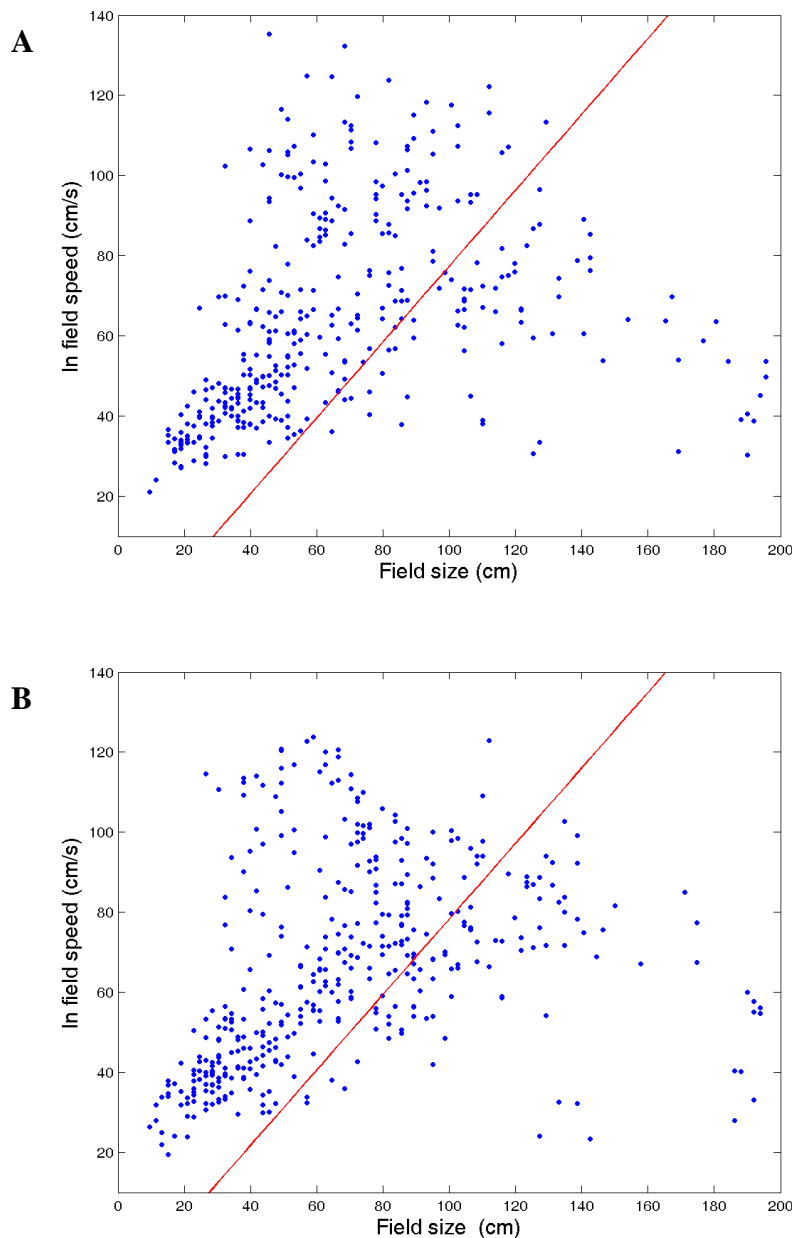
Figure 4.6 Field size vs. in-field average speed during baseline trials

for eastward (A) and westward (B) firing cells. . Red lines: linear fits, minimising perpendicular distance to points. The x-axis indicates the field size, measured in cm. The y-axis indicates in-field speed measured in cm/s.

A similar relationship holds for probes (see figure 4.7) and although weaker in terms of correlation coefficient, it is still highly significant [R=0.14, p=0.004 (eastward firing cells), R=0.16 (westward firing cells), p=0.0005]. This is due to the rat being slower in the probe trials, which is apparent if one compares across panels in figures 4.6 and 4.7. The scatter plots in figure 4.7 are "flatter" [*i.e.* closer to the horizontal axis].
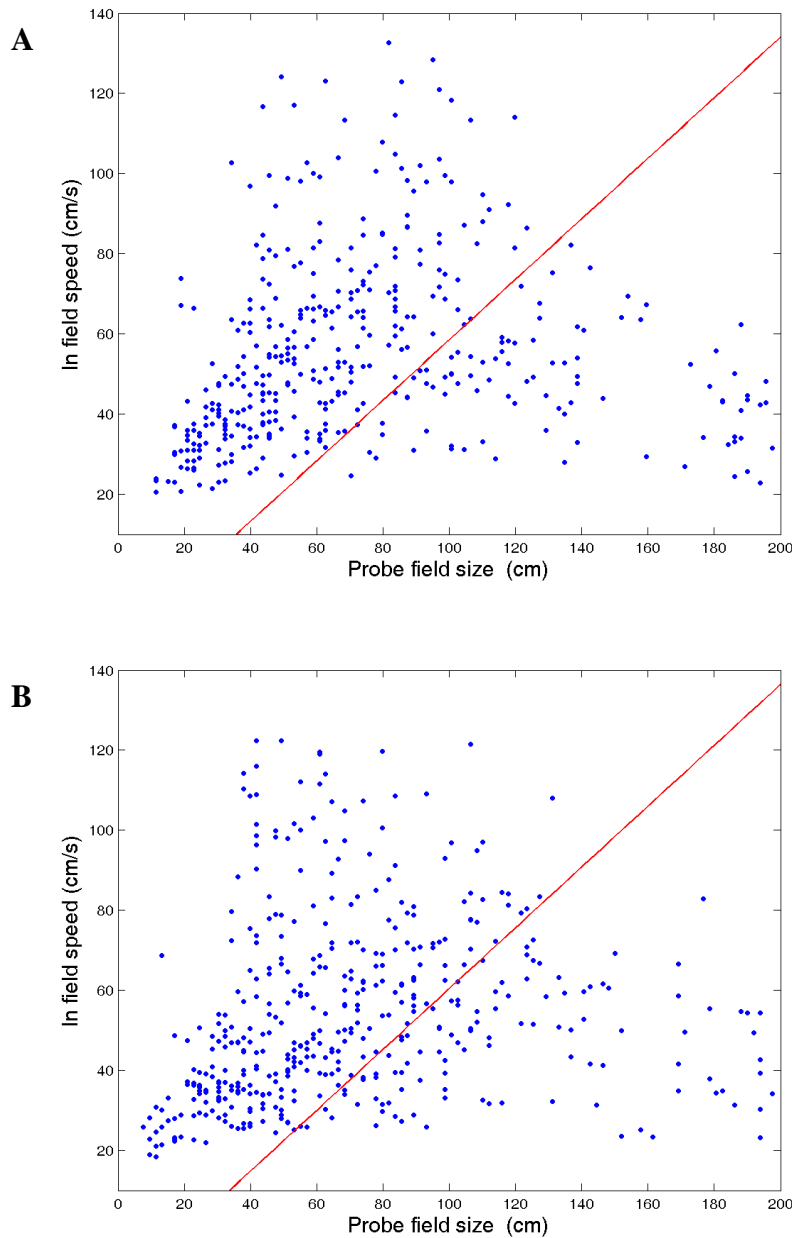
Figure 4.7 Field size vs. in-field average speed in probe trials for eastward (A) and westward (B) firing cells. Red lines: linear fits, minimising perpendicular distance to points. The x-axis indicates the field size, measured in cm. The y-axis indicates in-field speed measured in cm/s.

Field size and the slope of phase precession are strongly inversely correlated [R= -0.47 (eastward firing cells), R= -0.58 (westward firing cells), p<10^{-15}], namely the larger the field the shallower the slope of the precession, as shown in figure 4.8. The relationship holds for all trial types [see Supplementary Table 6.7]
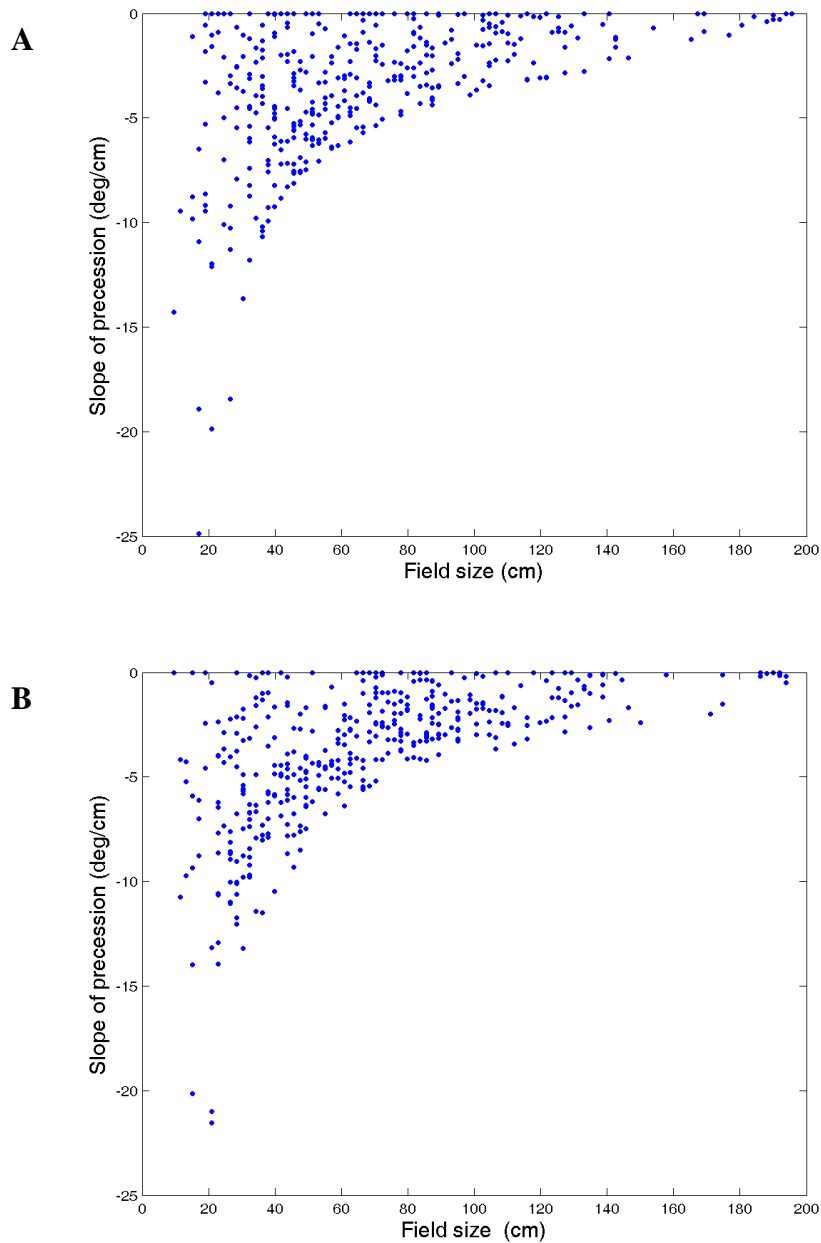
Figure 4.8 Field size vs. slope of phase precession during baseline trials for eastward (A) and westward (B) firing cells. The x-axis indicates the field size, measured in cm. The y-axis indicates slope of phase precession measured in deg/cm.

There is no significant correlation between field size and peak firing rate, skew, bits per second information or amount of precession (all p>0.1). Correlation of field size with bits per spike information is around –0.9 for all cells, as expected.

In summary, field size is related to the speed at which the field is traversed, and this stems from the fact that both variables are related to the position of the field on the track. Moreover, field size is strongly correlated with the slope of phase precession, with larger fields exhibiting a slower precession rate.

4.1.5 Other measures

Peak firing rate is not correlated with any other field characteristic, except bits per second information [R around 0.90] to which it is computationally related. Figure 4.9 illustrates that there is no relationship between the position of the field on the track and its peak firing rate. Figure 4.10 shows precession slope and peak firing rate are not related.
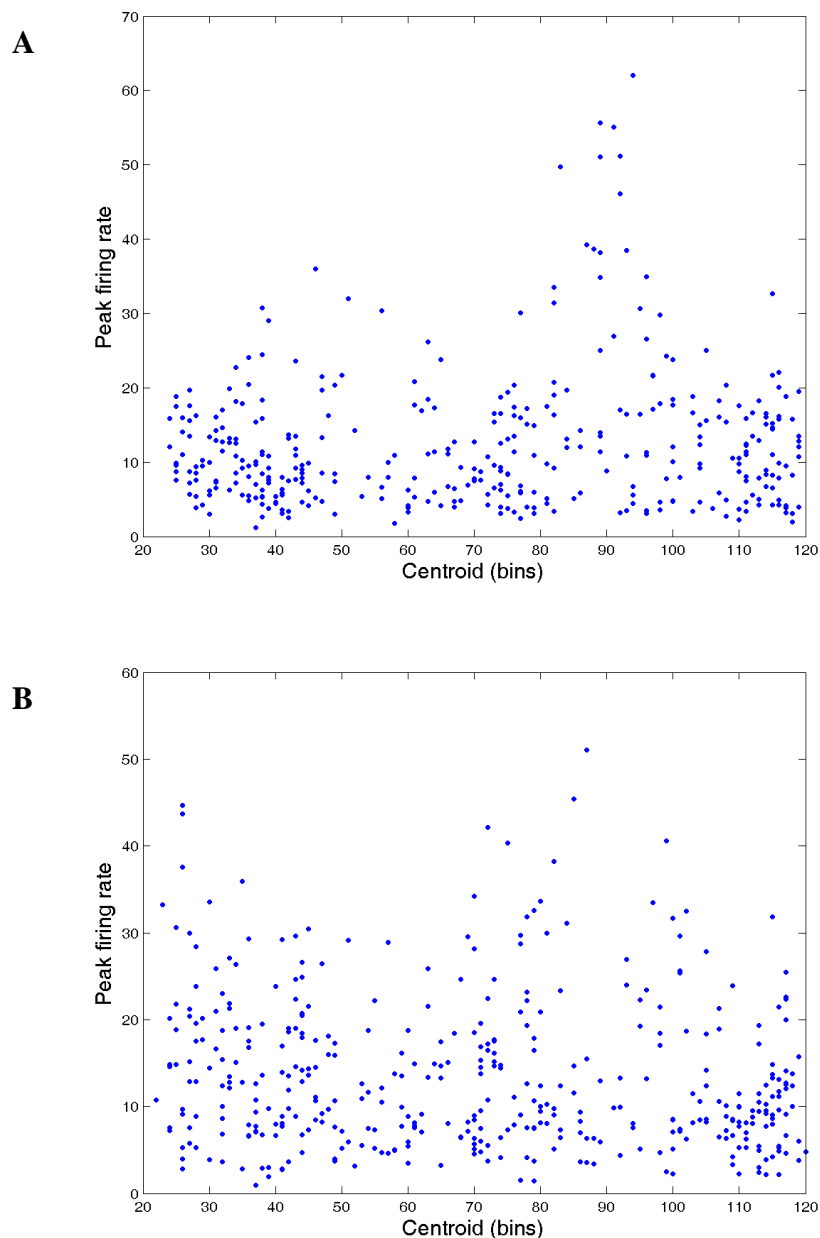
Figure 4.9 Peak firing rate vs. the centroid of fields during baseline trials for eastward (A) and westward (B) firing cells. The x-axis indicates the field centroid, measured in bins. The y-axis indicates peak firing rate measured in Hz.

Figure 4.10 Peak firing rate vs. precession slope during baseline trials for eastward (A) and westward (B) firing cells. The x-axis indicates the slope of precession, measured in deg/cm. The y-axis indicates peak firing rates measured in Hz.
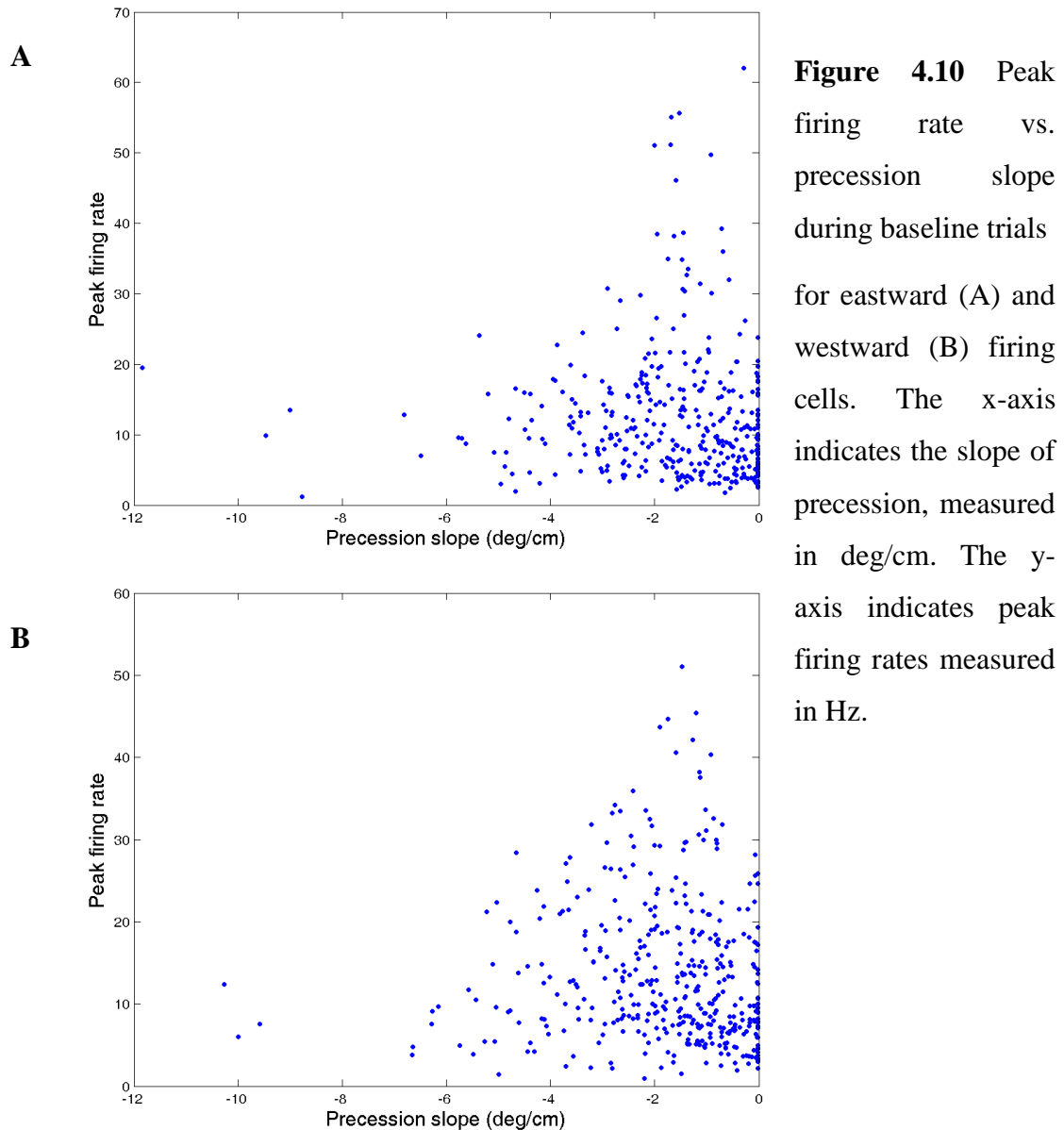
Supplementary section 6.2 analyses in detail changes in peak firing rate across successive trials. There appears to be a reduction in firing rate during probes versus prior baselines as compared to successive baselines, although this is not always significant. Furthermore, changes in peak rate do not correlate with changes in any other field measure.

Field skew is not correlated with in field speed or any information or precession measure. Changes in skew do not correlate with changes in any other measure [results not shown].

Bits per spike information correlates significantly with the slope of precession [R: –0.57 to –0.25, all p<0.01], with shallow precession being associated with little information. This stems from the association between the field size and bits per spike information measures. For the same reason, there is also a small degree of correlation between precession slope and in field average speed, but this is not always significant.

4.1.6   Summary of basic field properties on the linear track

As shown in this section, place field measures are related by the position of the field on the track. Middle fields are larger and less skewed, precess at a slower rate and are traversed at a higher speed. Fields closer to the end walls are smaller and skewed towards the middle of the track, tend to precess at a higher rate and are traversed at a lower speed.

The size of the field is associated with the speed at which it is traversed, and this is because fields in the middle of the track are larger and are traversed at a higher speed. More importantly, field size is strongly correlated with the slope of phase precession, with larger fields precessing more slowly. Furthermore, changes in these measures are related, as explored in section 4.4.1. This relationship also induces a connection between the position of the field on the track and the slope of phase precession.

4.2   Analysis of moving treadmill probes: Cells shift with the treadmill

To investigate the effect of the moving treadmill on field position on the track, differences in field centroid were computed for each probe versus its preceding baseline (**delta probe**) and for successive baselines (**delta baselines**, *i.e.* "subsequent – preceding baseline"). Numerically, this results in negative shifts for any cells whose centroid moves west on the track and positive shifts for any cells that move east when the treadmill is in motion.

Results are reported for all (westward and eastward) cells pooled together. In addition, similar to the previous section, results are reported for cells separated by preferred direction of firing to help identify any effects induced by the cell's directionality.

Figures 4.11 and 4.12 show typical examples of eastward and westward firing fields that shift with the treadmill. In figure 4.11, cell 1 shifts in the direction of treadmill movement in all moving treadmill probes, but more so in the ws and wf probe than the es and ef probes. Cell 2 also shifts in the direction of the treadmill in all moving treadmill probes but the amount of shift is smaller than for cell 1. Cells 1 and 2 also shift more when the treadmill is moving at a fast speed than when it is moving at a slow speed. Cells 3 and 4 provide an example of cells that move in the direction of the treadmill in most probes, but not the wf one. Cell 5 moves with the treadmill in the eastward moving probes (es/ef) but moves against the treadmill in the westward moving probes (ws/wf).

In figure 4.12, cell 1 shifts in the direction of treadmill movement in all moving treadmill probes, but more so in the ws and wf probe than the es and ef probes. Cell 2 shifts in the direction of the treadmill in all probes except es, when it shifts against it. Cell 3 is stationary in all probes except ef, when it moves with the treadmill. Cell 4 is stationary in all probes. Cell 5 shifts westwards irrespective of probe type.
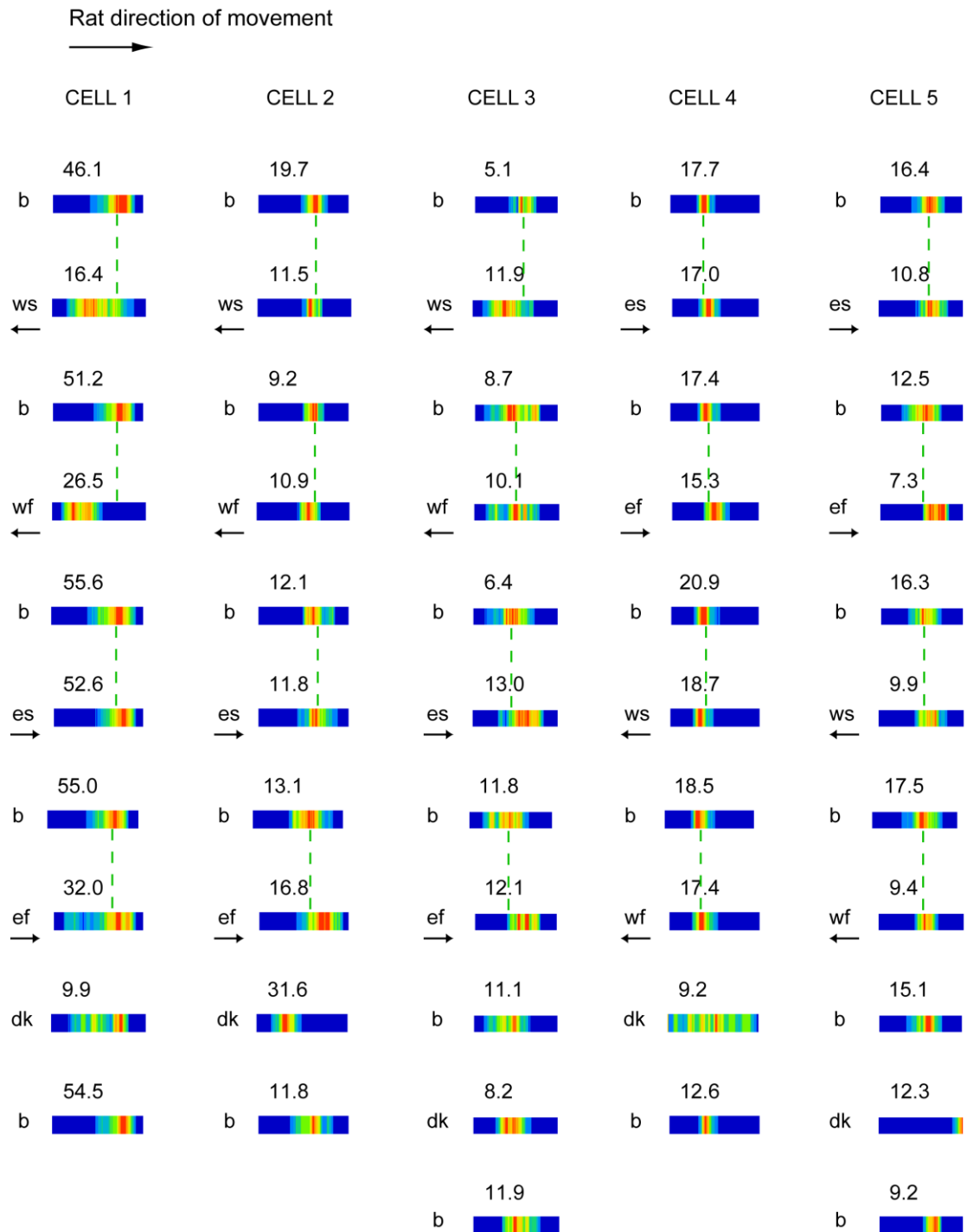
Figure 4.11 Rate maps for five eastward firing place cells during a day of recording. Each column represents one cell. Baselines are labelled b and each probe is indicated by its type (es, ef, wf, ws, dk). Baselines and probes are shown in the order in which they were given. The order of east and west to probes was balanced across cells. For moving treadmill probes, an arrow indicates the direction in which the track is moving. Numbers above rate maps indicate peak firing rate. Dashed green lines indicate the centroid location in the prior baseline for each moving treadmill probe.
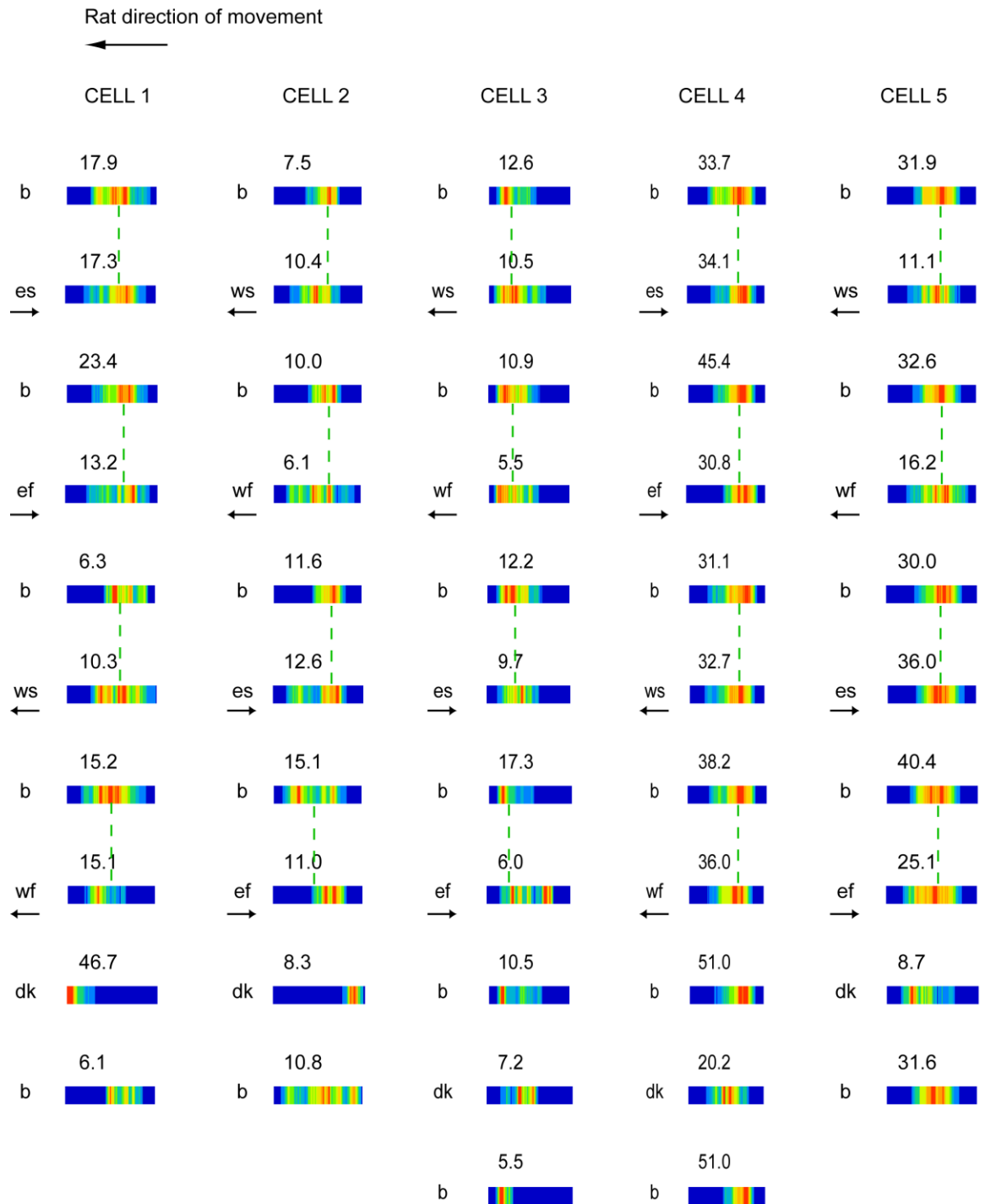
Figure 4.12 Rate maps for five westward firing place cells during a day of recording. Each column represents one cell. Baselines are labelled b and each probe is indicated by its type (es, ef, wf, ws, dk). Baselines and probes are shown in the order in which they were given. The order of east and west to probes was balanced across cells. For moving treadmill probes an arrow indicates the direction in which the track is moving. Numbers above rate maps indicate peak firing rate. Dashed green lines indicate the centroid location in the prior baseline for each moving treadmill probe.

Results for all the cells pooled together and for both eastward and westward firing cells are summarised in Table 4.1. Note that the medians of the probe shifts are positive when the treadmill is moving east and negative when the treadmill is moving west, indicating that, overall, the cells shift in the direction of the treadmill, but that the magnitude of the effect is small. The reasons for this will be explored section 4.2.6.

Also of note is that, as indicated by the difference in the mean and median values in Table 4.1 [and confirmed by Lillieforts tests, results not shown], the shift data are not normally distributed. To account for this, all further analysis will be based on nonparametric tests [which do not assume an underlying normal distribution of the data]. The level of significance for reporting p-values was generally taken to be 99%.

Table 4.1 CENTROID SHIFT

WESTWARD FIRING CELLS

Probe type	ef	es	wf	ws
No of fields	93	99	94	100
Median **delta probe** (in bins)	**1**	**1**	**-3**	**-1**
Mean delta probe (in bins)	-0.97	2.34	-4.31	-0.79
St. dev. delta probe (in bins)	20.96	11.17	11.35	14.08
Median **delta baselines** (in bins)	**0**	**-1**	**0**	**0**
Mean delta baselines (in bins)	0	-0.53	0.23	-0.70
St. dev. delta baselines (in bins)	4.08	5.60	5.76	5.43

EASTWARD FIRING CELLS

Probe type	ef	es	wf	ws
No of fields	82	94	88	92
Median **delta probe** (in bins)	**4**	**2**	**-2**	**-1**
Mean delta probe (in bins)	5.54	4.04	-1.06	1.22
St. dev. delta probe (in bins)	11.56	12.03	14.94	15.58
Median **delta baselines** (in bins)	**0**	**1**	**0**	**0**
Mean delta baselines (in bins)	-0.07	1.01	0.41	0.22
St. dev delta baselines (in bins)	5.87	4.47	5.81	4.75

ALL CELLS

Probe type	ef	es	wf	ws
No of fields	175	193	182	192
Median **delta probe** (in bins)	**2**	**2**	**-2**	**-1**
Mean delta probe (in bins)	2.09	3.17	-2.75	0.18
St. dev. delta probe (in bins)	17.47	11.60	13.27	14.82
Median **delta baselines** (in bins)	**0**	**0**	**0**	**0**
Mean delta baselines (in bins)	-0.03	0.22	0.32	-0.26
St. dev delta baselines (in bins)	4.98	5.12	5.77	5.13

4.2.1 Baseline stability: Do probes influence shifts of adjacent baselines?

Before assessing how cells shift during probes, it is useful to get a benchmark reference level by looking at how fields change across successive baselines. This can be achieved by quantifying the delta baseline. One can immediately ask two questions. Firstly, are the baselines stable and, by comparison, is the magnitude of the shift across successive baselines less that the delta probe one? Secondly, does the intervening probe influence the following baseline by, inducing a predictable shift or, put otherwise, is there any hysteresis effect?

The first result is that fields do not shift in a consistent manner across successive baselines. A one-sample Wilcoxon signed rank test revealed that the delta baselines did not have a median value significantly different from 0 [see Supplementary Table 6.8].

Moreover, probes did not influence adjacent baseline shifts at the population level. Firstly, all possible data set pairings of delta baselines, across all probe types were compared [*i.e.* the delta baselines spanning the ef probe was compared to the delta baselines of all other probes (es, wf, ws), in turn, *etc*]. Since the number of fields in each sample is different, ranksum tests were used. No results were significant [see Supplementary Table 6.9]. Because this approach implies multiple comparisons, which might induce spurious results, a Kruskal Wallis analysis was also used to confirm the

results. This also did not revealed any significant difference in delta baselines, irrespective of the intervening probe type [p=0.52, χ^2=2.23, df=3 (all cells); p=0.16, χ^2=5.09, df=3 (westward firing cells); p=0.57, χ^2=2.02, df=3 (eastward firing cells); where p is the p-value, and df are the degrees of freedom associated with the Kruskal Wallis analysis].

To confirm that the intervening probe induced no consistent trend in the delta baselines, the sign of this shift was considered [*i.e.* the precise magnitude of the shift was ignored but the direction was preserved]. Ranksum tests were again not significant [see Supplementary Table 6.10].

Furthermore, the distributions of the delta baselines across probe types are not significantly different [Kolmogorov-Smirnov tests, see Supplementary Table 6.11].

In conclusion, baseline centroids are not influenced by the intervening probe. This indicates that there is no overall hysteresis effect induced by the movement of the treadmill and that successive baselines are stable. This finding justifies using the shift across baselines as a valid benchmark against which to assess the probe-induced shift.

4.2.2   *Treadmill movement causes field shifts in the direction of movement*

To establish whether the moving treadmill induces significant field shifts in its direction of movement, delta probe were compared to delta baselines. The shift during probe conditions is significantly larger than the shift during baselines [matched sample Wilcoxon sign rank tests summarised in Table 4.2 below]. See also figures 4.14-15 and Supplementary figures 6.2-3.

Table 4.2 SIGN RANK for SHIFT: DELTA BASELINES vs. DELTA PROBE, one tailed P-VALUES

Probe type	ef	es	wf	ws
All cells p-values	4.5×10^{-5}	1.8×10^{-9}	7.2×10^{-7}	1.9×10^{-3}
Westward firing cells p-values	3.6×10^{-5}	1.0×10^{-7}	1.2×10^{-8}	2.4×10^{-3}
Eastward firing cells p-values	4.10×10^{-3}	1.3×10^{-6}	1.7×10^{-7}	3.6×10^{-3}

These results are confirmed by a Kruskal Wallis analysis where all the moving treadmill probes are considered [χ^2=39.64 (westward firing cells), χ^2=43.72 (eastward firing cells), χ^2=82.3 (all cells), all $p<10^{-15}$ and df=3]. The associated Bonferroni corrected multicomparison [at 99% significance] reveals fields shift with the treadmill in all the probes, namely shifts in probes where the track is moving eastwards (which are positive) are significantly different from shifts in westward moving treadmill probes (which are negative).

Thus, as predicted, the moving treadmill affects the position of the place fields on the linear track and is consistent with the hypothesised effect that, if the rat is moving with or against the treadmill the fields are translated, overall, along the direction of the treadmill movement.

4.2.3 Does the field shift during probes predict field shift during subsequent baselines?

We are now in a position to address the hysteresis question from section 4.3.1 from a different perspective, namely: Does a shift in a particular direction induced by a probe result in a similar direction shift of the following baseline with respect to the prior baseline?

One way of looking at this question is to correlate the delta probe with the delta baselines shifts. However, this approach is flawed in the present circumstances as both shift measures are computed with respect to the same quantity, prior baseline.

Mathematically, this makes the correlation coefficient that we would obtain dependent on the variance inherent in the measurement of the prior baseline centroid, which we cannot estimate from the data.

To circumvent partially the problem of variance estimation, I have compared the sign of the shift for delta probe with that of the corresponding delta baselines shift using a 2 tailed Fisher's exact test (2x3, *i.e.* delta baselines/probe versus 3 possible signs: 1,0 and -1). We would expect that, at the population level, if the sign of the shift during successive baselines were indicative of the sign of the shift from prior baseline to probe, we would observe similar distributions for the signs of the shifts. If cells shifted in the same direction, irrespective of the magnitude of this shift, in probes and across successive baselines we would obtain two similar distributions for the signs of these shifts. With minor exceptions (*e.g.* westward firing cells ef and ws probe), the results of the Fisher exact test are significant, indicating that one can reject the null hypothesis that signs of shifts come from populations with similar distributions [see Supplementary Table 6.12].

Thus, there is no evidence to suggest that the direction of the shift with respect to the prior baseline during probes will influence the direction of the shift in the following baselines. This is consistent with the results in section 4.3.1, which found no difference between successive baselines and no indication of a hysteresis effect.

4.2.4   Treadmill speed does not influence the magnitude of the field shift

There is no significant difference, at the population level, between the magnitudes of the shift during fast versus slow moving track probes, except for the westward firing cells in the wf vs. ws probe [see Supplementary Table 6.13].

Before concluding that the speed of the moving treadmill exerts no influence on the amount of shift, it is worth noting that the highest speed of the treadmill [10cm/s] is only a fraction of the maximum speed that the rat achieves on this linear track [up to 2m/s, *i.e.* 20 times larger]. Higher magnitude treadmill speeds might yield statistically

significant results. Unfortunately, this was not possible with the present set-up as the rat had to learn to comfortably back-pedal as *it* reached the end wall in order to eat the food from the cup there, thus severely restraining the speed at which the treadmill could be operated.

4.2.5 *An interaction between cell's direction of firing and treadmill movement direction*

We consider the possibility that a cell might react differently to movement of the treadmill with or against its preferred direction of firing. For example, an eastward firing field might shift more in an eastward moving treadmill probe than in a westward one. Cells 1 and 2 in figure 4.11 provide such an example. To enable a direct comparison, the eastward treadmill probe shifts and the negative of the westward ones were considered. Now positive shifts signify a shift in the same direction as the treadmill, and we can look at effects across different directions of treadmill movement.

A Kruskal Wallis analysis yielded significant p-values [p=0.03, χ^2=8.65, df=3 (westward firing cells), p=0.006, χ^2=17.36, df=3 (eastward firing cells), p=4.2 x 10^{-5}, χ^2=22.93, df=3 (all cells)]. When considering all the fields, a Bonferroni corrected multicomparison [at 99% significance] revealed that fast movement of the treadmill in the same direction as that of the cell [*i.e.* eastward firing cells in ef and westward firing cells in wf] induces greater shifts than slow/fast movement of the treadmill against the cell's direction of firing [*i.e.* eastward firing cells in wf/ws and westward firing cells in ef/es]. However, when cells are separated by preferred direction of firing, the multicomparison procedure [95% significance] reveals that only the eastward firing cells shift more in the ef probe than in the wf/ws ones.

Furthermore, the same results hold when considering only cells that were common to both sets [*e.g.* eastward firing cells that were included in both the ef and wf set], which allows us to perform matched sample Wilcoxon sign rank tests [see Supplementary Table 6.14].

In summary, the statistical analysis is suggestive of a trend for cells to shift more when the rat moves with the treadmill than when it moves against it. The results indicate a significant difference between these two types of manipulation for eastward firing cells, both at the data set level and at the individual cell level. Results for westward firing cells fail to reach significance. This finding points to the fact that the distribution of the fields on the track might play a role in determining the magnitude of the shift and the next section will explore this possibility.

4.2.6   Is shift consistent with path integration?

One question is whether the position of the field on the linear track influences the amount of the shift during moving treadmill probes. For example, a path integration mechanism might predict a cumulative shift in the field as the animal ran farther from the start wall. To see whether this is the case, the amount of shift during probes was plotted against the field centroid position of the prior baseline. One example is provided in figure 4.13 which depicts the shift distributions (delta probe) for the eastward firing cells in the ef probe and westward firing cells in the wf probe [for a complete overview see Supplementary figures 6.1].

If a path integration mechanism generated a cumulative shift, the results would be well fitted by a linear relationship. However, outliers generate poor least square fits [green line]. To account for this, lines were refitted by minimizing absolute [rather than least square] distance (red line), and these fits were used for subsequent analysis. To quantify the goodness of the fit, a null distribution was constructed by randomly shuffling the data points in each graph 5000 times to obtain p-values, as summarized in Table 4.3 below. Each p-value denotes the percentage of shuffles that gave a better fit than the original data (as quantified by the sum of absolute distances of each point from the fitted line). None of these p-values are significant, indicating that the linear fit is very poor.

Table 4.3 LINEAR FIT P-VALUES (one tailed)

Probe type	Westward firing cells	Eastward firing cells
ef	0.98	0.89
es	0.11	0.12
wf	0.97	0.99
ws	0.25	0.80
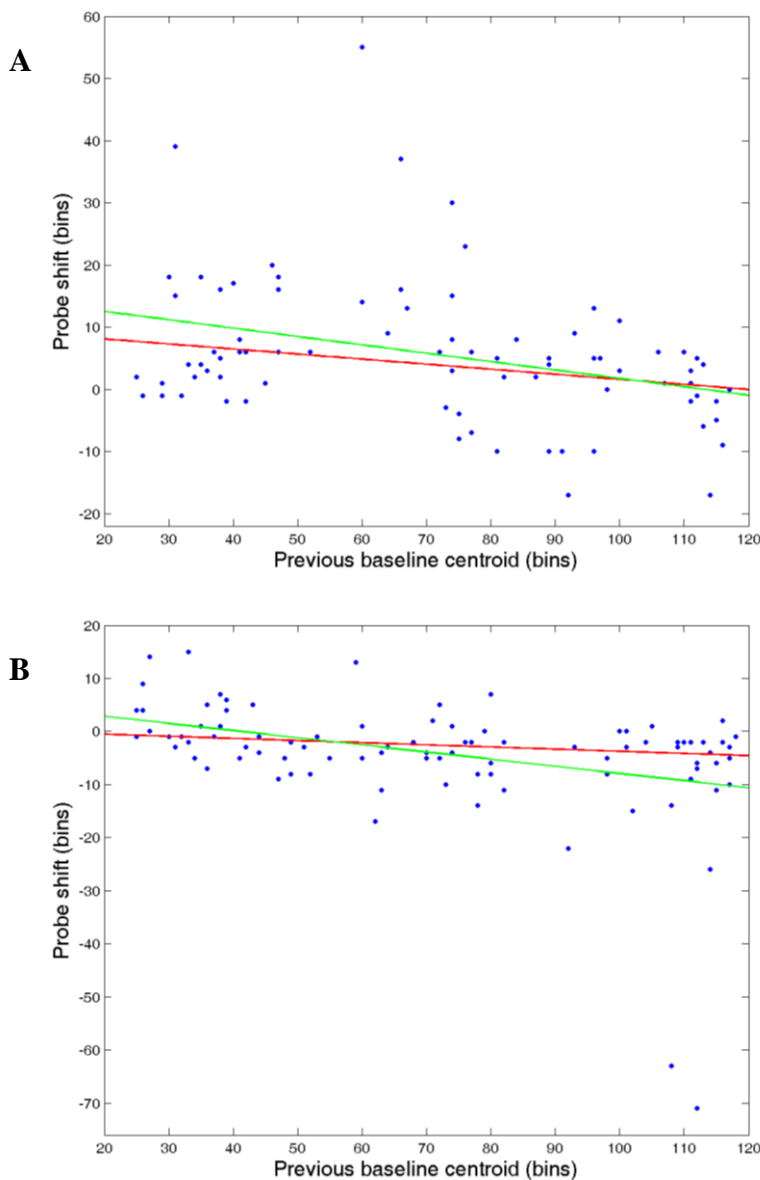
Figure 4.13 Shift vs. field's centroid in the prior baseline

for eastward firing cells in the ef probe (A) and westward firing cells in the wf probe (B). Green curve: least squares linear fit, which is unduly affected by outliers. Red curve: absolute distance robust fit. The x-axis indicates the centroid of the field in the prior baseline, measured in bins. The y-axis indicates the shift, measured in bins.

An alternative hypothesis, suggested by Gothard at al (1996a) is that two reference frames bind fields on the linear track: that of the track and that of the experimental room. In these experiments, fields closer to a mobile start box maintain a close

relationship to this landmark, while fields further away from this box, and closer to the end wall, are bound to the room reference framework. To test for the presence of this effect, I have fitted a quadratic relationship to the data in figure 4.13. These are depicted in figures 4.14 for eastward firing cells in the ef probe and figure 4.15 for westward firing cells in the wf probe, for both delta baselines and delta probes shift [for a complete overview see Supplementary figures 6.2 and 6.3]. Again, green lines indicate the least squares fit and red lines indicate the robust, absolute distance fit.
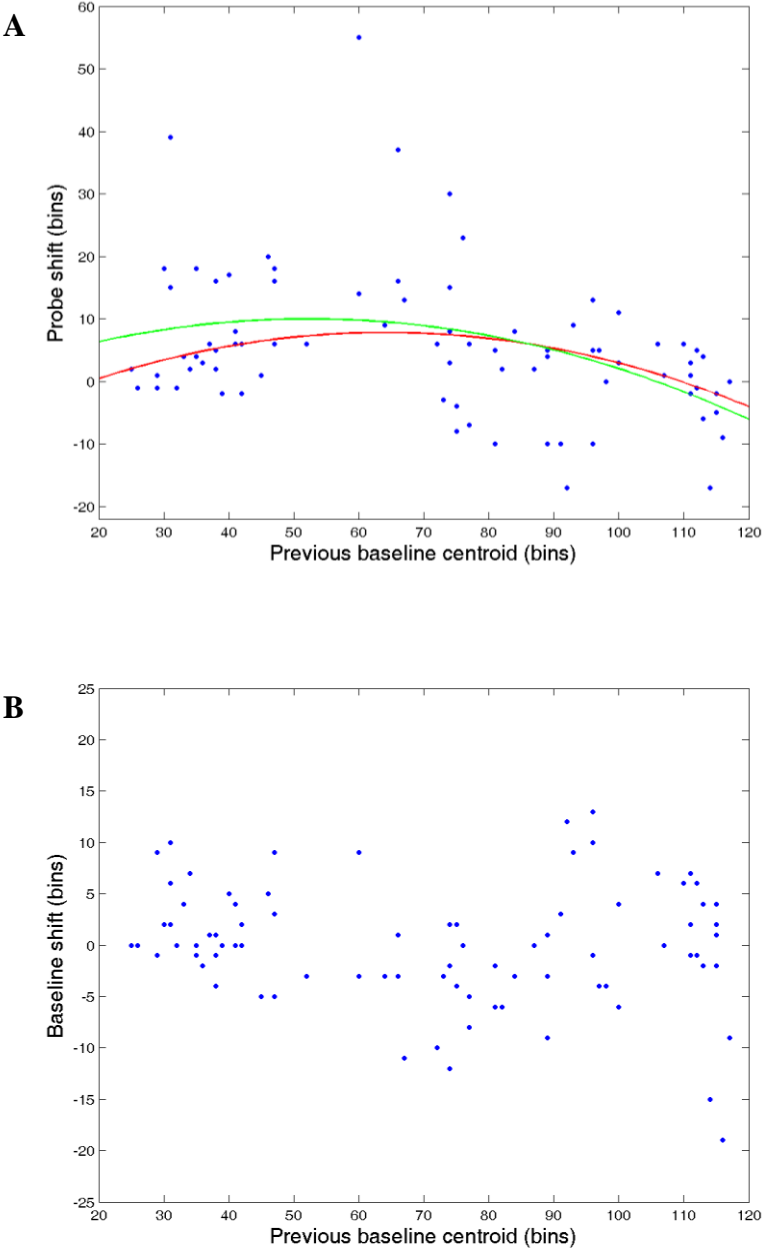
Figure 4.14 Shift vs. field's location on the track for eastward firing cells in the ef probe.

A: Delta probe shift vs. the field's centroid in the prior baseline Green curve: least squares quadratic fit. Red curve: absolute distance robust fit. The rat moves left to right. Both curves are convex, *i.e.* fields shift in the direction of treadmill movement.

B: Delta baselines shift vs. field's centroid in the prior baseline for same cells as in A.

The x-axis indicates the field's centroid in the prior baseline and the y-axis indicates the shift, both measured in bins.
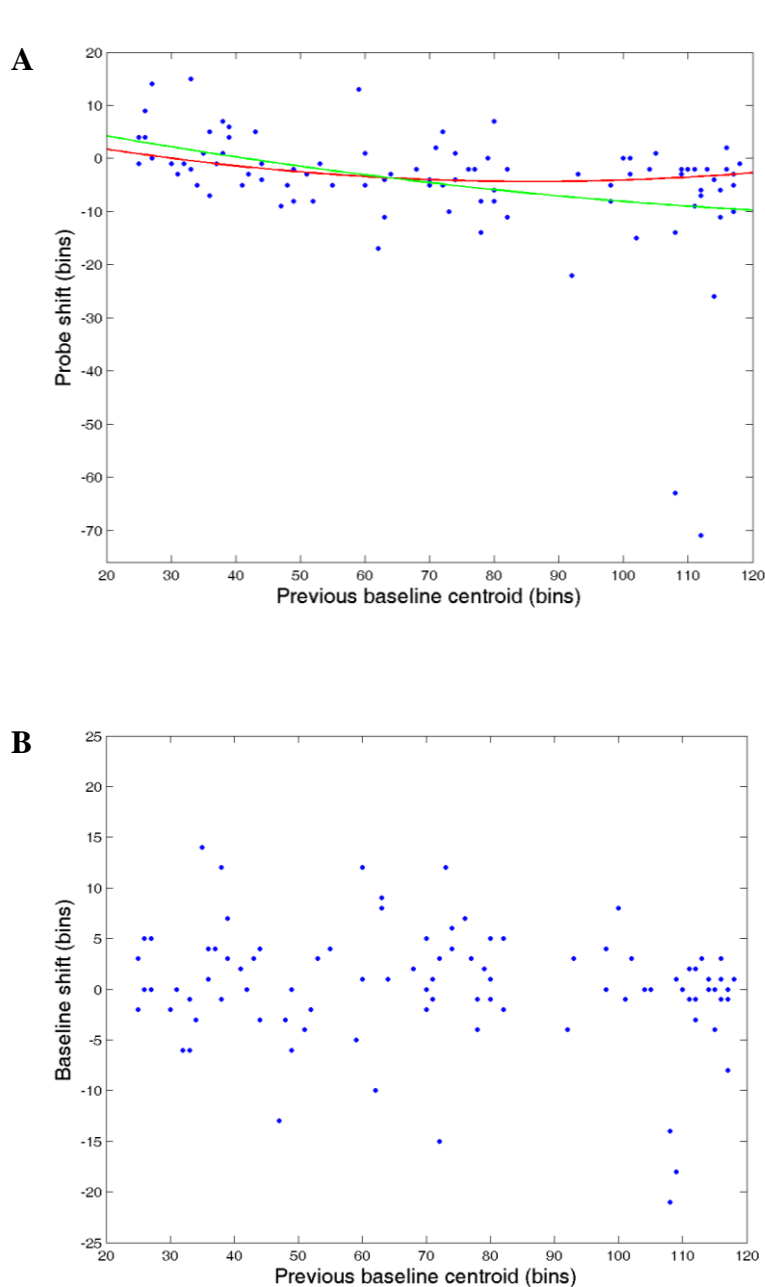
Figure 4.15 Shift vs. field's location on the track for westward firing cells in the wf probe.

A: Delta probe shift vs. field's centroid in the prior baseline. Green curve: least squares quadratic fit. Red curve: absolute distance robust fit. The rat moves right to left. Both curves are concave, *i.e.* fields shift in the direction of treadmill movement.

B: Delta baselines shift vs. the field's centroid in the prior baseline for same cells as in A.

The x-axis indicates the field's centroid in the prior baseline and the y-axis indicates the shift, both measured in bins.

As seen in Table 4.4 below, the relationship between the field's prior baseline centroid position and shift induced by the moving treadmill is well fitted by a quadratic relationship. P-values were obtained using the same 5000 shuffles of the data as for the linear fit. A p-value of 0 indicates that no shuffled data gave a better fit than the original data. Because of the robust fitting algorithm, an F test cannot be used to assess whether adding a quadratic term is significant. However, the p-values for the quadratic fit are generally significant, unlike those for the linear fit (see Table 4.3).

Table 4.4 QUADRATIC FIT P-VALUES (one tailed)

Probe type	Westward firing cells	Eastward firing cells
ef	0.12	**0.00**
es	0.16	**0.00**
wf	**0.002**	0.18
ws	**0.01**	0.75

Unlike the linear fit, the quadratic fit is significant when the track is moving in the preferred firing direction of the cell. This is consistent with two reference frameworks similar to the results of Gothard *et al* (1996 a). However, this appears not to be the complete story as the quadratic relationship is not significant when the cell's preferred direction of firing does not coincide with the direction that the treadmill is moving in.

One possible explanation is that the rat uses both landmarks and path integration to compute its exact location. In this case, it would be expected that it is more certain about its position if obvious cues are available, such as the start and end walls of the track, where it stops for food.

To test this hypothesis, the track was divided into 3 equal sections, as indicated in the Table 4.5 below: beginning, middle and end [this did not generate and equal number of cells in each category, but kept the same divisions for all probes/preferred direction of firing]. A ranksum test was used to assess if the fields in the middle section of the track shift significantly more than fields closer to its ends [beginning and end sections]. For complete results, see Supplementary Table 6.15.

Table 4.5 SCHEMA OF THE LINEAR TRACK DIVIDED IN 3 SECTORS

EASTWARD FIRING CELLS

Beginning	Middle	End

WESTWARD FIRING CELLS

End	Middle	Beginning

When the cell's preferred direction of firing coincided with the treadmill's direction of movement [eastward firing cells ef/es probe and westward firing cells wf/ws probe] the cells situated in the middle of the track shifted significantly more than the cells situated in the end section of the track but not the cells situated in the beginning section of the track. Cells in the beginning section also shifted more than cells in the end section. When the treadmill moved against the cell's preferred direction of firing, there was no significant difference among the three track segments for eastward firing cells [*i.e.* in wf/ws probes]. Westward firing cells shifted significantly more in the middle section than in the beginning section, but not the end section.

There is good agreement between these results and the quadratic fitting results. In the case where the rat moves with the treadmill, the shifts of fields located at the end of the track are significantly smaller than those of fields in the beginning and middle sectors of the track, as seen in figures 4.14 and 4.15. This is consistent with the rat seeing the end wall or switching to a room-based reference frame as it approaches the end wall. An alternative explanation is that, when the rat is moving with the treadmill, fields located next to the end wall have "nowhere to shift" [*i.e.* if they would shift forward they would "fall off" the track].

The results from probes when the rat moves against the treadmill can be interpreted in the same way. However, in these probes the rat has to travel farther than in baselines conditions, as it needs to overcome the backward movement of the track. This suggests that, if it uses reference frame switching, the switch between the two navigational modes should occur earlier [i.e. closer to the start of the track]. This hinges on the assumption that the switch point is governed by the path integration mechanism. Alternatively, if the switch is reset by a landmark, it should occur at the same point on the track as in the moving treadmill probes.

The results are suggestive of a trend supporting the first assumption [i.e. an earlier switch governed by a path integration mechanism]. Both eastward and westward firing cells do not shift more in the middle sector of the track than in its end sector. However, westward firing cells shift significantly more in the middle sector than in the start section of the track, indicating a cumulative shift as the rat runs farther. Data for eastward firing cells fail to reach significance.

The interpretation of these results is that, at the population level, it is not justified to categorize cells into populations of "path integrators" and "landmark-bound". Rather, as seen in figures 4.14-15 cells that shift with the treadmill are distributed over the entire length of the track. It is possible that all cells use both interoceptive and exteroceptive cues, but that the particular weight assigned to these cues varies as a function of a field's position on the track. This hypothesis is further explored in the next section.

4.2.7   Looking at path integration on a run by run basis

We can take advantage of the way the rat runs in stereotypical trajectories on the linear track to compute the inferred position of the rat as calculated by its path integrator, rather than its absolute position as tracked by the camera. On a run-by-run basis, the position of the rat can be determined as the integral of the time it has travelled from the start wall multiplied by its speed of movement relative to the track (*i.e.* discounting the speed of movement of the track itself).

To this end, the position data were split into individual runs. The start of the run was identified as the point after which the rat turned and proceeded to run in a straight line at more than 3 cm/s. Note that the runs don't always start from the same point, therefore a "start line" was drawn at 20 bins (48 cm) along the track from the start wall. If a run started before this line it was considered valid, otherwise it was excluded from further analysis. The current position of the rat was redefined as time elapsed from this line (in seconds) multiplied by the rat's momentary speed (in cm/sec). While this poses no problem for probes when the rat moves against the treadmill, in the opposite case it causes positions nearing the end of the track to "fall off" the end of the track. Therefore, these positions and associated spikes were excluded from further analysis.

For each field, rate maps were then reconstructed using the same procedure as for the original data, taking care to include only valid spikes [*i.e.* the ones that satisfied the good behaviour criteria as described in chapter 3].

We expect that, to the extent to which a field is governed by path integration, these reconstructed fields should show no shift in the moving treadmill probes and the fields should be smaller in terms of field size. On the other hand, if a field is bound to environmental landmarks, the shift and the size of the place field should be larger than in the original maps. Figures 4.16 and 4.17 plot the centroid of the field during probes versus the centroid in the prior baseline for both the original and the shifted data for eastward firing cells in the ef probe and westward firing cells in the wf probe [for all probes refer to Supplementary figures 6.4 and 6.5] . Diagonal lines indicate where the cell fields should be located if the moving treadmill did not induce a shift. For the original data, cells closer to the line should be cells governed by exteroceptive cues, whose fields are not affected by the moving treadmill. For the reconstructed data, cells closer to the line are cells that are governed by path integration (interoceptive information) and for which position corrected any original shift. Note that the rat moves from left to right for eastward firing cells and right to left for westward firing cells. Also, note that the data in Panel A is the same data as in figures 4.14 and 4.15 Panel A.

One can immediately observe in figures 4.16 and 4.17 that neither the original data nor the reconstructed data result in smaller shifts overall. This is consistent with the fields of some cells being primarily controlled by exteroceptive cues and those of others being primarily controlled by path integration cues, as there are cells close to the diagonal guidelines in both graphs. However, a large majority of cells are close to neither line, indicating that they use a combination of the two strategies.

A

B
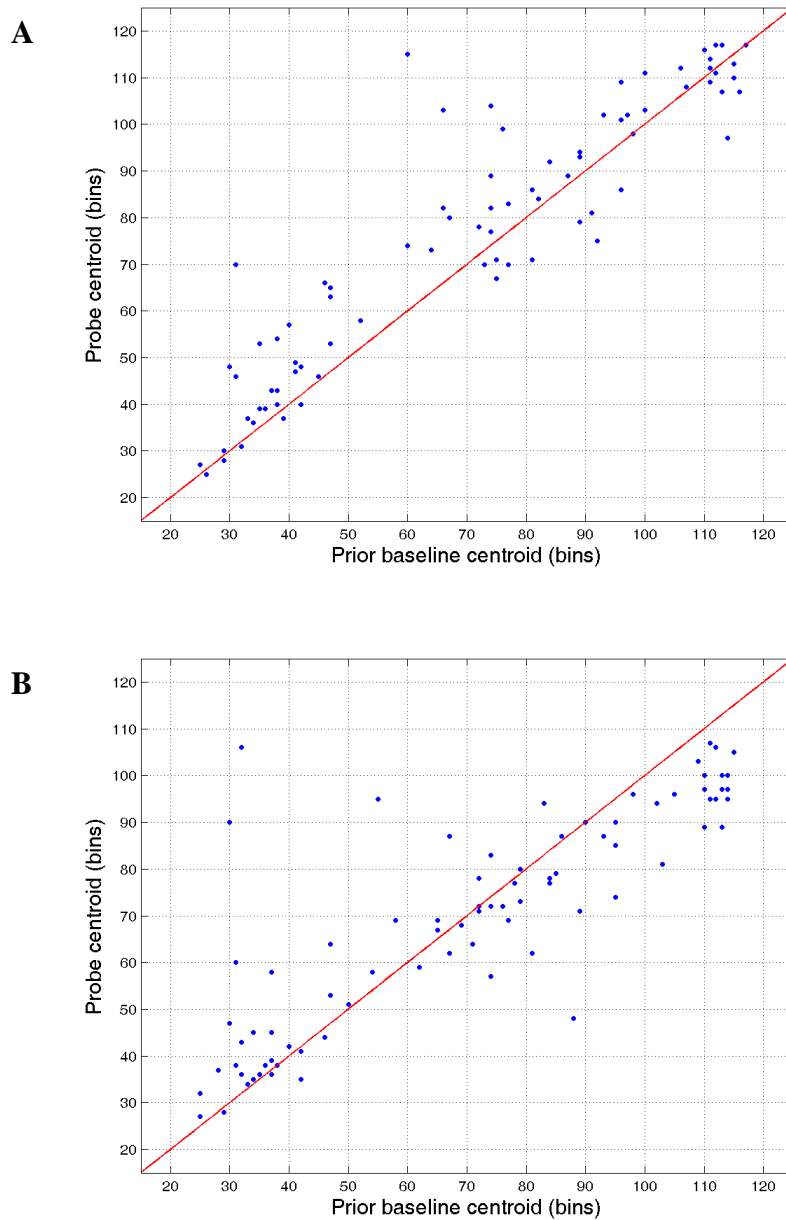
Figure 4.16 Two data plotting modes for eastward firing cells in the ef probe.

Prior baseline centroid (x-axis) vs. probe centroid (y-axis) for the original data (A) and the reconstructed data (B). Red lines indicate the no shift location. In A the red line is consistent with cells that are bound to an environment frame of reference, while in B the red line is consistent with cells relying 100% on path integration. The rat is moving left to right.
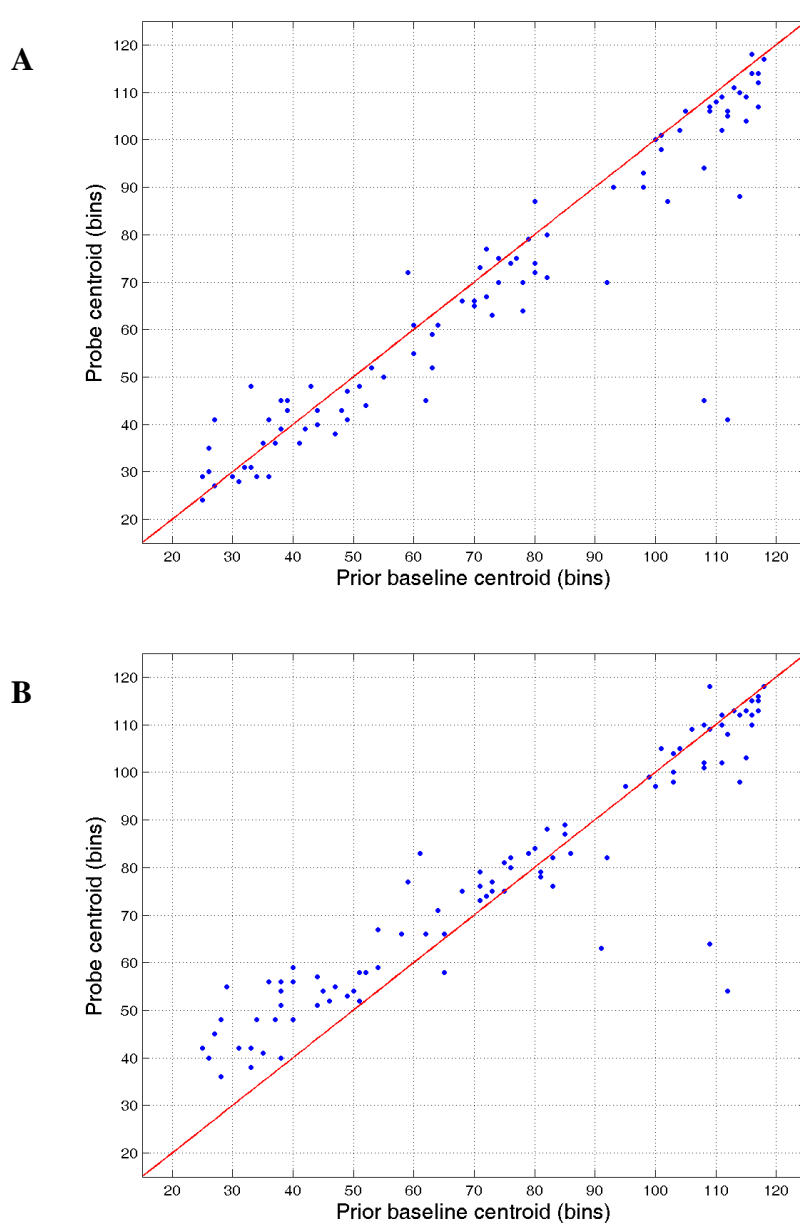
Figure 4.17 Two data plotting modes for westward firing cells in the wf probe.

Prior baseline centroid (x-axis) vs. probe centroid (y-axis) for the original data (A) and the reconstructed data (B). Red lines indicate the no shift location. In A the red line is consistent with cells that are bound to an environment frame of reference, while in B the red line is consistent with cells relying 100% on path integration. The rat is moving right to left.

The other observation is that reconstructing the data "overcorrects" for cells situated closer to the end wall. Note that the scatter plot "curves" away from diagonal at the end of the track. In figure 4.16 B, the rightmost points curve below the red diagonal while in figure 4.17 B the leftmost points curve above the red diagonal. This is consistent with the idea that they are less governed by path integration the further along the track the rat needs to travel.

In terms of which framework generates smaller shifts, one can compare the amount of shift across frameworks [*i.e.* panels A and B in figures 4.16 and 4.17]. The percentage of cells that shift less in the original framework is 58%‑72% for each probe type (mean

64.99%, std 4.69%) for fields situated on the first 2/3 of the track's length. Note that similar results hold for the entire length of the track but, as discussed previously, when the rat is moving in the same direction as the treadmill, some of the data have to be discarded, which will induce a bias for the field measures computation. Thus, in the present data, cells appear more governed by exteroceptive cues. Table 4.6 presents percentages for the track divided in 3 sections as previously discussed.

Table 4.6 PERCENTAGE OF CELLS THAT SHIFT LESS IN THE ORIGINAL DATA PLOTTING MODE WITH THE TRACK DIVIDED IN 3 PARTS

Probe type	ef	es	wf	ws
Westward firing cells beginning	64.29%	79.31%	24.24%	38.24%
Westward firing cells middle	59.38%	55.88%	60.00%	41.67%
Westward firing cells end	66.67%	75.00%	83.87%	83.33%
Eastward firing cells beginning	36.67%	36.11%	51.72%	54.05%
Eastward firing cells middle	27.27%	53.85%	75.86%	63.64%
Eastward firing cells end	80%	71.88%	60.00%	72.73%

It appears that when the treadmill and cell firing direction coincide [eastward firing cells in ef/es probes and westward firing cells in wf/ws probes] the percentage of cells that shift less in the original (absolute spatial coordinates) data plotting mode is smaller when compared to the treadmill moving against the cell's preferred direction of firing [eastward firing cells in wf/ws probes and westward firing cells in ef/es probes]. This is true for both the beginning and middle sectors of the track. In the end sector of the track, a high percentage of cells shift less in the original data plotting mode (but, for the reasons noted above, caution is required when interpreting results for probes when the rat moves with the treadmill).

This result provides an explanation as to why the quadratic fits in figures 4.14 and 4.15 were only significant when the treadmill and cell's firing direction coincided, as path integration appears to influence a higher percentage of cells in these probes. Conversely, in probes when the rat moves against the treadmill, exteroceptive cues appear to play a more salient role.

A similar conclusion can be drawn from the framework in which the cells shifted less and the correspondence between this and the framework in which the field was "tighter". This implies that if a cell's spatial selectivity is significantly biased either towards exteroceptive or interoceptive information, this should be reflected in the "accuracy" of its firing. Only 50-69% (mean 57.72%, std 6.31%) of the cells located on the first 2/3 of the track's length conform to this pattern. Results are slightly worse when looking at peak firing rate instead of field size 40-55% (mean 49.06%, std 5.28%) as an indicator of field "tightness", but this measure is presumably more sensitive to the replotting procedure. This leaves a significant percentage of cells in a fuzzy category, for which a smaller shift does not imply a tighter field.

4.2.8 Is field shift correlated with changes in other measures of field size?

The field shift did not correlate with changes in any other field measure [results not shown]. The following sections will highlight results for field size and precession in detail.

4.3 Field size is unaffected by the moving treadmill

Another potential effect of the moving treadmill probes might be that the rat perceives the environment as elongating or shrinking depending on whether it moves against or with the treadmill, respectively. Huxter *et al* (2003) have shown that altering the size of the linear track by moving the end walls induces a proportionate distortion in the place fields, which is dependent on the position of the field on the track [*i.e.* the closer the field to the end wall that moves, the greater the field shift in the same direction]. Also, the larger the field the more it shrinks as the track is compressed. Furthermore, recall that the magnitude of the change in field size was directly related to the magnitude of the change in phase precession slope.

To look for such an effect in these data, the difference in field size from prior baseline to probe (delta probe) and across successive baselines (delta baselines) was considered [see Supplementary Table 6.16].

The change in field size across baselines or from prior baseline to probe was not significantly different from 0 [see Supplementary Table 6.17].

There was no difference in field size change across baselines as quantified by a ranksum test, namely, fields were similarly distorted between successive baselines, irrespective of intervening probe [see Supplementary Table 6.18].

Probes did not induce significantly different changes in field size when compared to successive baselines [matched sample Wilcoxon sign rank test in Table 4.7], except the wf probe.

Table 4.7 SIGN RANK DELTA BASELINES vs. DELTA PROBE FIELD SIZE two tailed P-VALUES

Probe type	ef	es	wf	ws
All cells	0.014	0.11	0.0001	0.27
Westward firing cells	0.08	0.43	0.001	0.39
Eastward firing cells	0.09	0.14	0.003	0.48

Moreover, there was no difference in field size change from baseline to probe [ranksum test, see Supplementary Table 6.19], irrespective of probe type. A Kruskal Wallis analysis grouped by probe type was not significant in all cases [p= 0.56, χ^2=2.04, df=3 (westward firing cells); p=0.62, χ^2=1.78, df=3 (eastward firing cells); p=0.75, χ^2=4.27, df=7 (grouped by both probe type and preferred direction of firing)].

In conclusion, the moving treadmill did not cause fields to distort as would be predicted if the rat perceived such probes as an extension/compression of the environment.

4.3.1   Is the change in field size related to changes in any other measure?

As expected, the change in field size is strongly correlated with the change in bits per spike information. However, although field size and in-field average speed are related measures, their changes do not correlate with each other. For moving treadmill probes, this can be explained by the fact that fields shift their location on the track.

The change in field size is also significantly correlated [see section 4.4.1] with the change in the phase precession slope but not with the change in the amount of phase precession. This is consistent with the previous finding that the slope of precession correlates with field size and with the results of Huxter *et al* (2003). However, in contrast to the way the fields shift and in contrast to the compressing runway results, there is no relationship between the position of the field on the track and its size change [results not shown].

This section has shown that the interpretation of the changes in field size is not consistent with the results elicited by compressing/expanding the runway experiments.

4.4   Phase precession

For each cell, a phase precession line was fitted to the spikes versus position plot of each cell using an unwrapping algorithm based on minimizing the cos distance [see chapter 3]. For westward firing cells, the x-axis was flipped so that all precession lines have negative slope. Once phase angles were unwrapped, the amount of precession for each cell was defined as the length of the precession line (in degrees) and a phase-position correlation coefficient was computed.

A summary of measures is available in Supplementary Tables 6.18-20 for cells grouped by preferred direction of firing. No attempt was made to select cells that do not appear to precess and results are reported for all cells. Thus, the reported results

generally underestimate the strength of the precession effect. Darkness trials are also included in this analysis.

No differences were found, at the population level, in terms of precession slope, amount or phase-position correlation across successive baselines or from baseline to probes [see Supplementary Section 6.3].

When considering all eastward and westward fields in all trials, as described in the beginning of this chapter, there is a strong correlation for all precession measures between successive baselines [SLOPE: R=0.61 (eastward firing cells)/0.56 (westward firing cells); AMOUNT: R=0.50 (eastward firing cells)/0.47 (westward firing cells); PHASE-POSITION CORRELATION: R=0.49 (eastward firing cells)/0.43 (westward firing cells); all $p<10^{-5}$]. Figure 4.18 illustrates this for phase precession slope. Precession measures for moving treadmill probes also correlated significantly with prior baselines ones [SLOPE: R=0.40 (eastward firing cells)/0.42 (westward firing cells); AMOUNT: R=0.38 (eastward firing cells)/0.35 (westward firing cells); PHASE-POSITION CORRELATION: R=0.35 (eastward firing cells)/0.30 (westward firing cells); all $p<10^{-5}$]. The relationship between precession slopes in probes versus prior baselines is depicted in figure 4.19. The same results hold when grouping fields by direction of firing and probe type [see Supplementary section 6.3]. Interestingly, the only non-significant correlations between probe and prior baseline measures were for darkness probes [$p>0.35$ for all measures], and this is partly responsible for the correlations between probes and baselines being smaller than those between successive baselines. The reason for this will be explained in the next section.

In summary, the phase precession phenomenon does not appear to be disrupted by the moving treadmill probes, despite the fields shifting their location on the linear track. All the investigated measures of precession remain stable across various trials and correlate well with each other.
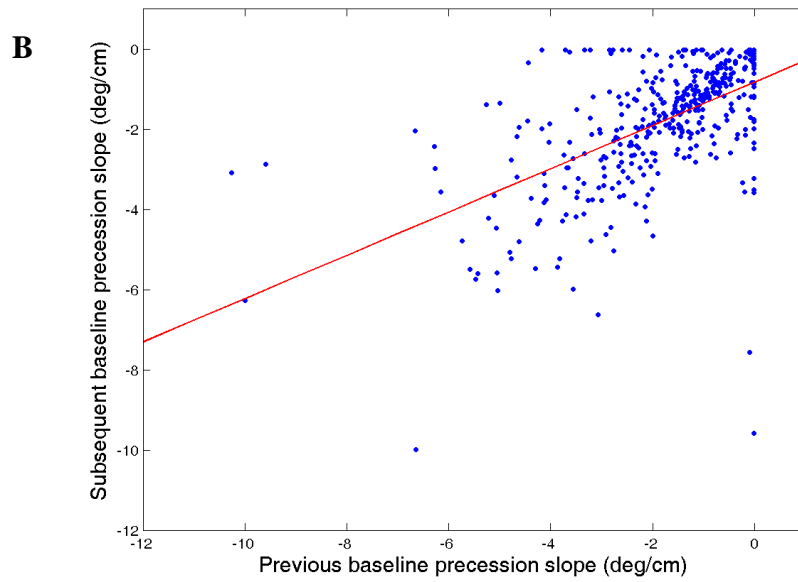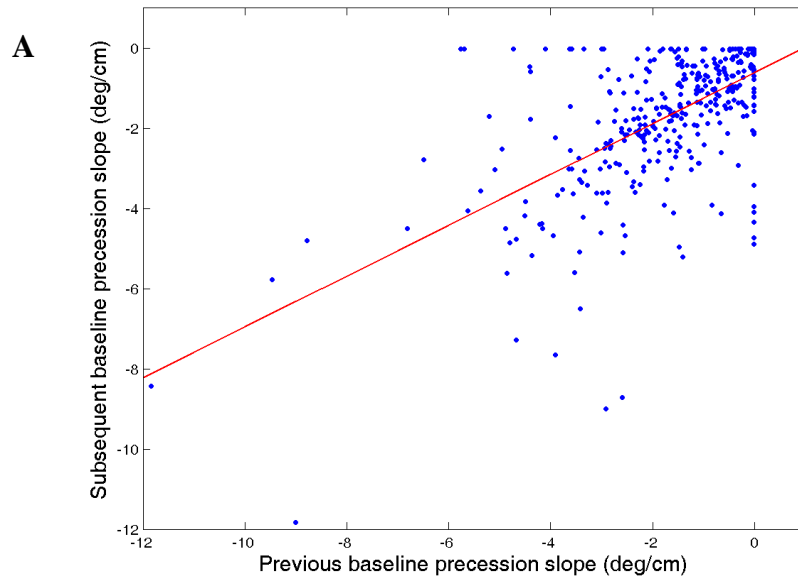
Figure 4.18 Comparison of baseline precession slopes.

Prior baseline precession slope (x-axis) vs. subsequent baseline precession slope (y-axis) for eastward firing cells (A) and westward firing cells (B).
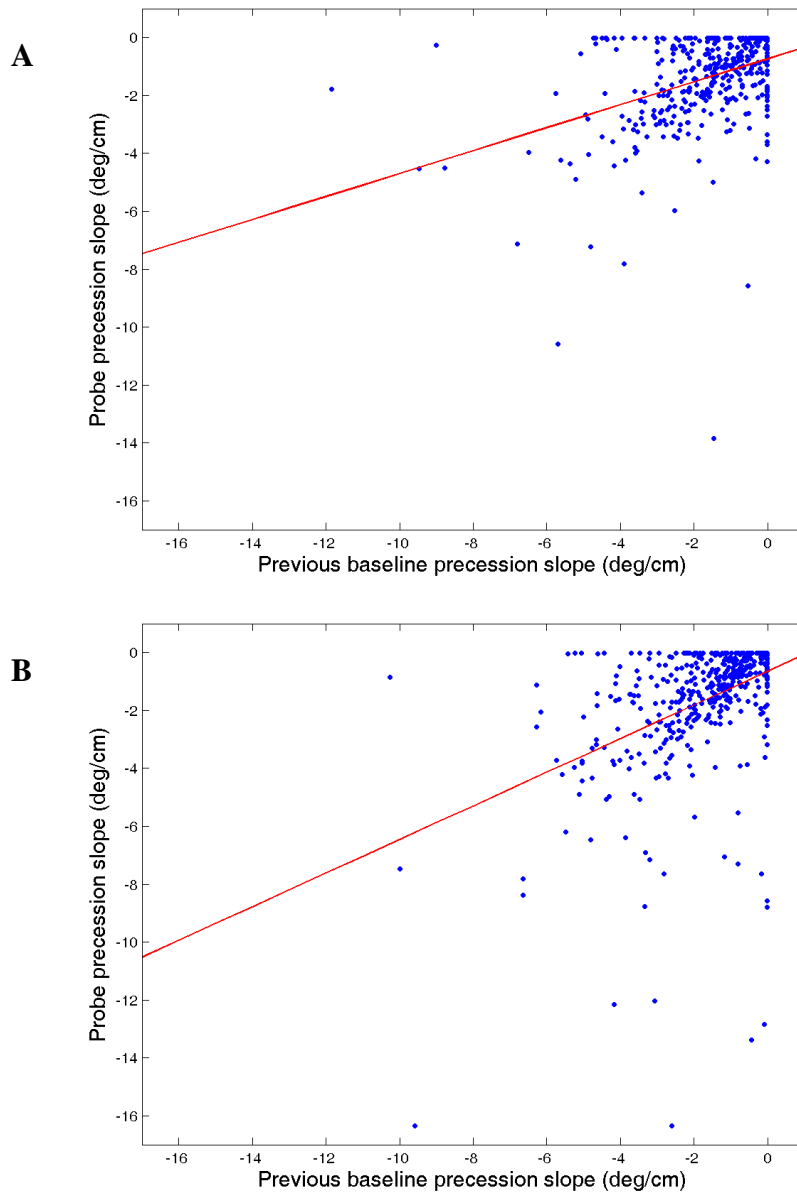
Figure 4.19 Baseline vs. probe precession slopes.

Prior baseline precession slope (x-axis) vs. probe precession slope (y-axis) for eastward firing cells (A) and westward firing cells (B).

4.4.1 The slope of precession is related to the size of the field

As shown previously, the slope of phase precession is related to the size of the field and its position on the track. It is therefore of interest to see if changes in precession slope are related to changes in any other field measures at the individual cell level.

Indeed, when considering all eastward and westward fields in all trials, as described in the beginning of this chapter, changes in precession slope across successive baselines and from probes to the prior baseline correlate with changes in field size [successive

baselines: R=0.24 (eastward firing cells)/0.30 (westward firing cells); probe to prior baseline: R=0.34 (eastward firing cells)/0.37 (westward firing cells); all $p<10^{-5}$]. These correlations are depicted in figures 4.20 for delta probe and 4.21 for delta baselines. Results for cells grouped by trial type are presented in Supplementary section 6.3. Similar results were found for the bits per spike information, a measure associated with field size. However, there were no significant correlations with the changes in average in field speed, even though this is related to field size.
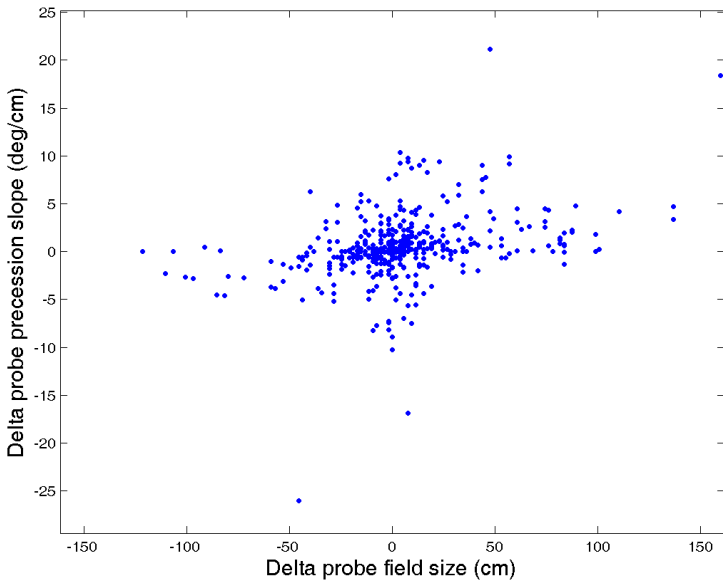
Figure 4.20 Comparison of delta probe for field size vs. precession slope.

Delta probe field size (x-axis) vs. delta probe precession slope (y-axis) for eastward firing cells (A) and westward firing cells (B).
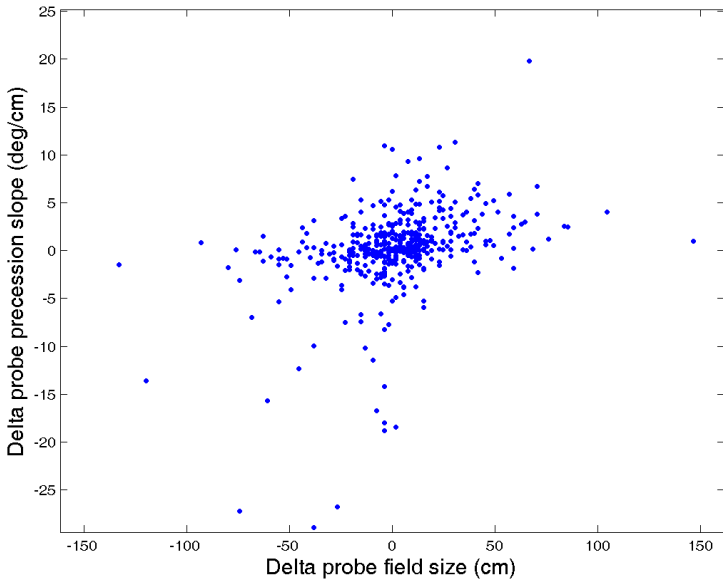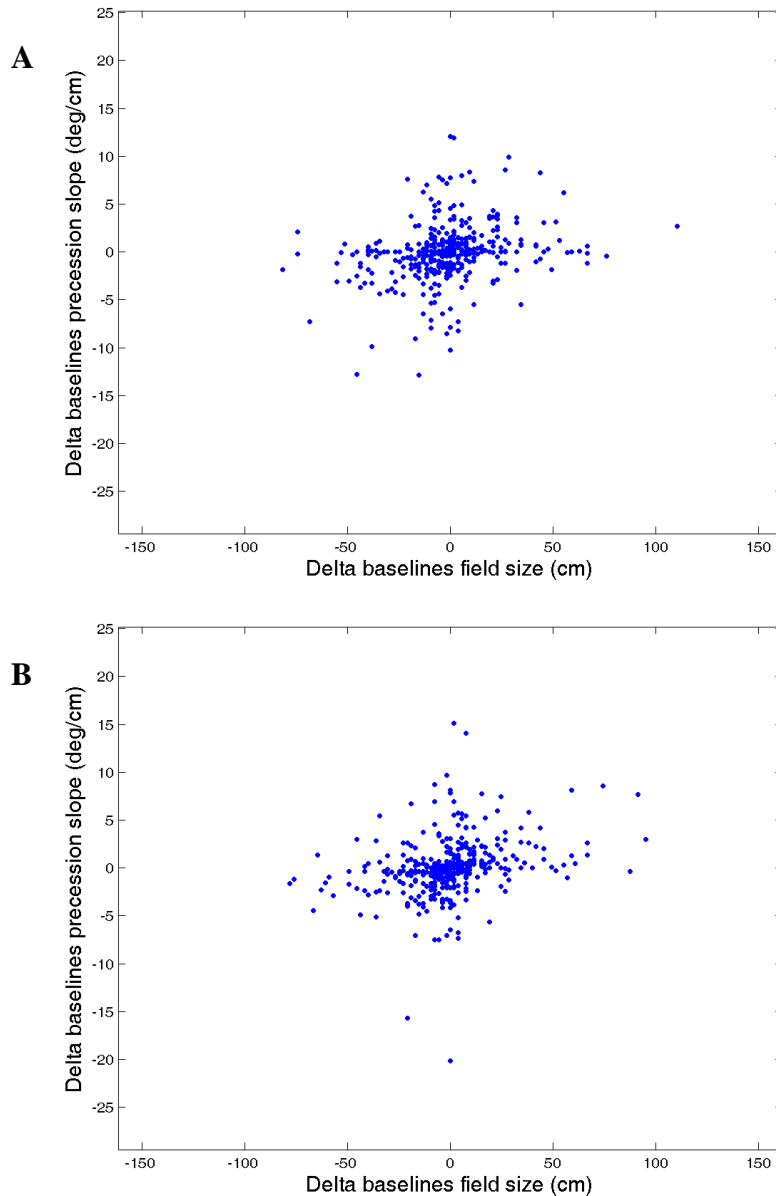
Figure 4.21 Comparison of delta baselines for field size vs. precession slope.

Delta baselines field size (x-axis) vs. delta baselines precession slope (y-axis) for eastward firing cells (A) and westward firing cells (B).

4.5 Darkness trials

I also examined the control over field parameters by environmental cues by turning off the lights while the treadmill was moving at baseline speed. The first question of interest is whether cell fields were stable when the lights were turned off or whether a substantial number of them remapped. As summarized in table 4.8, the shift in the centroids of the fields during dark trials are substantial and exhibit a large degree of variability.

125

Table 4.8 DARK TRIALS CENTROID SHIFT

Probe type = DK	All cells	Westward cells	Eastward cells
No of fields	102	53	49
Median delta probe (in bins)	2	6	-3
Mean delta probe (in bins)	3.55	10.86	-4.36
St. dev. delta probe (in bins)	37.17	36.41	36.70
Median delta baselines (in bins)	0	0	0
Mean delta baselines (in bins)	0.22	-0.09	0.55
St. dev. delta baselines (in bins)	5.73	5.28	6.19

The baselines are stable as indicated by a one sample Wilcoxon sign rank test for 0 median for delta baselines [p=0.91 (westward firing cells), p=0.31 (eastward firing cells) and p=0.51 (all cells)]. The same holds for delta probe [p=0.06 (westward firing cells), p=0.41 (eastward firing cells) and p=0.40 (all cells)], indicating that the dark trials do not induce a shift in any particular direction. Probe shift is not significantly different from across baselines shift [matched sample Wilcoxon sign rank test: p=0.06 (westward firing cells), p=0.31 (eastward firing cells), p=0.50 (all cells)]. There is however substantially more variance in how cells shift during darkness probes [Ansari-Bradley test (two tailed): $p=3.5 \times 10^{-9}$ (westward firing cells); $p=5.4 \times 10^{-9}$ (eastward firing cells); $p=4.9 \times 10^{-18}$ (all cells)].

When considering the position of the field on the track, as indicated by its centroid in the prior baseline, there is a highly significant correlation between the location of the field and the amount of shift during darkness trials [$R=-0.60$, $p=1.8 \times 10^{-6}$ (westward firing cells), $R=-0.74$, $p=1.3 \times 10^{-9}$, $R=-0.67$, $p=1.4 \times 10^{-14}$ (all cells)]. This partly stems from the fact that cells near to the end walls can only shift towards the middle of the track, whilst cells in the middle of the track move either right or left as seen from figure 4.22. However, it is not consistent with the idea that cells closer to the end walls are more "anchored" to the linear track, either by local cues or by a path integration mechanism that did not yet have the opportunity to accumulate much error. Rather, there seem to be two qualitatively different types of cells: the ones that stay more or less where they were (small shifts) and the ones that remap (large shifts). This is in

stark contrast to both figure 4.13 and figures 4.14 –15 (which indicated that for the moving treadmill probes there is a quadratic relationship between the position of the field on the track and the amount of shift during probes).
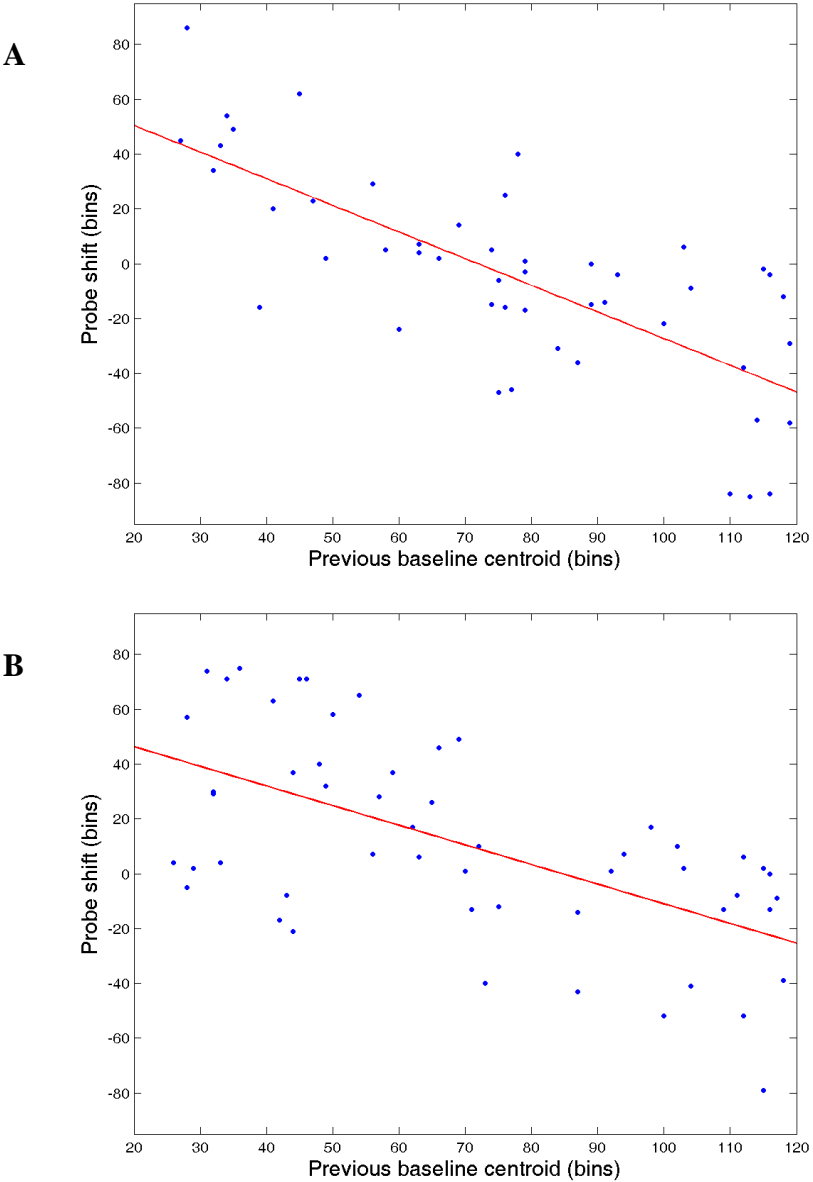
Figure 4.22 Shift vs. the field's location in the prior baseline in the darkness probe for eastward firing cells (A) and westward firing cells (B). Red curve: least squares regression line. Note that the rat moves left to right in A and right to left in B. The x-axis indicates the centroid of the field, in the prior baseline measured in bins. The y-axis indicates the shift, measured in bins.

Table 4.9 summarises the changes in field size in the darkness probe, as compared to the prior baseline.

Table 4.9 DARK TRIALS FIELD SIZE CHANGES

Probe type = DK	All cells	Westward cells	Eastward cells
Median delta probe (in bins)	0	-2	6
Mean delta probe (in bins)	0.96	-5.09	7.51
St. dev. delta probe (in bins)	25.99	22.34	28.22
Median delta baselines (in bins)	-3	-2	-4
Mean delta baselines (in bins)	-3.90	-3.18	-4.67
St. dev. delta baselines (in bins)	15.35	12.68	17.91

The median of delta probe field size is not significantly different from 0 [one sample Wilcoxon sign rank test, p=0.14 (westward firing cells), p=0.12 (eastward firing cells), p=0.92 (all cells)].

There is no difference in field size change in delta probe vs. delta baselines, except for eastward firing cells [matched sample Wilcoxon sing rank test, p=0.06 (all cells), p=0.51 (westward firing cells), p=0.003 (eastward firing cells)]. However, there is a significant difference in variance of the change in field size [Ansari Bradley test (two tailed): $p=1.3 \times 10^{-6}$ (all cells), p=0.006 (eastward firing cells), p=0.004 (westward firing cells]. This shows there is more variance in darkness probe field size change than across successive baselines, which was not the case for the moving treadmill probes. Thus, we cannot conclude that fields expand/contract during darkness on a consistent basis. Rather, as many cells remap in the darkness probe, as shown in figure 4.22, the comparison in field size is meaningless.

4.5.1 Comparison of moving treadmill and darkness probes

As demonstrated in the previous section, darkness probes have a drastic effect on the cells on the linear track. While cells shift moderately and in a predictable manner during moving treadmill probes, a substantial percentage of cells remap in the darkness trials. Furthermore, there is substantially more variance in the amount of shift and change in field size when compared to baselines for the darkness trials. Thus, it is difficult to make inferences about how the behaviour of a cell in a darkness trial relates to its behaviour on the moving treadmill probes. The ideal comparison would have been between stationary and moving treadmill darkness probes but, unfortunately, pilot studies showed that this combination was too disruptive for the rat's behaviour [*i.e.* rats got too scared to shuttle back and forth]. Nonetheless, this section will attempt a comparison.

In terms of cells that became quiescent, 32 eastward firing cells and 33 westward firing cells satisfied the good baseline criteria for prior and subsequent baselines but did not fire enough during the darkness probe to be included in the analysis. This is significantly more than the cells that were excluded on the same grounds from the moving treadmill analysis. Adding excluded (*i.e.* quiescent) + included cells and expressing excluded as a percentage of total number of cells for each probe, we find that 38.92% cells were quiescent during darkness probes [see Supplementary Table 6.23]. By comparison, 14.21% were quiescent in ef probes, 2.03% in es probes, 9% in wf probes and 4.44% in ws probes.

There are also a small number of cells (17) that only fire in darkness probes. These were not part of any analysis [either included or excluded cells in the previous paragraph] and did not fire more than 30 spikes in any of the adjacent baselines, but fired more than 60 spikes in the darkness probes.

The majority (75-90%) of the cells that became silent during darkness trials were included in at least one of the moving treadmill data sets. Inspecting their position on the track reveals no clear pattern, except for a weak tendency to be clustered near the end walls. In the majority of cases, matched sample Wilcoxon sign rank tests (comparing delta probe vs. delta baselines in the moving treadmill probes) are not

significant, except for westward firing cells wf/ws probes and eastward firing cells es probe [results not shown]. This indicates that these cells do not shift much during moving treadmill probe trials.

The fact that they appear to be mainly located by the end walls is consistent with the idea that these cells are rather strongly influenced by visual inputs, in the sense that visual inputs from the end wall is required to establish a place field. This is consistent with these cells not shifting significantly during moving treadmill probes. However, there is little data here to form a strong conclusion, because they are neither particularly clustered nor significantly stable [*i.e.* not shifting more than across baselines] in all trials.

More than 75% cells that fired in the dark also fired during moving treadmill probes [see Supplementary Table 6.24]. A rapid inspection showed that they are roughly uniformly distributed on the track. Matched sample Wilcoxon sign rank tests comparing delta probe versus delta baselines shifts in the moving treadmill probes are significant, indicating that these cells generally shift with the treadmill, except in the ws probe. Ansari Bradley tests for difference in variance across samples were all not significant, indicating that the variance of the shift is not significantly different in probes as contrasted to successive baselines.

Cells that fire both during moving treadmill and darkness trials can be considered to be governed by both path integration and visual cues. The fact that these cells move with the treadmill points to at least some of them relying on path integration to establish spatial selectivity. This would predict that the firing fields of such cells should be larger during darkness trials, as path integration is an error prone computational strategy. However, since many cells remap during darkness probes, it is meaningless to consider field size changes with respect to adjacent baselines.

5 Discussion

As originally suggested by O'Keefe (1976), place cells integrate a range of exteroceptive environmental information as well as interoceptive information about the animal's own movement to establish their spatial selectivity. The main purpose of this thesis has been to investigate the interplay between these two sources of information by directly manipulating two key inputs. On the one hand, the contribution of self-motion information was explored in the moving treadmill experiments. On the other, this was contrasted with the effects of removing visual input in the darkness probe.

The main finding of this thesis is that place cells shift in the direction of the treadmill during moving treadmill probes, indicating that self-motion information provides a key input for place cell spatial selectivity. Secondly, the darkness manipulations have shown that visual input is also essential, as many cells became quiescent or remapped during this type of manipulation.

These manipulations confirm that place cells use both interoceptive and exteroceptive cues to establish their place fields, and here I discuss their relative contributions and possible interplay of these sources of information. The organisation of this chapter follows that of chapter 4. I will first discuss the general place field properties on the linear track, and then move on to the effects of the moving treadmill and darkness manipulations.

5.1 Place field properties are dictated by their position on the track

This thesis shows that place field measures correlate with the field's position on the track. Fields in the middle of the track are larger, are traversed at a higher speed, are less skewed and phase precess at a slower rate. In contrast, the peak firing rate, the amount of precession and the phase-position correlation do not depend on the location of the field on the track. These properties hold for both baselines and probes.

5.1.1 Field size

The field size correlation with its location on the track is consistent with the effects of environment geometry on field size and shape observed by of O'Keefe and Burgess (1996), Huxter *et al* (2003) and Fenton *et al* (2008).

We explored the hypothesis that fields show a uniform distribution on the track. This was found not to be the case, with the distribution of the present data being trimodal. Fields were more clustered in three regions: closer to the end walls and in the middle of the track.

One explanation for the difference in field size along the track is that the precision of the spatial representation is higher nearer the end walls of the track. This could be due to the availability of more salient local cues or to the presence of the goal in these locations.

An alternative hypothesis is that that field size is related to the speed at which the field is traversed, in the sense that both variables depend in a similar fashion on the field's position on the track. While there were no correlations between in-field average speed changes and changes in field size across trials, this cannot entirely rule out an effect of speed on field size, which might be apparent if, instead of mean speed, we considered a more accurate measure of this variable, such as an in-field profile/distribution of

speed across the entire place field. Indeed, evidence suggests that speed is an important input for place cells firing properties [McNaughton *et al*. 1983, Geisler *et al* (2007), Huxter *et al* (2003)]. Elucidating this point would require a method of defining functions for speed profiles and comparing them, an important question which remains to be addressed in the future.

The departure from uniformity of the fields' distribution on the track and the confounding relationship between both field size and in-field speed do not allow us to establish whether, in this experiment, the field size is determined by sensory information stemming from the proximity to end walls or by the rat's behaviour. Answering this interesting and debated question would require gathering a large data-set in which speed-matched runs on the linear track could be compared. This would require the same animal be run for very long trials, which was not possible using the present set-up.

5.1.2 Field skew

Mehta and colleagues [Mehta *et al* (1997), Mehta *et al* (2000)] have shown that place fields on the linear track become negatively skewed with experience across successive individual runs through the field [but see also Schmidt *et al* (2009), Lee and Knierim (2007) for a competing view]. In the experiments presented here, where the rat experiences the track for a considerable number of trials each day, the model of Mehta and colleagues would predict that all fields should eventually become negatively skewed.

Here I show that there is a relationship between field skew and the position of the field on the track. Fields in the middle of the track are more symmetrical, while fields closer to the end walls are skewed towards the middle of the track. Skew or changes in skew across probes are not correlated with changes in any other measures.

These data show that, although it is theoretically possible that, overall, an asymmetrical expansion of fields takes place (as proposed by Mehta *et al.* (1997)), this effect is negligible, since it can be overpowered by the field's position on the track and does not appear to hold for fields in the centre even after considerable experience.

5.2   Characteristics of shifted fields are preserved

This thesis shows that moving treadmill probes do not induce changes in any other place field related measures, other than their location on the track.

The fields do not expand or contract in a coherent manner during moving treadmill probes, as would be predicted if the rat perceived the environment as shrinking or elongating as shown by Huxter *et al* (2003) [see also optic flow discussion below].

Indeed, the only measures whose changes are correlated are field size and the slope of phase precession, as found by Huxter *et al* (2003) and Schmidt *et al* (2009). This holds across all trial types except the darkness probes. As many cells remap during darkness manipulations, their field sizes in baselines versus probes are not related.

There was no relationship between peak firing rate and precession measures, as would be predicted by the models of Harris *et al* (2002) and Mehta *et al* (2002).

5.3 Place cells integrate self-motion cues

In the moving treadmill probes, the place fields shift in the direction of the treadmill. This is consistent with the rat integrating self-motion cues. The moving treadmill probes do not influence place fields during the subsequent baselines. In this thesis, I found that place fields are stable during baselines and that there is no hysteresis effect induced by moving treadmill probes.

When the rat moves with the treadmill, it travels farther in a given time interval, as its speed increases relative to absolute spatial coordinates. Therefore, if the rat keeps track of its own movement, place fields should be translated forward (*i.e.* farther away from the start of the run). Conversely, place fields should be translated backwards when the rat moves against the treadmill. The moving treadmill manipulations have shown that this is indeed the case, providing direct evidence that place cells use idiothetic input to establish their spatial selectivity. Moreover, this input is used even when visual cues are available and conflict with the rat's idiothetic computation of location.

In the experimental set-up used here, there was no difference in the magnitude of field shift caused by the slow (5 cm/sec) and fast (10 cm/sec) speeds of the moving treadmill. A limitation of these experiments is that the speed of the treadmill is much smaller than the rats' running speed, which can reach up to 2m/sec. Using a linear track paradigm puts a physical limit to experimenting with the treadmill speed, since the rat has to stop for reward consumption and turn at the end of the track. Therefore, extending these data to faster treadmill speeds could only be achieved by changing the experimental paradigm, *e.g.* using a circular track.

Consequently, it is conceivable that the difference between the slow and fast speeds used in the present experiments is too small to generate statistically significant differences in the magnitude of shift between the two conditions.

The interesting finding is that even a slow displacement speed of the treadmill causes significant shifts in its direction of movement, indicating that place cells are highly sensitive to self-motion input.

5.4 Sources of self-motion information

The moving treadmill disrupts two obvious sources of self-motion information. One is motor efference copy and the other is optic flow. Unfortunately, this manipulation does not provide a means of disambiguating between these two sources of information.

Likely sources for the motor efference copy are step counting or a signal related to the amount of muscle effort elicited by active walking. It is possible that on the moving treadmill the rat runs in a different way, as measured by locomotor parameters such as stride, gait and step frequency. Another source might be the deflection of the vibrissae of the rat caused by air flow or the vibrissae touching the side walls of the environment. Unfortunately, the present set-up did not allow us to monitor these parameters.

Optic flow might also arise from different sources, such as the looming of the end walls, the flow of the side walls or perhaps by the moving belt of the treadmill. One interesting observation is that that the optic flow from the belt and the side walls of the track and other room cues are divergent. The optic flow from the belt is commensurate with the rat's own speed of movement, while that from the side walls/room cues is faster/slower when the animal is moving with or against the track, respectively, as it is governed by the rat's absolute speed (i.e. compounded with that of the treadmill).

However, as discussed in Introduction, evidence from other studies points to the fact that optic flow is secondary in importance to locomotion.

Lu and Bilkey (2009) and Terazzas *et al* (2005) found that increasing/reducing optic flow stimulation induces the place fields to shrink/enlarge and did not affect their position on the track (i.e. no remapping was observed) when optic flow manipulations were performed on their own [Lu and Bilkey (2009)]. This was not found to be the case in the present study. The size of the place fields did not change during all baselines and moving treadmill probes.

On the other hand, restraining or passively translating the rat [see Introduction for discussion] severely disrupts place fields, which either become quiescent [Foster *et al* (1989)] or remap [Lu and Bilkey (2009), Song *et al* (2005), Terrazas *et al* (2005)]. These results suggest that locomotion *per se* provides an important input to place cells. Indeed, Dayawansa *et al* (2006) found cells whose fields were directly governed by locomotion. This is corroborated by behavioural evidence in other species [Wittlinger *et al* (2006), Dominici *et al* (2009), Mittelstaedt and Mittelstaedt (2001)] showing that step length and rate are crucial for distance estimation.

In contrast to the above experiments, the moving treadmill manipulations are designed to allow the rat to move as naturally as possible and, rather than abolishing locomotion input, they put it in conflict with exteroceptive information. This conflict does not disrupt place cell activity. I showed here that only a very small percentage of cells become quiescent during moving treadmill probes [see section 4.5.1] or remap [see Supplementary figures 6.2]. The results reveal that idiothetic input is an important factor for place cells as fields shift in the direction of the treadmill.

The present results fit best with those of Sharp *et al* (1995) who found that rotational visual motion in conjunction with corroborating vestibular input are a very efficient driver of place field spatial selectivity. The moving treadmill manipulations induce concomitant changes in optic flow and motor efference; this information is integrated by the place fields that shift with the treadmill at the expense of exteroceptive information.

5.5 Relative importance of interoceptive and exteroceptive cues is related to the field's position on the track

The thesis shows that the relative importance of these two sources of information about the rat's location is governed by the position of the field on the track. Fields in the start and middle sectors of the linear track shift more than fields in the end sector of the track, particularly when the rat moves with the treadmill. The amount of shift relates to the centroid of the field in a quadratic (rather than linear) way. This is in agreement with the results of Gothard *et al* (1996a/b), Gothard *et al* (2001), Redish *et al* (2000) and Rosenweig *et al* (2003). Their proposed interpretation for this finding was that fields located closer to the start of the track are established based on a path integration computation of location in a track-bound reference framework. Farther along the track, the rat switches to a to a room-based reference, causing fields to shift less.

This conclusion is further strengthened by reconstructing the position of the rat by its path integration (*i.e.* by integrating speed and distance travelled to infer current position). When the rat moves with the treadmill, a large percentage of cells in the first 2/3 of the track shift less in the reconstructed framework than in the original, absolute spatial coordinate framework. This indicates that self-motion input is more important than landmark information for these cells.

When the rat moves against the treadmill, the majority of the cells shift less in the original, absolute framework, explaining why the quadratic fit between the position of the field and its shift during moving treadmill probes is not significant on these probes. Two explanations are consistent with this finding: either (1) the rat switches reference frameworks earlier or (2) it ignores idiothetic cues. These are discussed separately in the following sections.

5.5.1 Earlier reference frame switch

When the rat moves against (as opposed to with) the treadmill, it walks more than in baselines, both in terms of step number and time. If, as proposed by Gothard *et al* (1996a), the rat relies on path integration up to a certain length on the track and then switches to a room based reference framework, this switch should occur earlier when the rat moves against the treadmill (assuming that it is governed by the path integration mechanism rather than by some fixed landmark). The possible hallmarks of such an effect are discussed bellow.

The overall shift in the place cell population should be less than in the moving treadmill probes, particularly for cells situated closer to the beginning of the run. Section 4.2.5 shows that, for eastward firing cells the magnitude of fields shifts is less when the rat moves against the treadmill than when it moves with the treadmill. However, this result does not reach statistical significance for westward firing cells. One caveat of this analysis is that it does not take into account the position of the field on the track.

To correct this, we performed ranksum tests comparing the magnitude of the shift when the track was split into 3 sectors [see Supplementary Table 6.15]. For westward firing cells, when the rat moves against the track, the shift in the middle sector is significantly larger than the shift in the start sector, while for eastward firing cells, the shift in all 3 sectors is not significantly different. The difference in ranksum test indicates that when the rat moves against the track, the relationship of shift versus position of the field is different for eastward and westward cells. This might provide an explanation as to why for westward firing cells, the shift when the rat moves against the treadmill is not significantly lower than when it moves with the treadmill.

Consistent with the ranksum results, the quadratic fits are not significant but they are better (see lower p-values in table 4.4) for westward firing cells than for eastward firing cells when the rat moves against the track.

The difference in eastward firing versus westward firing cells could arise from: 1) statistical reasons (*i.e.* not enough power of the ranksum test to detect a significant

difference when comparing shifts with or against the treadmill or 2) an asymmetry in the east-west configuration of cues.

If the second possibility was the case, we should have observed differences in eastward- versus westward-firing cells in all the probes. In the present dataset, this was not observed. However, a rigorous test would require discriminating between the eastward and westward firing properties by examining cells that are bi-directional and have overlapping fields in both directions. In a linear track configuration, only a very small percentage of cells are bi-directional, the majority of which do not have overlapping place fields [Battaglia *et al* (2004)].

I propose therefore that the difference observed here is more likely due to the lack of power of the statistical tools used. This is supported by the fact that, when data are aggregated for eastward and westward firing cells, the shift is significantly larger for the rat moving with the treadmill than against it.

Another effect of an earlier reference switch should be that the quadratic fit of shift versus location should be flatter than in the moving with the treadmill probes. This would arise from more cells being influenced by the room-reference framework. This is confirmed by Supplementary figure 6.2, in which the quadratic fits are almost horizontal lines when the rat moves against the treadmill.

In summary of this first hypothesis, the data are suggestive of trend supporting an earlier reference frame switch.

5.5.2   *Learning effects: switching between use of exteroceptive and idiothetic cues*

Jeffrey *et al* (1997) and Knierim *et al* (1995) showed that rats ignore cues they learn to be unreliable. In the experimental paradigm used here, the rat might be able to learn that path integration is more disrupted when walking against the treadmill and it might choose to ignore idiothetic information in this case – *i.e.*, it might rely more on

exteroceptive cues in the probes where it moves against the treadmill. In these probes, the rat locomotes farther and thus dispenses more muscular effort to overcome the treadmill's motion. It is conceivable that, with experience, it can learn it will be more error-prone in estimating its location in such probes and therefore pay more attention to exteroceptive cues. Indeed, results in section 4.2.7 are also consistent with this interpretation, as more cells shift less in the original (absolute spatial coordinates) data plotting mode, indicating a stronger preference for exteroceptive cues in these probes.

However, the data here do not support a complete switch to exteroceptive cues, as place fields do exhibit significant shifts in the direction of the treadmill. Thus, this explanation is the less likely of the two.

Nonetheless, it cannot be excluded that the rat may learn to rely more on exteroceptive cues, as all the data presented here are obtained after the rat has had ample experience in this task. To quantify the extent of this learning effect would require one to record from cells on the first exposure to the moving treadmill. In practice, it is not possible to perform such experiments, since the behaviour of a naïve rat is too disrupted during its first exposure to the moving treadmill.

5.5.3   Conclusion of section: concomitant inputs

The general conclusion supported by this section is that place cells are neither path integrators nor landmark bound *per se*. Rather, they concomitantly use both types of inputs, and the relative strength of these inputs is governed by the field's location on the track. This is consistent with the result that cells shift in the direction of the treadmill in all probes and that cells showing this behaviour can be observed along the entire length of the track.

Further support for concomitant use of cues comes from the comparison of field size in the two data plotting methods (*i.e.* absolute spatial coordinates or with position inferred by the path integrator). One would expect that, if a cell is either a path

integrator or is landmark bound, it should have a tighter field in the corresponding data plotting framework. This was found to be the case only for about 50% of cells.

5.6   A preference for exteroceptive cues

This thesis shows that exteroceptive and interoceptive cues are used in combination and concomitantly by place cells, and that the relative weights of usage depend on the field's position on the track. To determine experimentally the weight of exteroceptive cues, I carried out darkness experiments in which the use of visual cues is abolished.

The darkness trial results are in agreement with those of Quirk *et al* (1990), Markus *et al* (1994) and Puryear *et al* (2006). All studies found cells that cease firing in the dark. Similar to the results reported is the present thesis, in studies carried out on a radial maze (an environment more closely related to the linear track), Markus *et al* (1994) and Puryear *et al* (2006)) found a large proportion of cells that remap or only have a field in the darkness condition.

My results show that more than a third of place fields become quiescent during darkness probes, indicating that visual input is essential for these cell's spatial firing properties. Consistent with this explanation, these cells generally did not shift significantly more during moving treadmill probes than during baselines.

The cells that fired during darkness trials either had a field similar to that in the baseline trials or remapped. These cells shifted significantly during moving treadmill probes, indicating that they are governed at least in part by interoceptive cues. However, the fact that many cells remapped during darkness trials, despite the rat being allowing to shuttle on the track with the lights on for a considerable period (so that it would perceive the environment had not changed) suggests that these cells required visual input as a path integrator anchor. Similarly, the cells that did not remap might use other types of cues [olfactory, tactile *etc* or vestibular, *e.g.* keeping track of turns at the end of the track] as a path integration anchor.

Overall, these results suggest that place cells prefer visual input to interoceptive cues. Some do so on an exclusive basis and therefore become quiescent when visual input is removed. Others can compensate by other types of cues [either interoceptive or non-visual exteroceptive], but this mechanism is imprecise and many cells remap. These results are in agreement with the fact that place cells make a hierarchical opportunistic use of available cues [see Introduction for discussion].

5.7   Future directions

The present experimental set-up is limited by the use of a linear track. This is because the rat has to stop for reward consumption at the ends of the track and therefore has to learn to back-pedal and then turn around in the probes where it moves against the track. Such movements are somewhat disruptive to the rat's behaviour and impose a stringent limitation on the speed at which the treadmill can be moved continuously. Furthermore, they make it impossible to perform darkness manipulations concomitantly with moving treadmill ones since the animal is afraid of running on the moving track in the dark.

One solution to this problem could be provided by the use of a circular track, where the rat would not have to back-pedal and turn. Another would be to have a variable speed belt which is controlled by the animal's position on the track. The second solution is technically very difficult and will not be discussed further here. Both solutions would allow for a greater range of manipulations to be performed, as discussed below.

The first question, which could be addressed by employing a larger range of treadmill speeds, is whether the amount of field shift is dependent on the speed of the treadmill and if this effect follows a linear (or possibly nonlinear) relationship. An interesting possibility is that, as the mismatch between the animal's actual location and its expected one increases, the rat's attention might actively focus on exteroceptive cues. This would reflect in the shift effect levelling off at high speeds.

Experiments on the linear track have shown that the amount of shift depends on the field's position on the track and suggested that the rat might use two reference frames (a track-bound and a room-bound one, each consistent with a different navigational strategy, i.e. path integration and landmark controlled, respectively) to establish its location. It would be interesting to see how this translates to a circular environment as in this environment there is no straightforward definition for a path integration origin point. Given this difference between the two environments, it is also possible that the relative importance that exteroceptive and interoceptive cues exert over place cells might differ across enclosures and a smaller/larger proportion of fields would shift with the treadmill or the magnitude of the shift would be different.

A third line of enquiry would rely on manipulations combining treadmill movement and darkness. This could provide a definitive answer about the extent to which cells that fire in darkness perform path integration or are established by local, non-visual exteroceptive cues. Furthermore, it would allow us to compare the relative weight assigned to path integration in light versus dark conditions at the level of individual cells. Additionally, it could ask if the shift with the treadmill in light conditions is "corrected" by exteroceptive cues (*i.e.* if cells shift more during darkness than in light conditions). If this were true, then it would constitute direct evidence that place cells integrate spatial cues in an "opportunistic fashion".

Finally, a similar paradigm could be applied to grid cells. It would then be very interesting to see how individual fields of a particular grid cell are affected by the moving treadmill paradigm, when such fields are traversed in sequence If indeed the rat uses two reference frameworks the prediction is that each field would shift by a different amount.

6 Supplementary results

This chapter follows the organisaton of chapter 4 and the same presentation order.

Please note, p-values of 0 indicate a value smaller than Matlab's numerical precision which is eps=2.22×10^{-16}. The differences in any measure between adjacent baselines, *i.e.* "subsequent - previous baseline", are labelled **delta baselines**. The differences of "probe - prior baseline" are labelled **delta probe**.

Table 6.1 QUADRATIC FIT CENTROID vs. FIELD SIZE

WESTWARD CELLS

Probe type	ef	es	wf	ws	dk
Baseline R^2	0.64	0.56	0.60	0.57	0.68
Baseline F statistic	81.40	62.12	6.73	65.30	53.55
Baseline P-value	0	0	0	0	0
Probe R^2	0.59	0.55	0.55	0.56	0.50
Probe F statistic	63.70	58.67	56.53	61.82	25.54
Probe P-value	0	0	0	0	0

EASTWARD CELLS

Probe type	ef	es	wf	ws	dk
Baseline R^2	0.60	0.52	0.59	0.53	0.58
Baseline F statistic	58.76	49.74	61.77	50.59	31.71
Baseline P-value	0	0	0	0	0
Probe R^2	0.54	0.49	0.61	0.55	0.55
Probe F statistic	46.37	43.90	67.26	54.38	27.84
Probe P-value	0	0	0	0	0

There is a strong convex relationship between field size and its position on the track, as measured by its centroid. This relationship holds for all baselines prior to probes (baseline) as well as for all the probes.

<center>***</center>

Table 6.2 QUADRATIC FIT CENTROID vs. IN-FIELD AVERAGE SPEED

WESTWARD CELLS

Probe type	ef	es	wf	ws	dk
Baseline R^2	0.57	0.43	0.51	0.49	0.69
Baseline F statistic	63.17	37.64	49.15	48.74	57.85
Baseline P-value	0	0	0	0	0
Probe R^2	0.23	0.37	0.31	0.44	0.46
Probe F statistic	14.22	28.86	21.60	38.98	22.10
Probe P-value	0	0	0	0	0

EASTWARD CELLS

Probe type	ef	es	wf	ws	dk
Baseline R^2	0.50	0.39	0.46	0.48	0.57
Baseline F statistic	43.81	27.25	37.39	52.53	25.03
Baseline P-value	0	0	0	0	5.9×10^{-8}
Probe R^2	0.35	0.29	0.28	0.31	0.31
Probe F statistic	26.69	17.61	16.54	20.76	10.69
Probe P-value	0	0	0	0	1.4×10^{-4}

There is a strong convex relationship between in-field speed and the position of the field on the track. This table indicates that the strength of this relationship is reduced during probes as compared to baselines, although it remain highly significant. This issue is investigated in Section 6.1 below.

<center>***</center>

6.1 Speed analysis

One topic of interest is how the probes affect the behaviour of the rat. This section investigates how the rat's speed changes during probes. As shown above, the position of the field on the track is related to the speed at which it is traversed. This stems from the fact that the rat runs faster in the middle of the track and this is associated with larger fields. This relationship holds true for both baseline trials and probe trials. A summary of the in-field speed changes is presented below.

WESTWARD CELLS IN-FIELD AVERAGE SPEED

Probe type	ef	es	wf	ws	dk
Median delta baselines (cm/s)	-2.76	2.77	2.59	0.08	-2.82
Mean delta baselines (cm/s)	-3.05	2.13	2.60	-0.22	-3.11
St. dev. delta baselines (cm/s)	9.52	11.16	11.72	8.32	11.12
Median delta probe (cm/s)	-19.69	-5.15	-7.17	-4.51	-19.45
Mean delta probe (cm/s)	-19.20	-6.09	-8.42	-7.81	-18.69
St. dev. delta probe (cm/s)	21.50	11.12	16.30	12.58	27.06

EASTWARD CELLS IN-FIELD AVERAGE SPEED

Probe type	ef	es	wf	ws	dk
Median delta baselines (cm/s)	0.55	-0.21	0.70	-0.08	0.61
Mean delta baselines (cm/s)	0.06	-1.19	1.77	0.66	3.26
St. dev. delta baselines (cm/s)	12.29	10.97	12.59	10.74	16.14
Median delta probe (cm/s)	-11.52	-3.95	-11.30	-7.10	-14.89
Mean delta probe (cm/s)	-11.40	-4.09	-10.80	-8.22	-17.79
St. dev. delta probe (cm/s)	14.52	11.69	16.75	15.83	30.61

A cursory glance of the data shows that in-field average speed changes by a few cm/s across successive baselines. However, in probes, the speed decreases substantially in all cases. This could reflect two things: 1) the rat runs slower during probes and 2) the position of the fields on the track changes in probes, which is reflected in the speed at which the field is traversed. Changes in field size would also affect the in-field average speed measure.

First a Kruskal Wallis comparing successive baselines reveals that all baselines are similar in terms of in-field speed and there is no intervening probe effect on baseline in-field speed. [p=0.77, χ^2=5.66, df=9 (eastward firing cells); p=0.94, χ^2=3.49, df=9 (westward firing cells) and p=0.97, χ^2=9.22, df=19 (all cells, also grouped by preferred direction of firing)].

Comparing the changes in speed in delta baselines versus delta probe the results are significant, in the sense that the speed at which the field is traversed is reduced during probes, except for east cells in the es probe [matched sample Wilcoxon sign rank tests below].

SIGN RANK IN-FIELD SPEED DELTA BASE vs. DELTA PROBE (two tailed)

Probe type	ef	es	wf	ws	dk
Westward cells p-values	6.7×10^{-11}	3.4×10^{-9}	2.9×10^{-9}	1.9×10^{-9}	2.3×10^{-5}
Eastward cells p-values	6.3×10^{-9}	0.17	3.5×10^{-8}	5.2×10^{-8}	1.2×10^{-4}

For both eastward and westward firing cells, a Kruskal Wallis analysis comparing prior baselines versus probes, grouped by trial type, yields significant results [p=0, χ^2=178.33, df=9 (westward firing cells) and p=0, χ^2=119.51, df=9 (eastward firing cells)]. A Bonferroni corrected multicomparison [at 95% significance] reveals that all probes induce a significant in-field speed decrease when compared to across baseline in-field speed changes, except for the east cells es probe (consistent with Wilcoxon tests). In all cases, the ef and dk probes cause the largest and comparable decrease in speed.

Further grouping cells by preferred direction of firing and comparing across all probe types yields similar findings [Kruskal Wallis p=0, χ^2=277.85, df=19]. A Bonferroni corrected multicomparison [at 95% significance] shows that speed changes across baselines are not significantly different, consistent with fields being stable (*i.e.* not shifting) and speed during baselines being similar. The multicomparison reveals that all probe types induce a similar speed decrease for both eastward and westward firing cells [*i.e.* running east or west, or with/against the track does not make a difference]. For both running directions, the ef and dk probes generate the largest speed decrease.

It would be interesting to establish how much of the speed decrease is due to a different running pattern during probes and how much is due to the field shifting to a different position. One prediction is that, if the observed effect is due solely to the field shifting during probes, large absolute shifts should be accompanied by large absolute speed differences and small shifts should be associated with small speed differences. This was found not to be the case [results not shown, generally correlation coefficients were small and not significant, and adding a quadratic trend did not improve the fit]. Thus, we can conclude that the main cause of the observed speed decrease is the rat running slower during probes.

The important question is whether running pattern has a significant effect. Changes in average in-field speed from baseline to probe do not significantly correlate with changes in any other field measures. Therefore, it is unlikely that speed differences bias the results in a particular way. Furthermore, since the effect is not significantly different across probe types, if there is a bias, this should affect all probes similarly.

<div align="center">***</div>

Table 6.3 QUADRATIC FIT CENTROID vs. PRECESSION SLOPE

WESTWARD CELLS

Probe type	ef	es	wf	ws	dk
Baseline R^2	0.38	0.19	0.33	0.33	0.29
Baseline F statistic	28.03	11.36	22.48	24.14	10.05
Baseline P-value	0	3.7×10^{-5}	0	0	2.1×10^{-4}
Probe R^2	0.34	0.32	0.22	0.25	0.32
Probe F statistic	23.60	23.36	12.61	15.86	11.85
Probe P-value	0	0	1.5×10^{-6}	1.1×10^{-6}	6.1×10^{-5}

EASTWARD CELLS

Probe type	ef	es	wf	ws	dk
Baseline R^2	0.27	0.15	0.16	0.06	0.19
Baseline F statistic	14.88	8.16	8.35	2.63	5.44
Baseline P-value	3.3×10^{-6}	5.5×10^{-4}	4.9×10^{-4}	0.08	0.007
Probe R^2	0.15	0.17	0.21	0.07	0.16
Probe F statistic	7.06	9.47	11.63	3.35	4.52
Probe P-value	0.001	1.8×10^{-4}	3.4×10^{-5}	0.04	0.01

There is a convex relationship between centroid and the slope of phase precession, with cells in the middle of the track exhibiting shallower precession slopes.

<center>***</center>

Table 6.4 CORRELATION CENTROID vs. FIELD SKEW

WESTWARD CELLS

Probe type	ef	es	wf	ws	dk
Baseline R	-0.34	-0.41	-0.27	-0.55	-0.29
Baseline P-value	0.0009	0	0.008	0	0.03
Probe R	-0.32	-0.30	-0.22	-0.42	-0.38
Probe P-value	0.002	0.002	0.04	0	0.004

EASTWARD CELLS

Probe type	ef	es	wf	ws	dk
Baseline R	-0.53	-0.36	-0.34	-0.40	-0.39
Baseline P-value	0	0.0004	0.001	0.0001	0.005
Probe R	-0.48	-0.46	-0.29	-0.28	-0.17
Probe P-value	0	0	0.005	0.006	0.23

Field skew and centroid are linearly related with fields closer to the end walls being skewed towards the middle of the track.

<center>***</center>

Table 6.5 QUADRATIC FIT CENTROID vs. BITS PER SPIKE INFORMATION

WESTWARD CELLS

Probe type	ef	es	wf	ws	dk
Baseline R^2	0.33	0.20	0.29	0.24	0.37
Baseline F statistic	22.49	11.88	18.45	15.52	15.04
Baseline P-value	0	2.4×10^{-5}	1.8×10^{-7}	1.4×10^{-6}	7.6×10^{-6}
Probe R^2	0.09	0.18	0.45	0.37	0.30
Probe F statistic	4.67	10.68	37.38	28.35	10.55
Probe P-value	0.02	6.5×10^{-5}	0	0	1.5×10^{-4}

EASTWARD CELLS

Probe type	ef	es	wf	ws	dk
Baseline R^2	0.23	0.21	0.36	0.17	0.27
Baseline F statistic	11.54	11.78	24.30	9.00	8.49
Baseline P-value	4.0×10^{-5}	2.8×10^{-5}	0	2.8×10^{-4}	7.2×10^{-4}
Probe R^2	0.48	0.26	0.09	0.26	0.40
Probe F statistic	36.43	16.00	4.00	15.25	15.24
Probe P-value	0	1.1×10^{-6}	0.02	2.0×10^{-6}	8.4×10^{-6}

There is a strong concave relationship between centroid and bits per spike information. Cells in the middle of the track exhibit less information than cells closer to the end walls.

<div align="center">***</div>

Table 6.6 CORRELATION FIELD SIZE vs. IN-FIELD AVERAGE SPEED

WESTWARD CELLS

Probe type	ef	es	wf	ws	dk
Baseline R	0.41	0.32	0.32	0.30	0.53
Baseline P-value	2.6×10^{-8}	9.4×10^{-8}	2.1×10^{-8}	1.1×10^{-6}	1.4×10^{-7}
Probe R	0.13	0.24	0.11	0.14	0.25
Probe P-value	0.22	0.02	0.30	0.16	0.08

EASTWARD CELLS

Probe type	ef	es	wf	ws	dk
Baseline R	0.35	0.27	0.27	0.41	0.30
Baseline P-value	$1.0\text{x}10^{-7}$	$1.4\text{x}10^{-6}$	$2.0\text{x}10^{-7}$	0	$4.2\text{x}10^{-4}$
Probe R	0.18	0.26	0.17	0.17	-0.02
Probe P-value	0.10	0.01	0.12	0.12	0.88

Field size and in field average speed are correlated, both during baselines and probes.

<center>***</center>

Table 6.7 FIELD SIZE vs. PRECESSION SLOPE

WESTWARD CELLS

Probe type	ef	es	wf	ws	dk
Baseline R	-0.61	-0.58	-0.59	-0.59	-0.52
Baseline P-value	0	0	0	0	$5.5\text{x}10^{-5}$
Probe R	-0.55	-0.58	-0.45	-0.52	-0.45
Probe P-value	0	0	$6.0\text{x}10^{-6}$	0	$7.6\text{x}10^{-4}$

EASTWARD CELLS

Probe type	ef	es	wf	ws	dk
Baseline R	-0.51	-0.44	-0.51	-0.44	-0.42
Baseline P-value	0	0	0	0	0.003
Probe R	-0.51	-0.43	-0.51	-0.46	-0.43
Probe P-value	0	0	0	0	0.006

Field size correlates strongly with the slope of phase precession, namely the larger the field the shallower the slope of the precession.

<center>***</center>

6.2 Peak firing rate analysis

The changes in peak firing rate across successive baselines (delta baselines) and from prior baseline to probe (delta probe) are summarized below.

WESTWARD CELLS PEAK RATE

Probe type	ef	es	wf	ws	dk
Median delta baselines (Hz)	-1.00	0.02	-0.54	-0.22	-1.10
Mean delta baselines (Hz)	-2.00	0.82	-1.03	-0.26	-0.69
St. dev. delta baselines (Hz)	5.51	5.48	5.23	4.58	4.79
Median delta probe (Hz)	-4.05	-0.45	-2.27	-1.36	-3.74
Mean delta probe (Hz)	-5.77	-0.91	-3.14	-2.09	-5.12
St. dev. delta probe (Hz)	6.40	6.12	5.97	5.63	9.95

EASTWARD CELLS PEAK RATE

Probe type	ef	es	wf	ws	Dk
Median delta baselines (Hz)	-1.25	-0.52	-0.77	-1.12	-0.58
Mean delta baselines (Hz)	-0.97	-1.06	-0.19	-0.37	-0.84
St. dev. delta baselines (Hz)	4.92	5.13	6.78	6.76	5.35
Median delta probe (Hz)	-2.08	-0.71	-1.26	-1.34	-2.94
Mean delta probe (Hz)	-2.24	-0.85	-2.49	-1.92	-4.10
St. dev. delta probe (Hz)	5.24	4.70	6.24	5.92	10.42

There is no difference in peak firing rate between successive baselines, irrespective of the intervening probe type [Kruskal Wallis: p=0.92, χ^2=3.83, df=9 (eastward firing cells), p=0.85, χ^2=4.82, df=9 (westward firing cells); p=0.28, χ^2=22.16, df=19 (all cells, further grouped by preferred direction of firing)].

A one sample Wilcoxon sign rank test for 0 median shows that, for both eastward and westward firing cells, the delta baselines change in peak rate is not significantly different form 0, except in the case of the ef probe for west cells.

SIGN RANK 0 MEDIAN: DELTA BASELINES PEAK RATE (two tailed)

Probe type	ef	es	wf	ws	dk
Westward cells p-values	0.002	0.19	0.09	0.35	0.22
Eastward cells p-values	0.04	0.02	0.20	0.18	0.14

However, a Kolmogorov Smirnov test shows that the distributions of delta baselines for peak rate are not significantly different across probe types [all p-values>0.01 for both eastward and westward firing cells, except p=0.005 for westward cells in ef vs. es probes].

A matched sample Wilcoxon sign rank test reveals that peak firing during probes is significantly lower, when compared to firing across successive baselines, for westward but not eastward firing cells.

SIGN RANK: DELTA BASELINES VS DELTA PROBE PEAK RATE (one tailed)

Probe type	ef	es	wf	ws	dk
Westward cells p-values	1.4×10^{-8}	1.2×10^{-3}	1.4×10^{-3}	8.0×10^{-4}	2.0×10^{-4}
Eastward cells p-values	0.04	0.39	1.9×10^{-3}	0.06	0.02

The changes in peak rate do not correlate with any other field measure [except the bits per second information to which it is computationally related]. Of interest is the fact that even though the rat runs more slowly through the field in probe trials, as shown in the previous section, this is not related to the changes in peak rate. Furthermore, while both speed and peak rate decrease for westward firing cells, they don't follow the same pattern for eastward firing cells [*i.e.* speed decreases significantly but rates generally do not].

<div align="center">***</div>

Table 6.8 SIGN RANK DELTA BASELINES P-VALUES (two tailed)

Probe type	ef	es	wf	ws
All cells p-values	0.98	0.99	0.15	0.68
Westward cells p-values	0.93	0.84	0.22	0.48
Eastward cells p-values	0.97	0.054	0.44	0.91

Fields do not shift in a consistent manner across successive baselines. The one-sample Wilcoxon signed rank test reveals that shift across successive baselines does not have a median value significantly different from 0.

***

Table 6.9 RANKSUM DELTA BASELINES

ALL CELLS P-VALUES (two tailed)

Probe type	ef	es	wf	ws
ef	-	0.95	0.27	0.86
es	-	-	0.26	0.83
wf	-	-	-	0.17

WESTWARD CELLS P-VALUES (two tailed)

Probe type	ef	es	wf	ws
ef	-	0.20	0.31	0.72
es	-	-	0.03	0.35
wf	-	-	-	0.16

EASTWARD CELLS P-VALUES (two tailed)

Probe type	ef	es	wf	ws
ef	-	0.24	0.57	0.91
es	-	-	0.52	0.21
wf	-	-	-	0.59

Probes did not influence adjacent baseline shifts at the population level. Ranksum tests for the difference in medians for the shift across successive baselines, across all probe types, failed to reach significance for all possible pairings.

***

Table 6.10 RANKSUM SIGN of SHIFT DELTA BASELINES

ALL CELLS P-VALUES (two tailed)

Probe type	ef	es	wf	ws
ef	-	0.94	0.20	0.93
es	-	-	0.22	0.87
wf	-	-	-	0.16

WESTWARD CELLS P-VALUES (two tailed)

Probe type	ef	es	wf	ws
ef	-	0.24	0.35	0.84
es	-	-	0.03	0.30
wf	-	-	-	0.24

EASTWARD CELLS P-VALUES (two tailed)

Probe type	ef	es	wf	ws
ef	-	0.19	0.38	0.92
es	-	-	0.64	0.22
wf	-	-	-	0.43

To confirm that the intervening probe induced no consistent trend in the delta baselines, the sign of the shift was considered [*i.e.* the precise magnitude of the shift was ignored but the direction was preserved]. Ranksum tests were not significant, indicating no differences across baselines.

***

Table 6.11 KOLMOGOROV SMIRNOV DELTA BASELINES SHIFT

ALL CELLS P-VALUES

Probe type	ef	es	wf	ws
ef	-	0.99	0.55	0.93
es	-	-	0.53	0.99
wf	-	-	-	0.49

WESTWARD CELLS P-VALUES

Probe type	ef	es	wf	ws
ef	-	0.55	0.79	0.92
es	-	-	0.11	0.75
wf	-	-	-	0.43

EASTWARD CELLS P-VALUES

Probe type	ef	es	wf	ws
ef	-	0.55	0.89	0.83
es	-	-	0.99	0.78
wf	-	-	-	0.81

The distributions of the shift across successive baselines, for all data sets, are not significantly different as revealed by Kolmogorov-Smirnov tests.

***

Table 6.12 TWO-TAILED FISHER 2X3 SIGN OF SHIFT DELTA BASELINES vs. DELTA PROBES

Probe type	ef	es	wf	ws
All cells p-values	0.002	9.97×10^{-5}	4.7×10^{-9}	0.04
Westward cells p-values	0.38	0.01	1.8×10^{-6}	0.15
Eastward cells p-values	8.7×10^{-4}	0.004	0.001	0.04

With minor exceptions (westward firing cells ef and ws probe), the results are significant, indicating that you can reject the null hypothesis that signs of shifts come from populations with similar distributions.

***

Table 6.13 RANKSUM DELTA PROBE SHIFT

ALL CELLS P-VALUES (two tailed)

Probe type	ef	es	wf	ws
ef	-	0.54	5.6×10^{-10}	8.7×10^{-7}
es	-	-	1.3×10^{-14}	5.0×10^{-10}
wf	-	-	-	0.036

WESTWARD CELLS P-VALUES (two tailed)

Probe type	ef	es	wf	ws
ef	-	0.93	1.9×10^{-5}	2.2×10^{-3}
es	-	-	2.0×10^{-8}	4.1×10^{-5}
wf	-	-	-	0.047

EASTWARD CELLS P-VALUES (two tailed)

Probe type	ef	es	wf	ws
ef	-	0.19	4.5×10^{-6}	8.1×10^{-5}
es	-	-	7.7×10^{-8}	7.2×10^{-6}
wf	-	-	-	0.24

There is no significant difference, at the population level, between the magnitudes of the shift during fast vs. slow moving treadmill probes. In the tables above, compare delta probe across same direction but different speed moving treadmill probes. Generally, ef vs. es and wf vs. ws pairs yielded no significant p-values [except the ws vs. wf probes for west cells], indicating no effect of treadmill speed. The p-values for eastward vs. westward treadmill moving probe pairs are all highly significant as, given that the fields shift in the direction of the track, their signs are different.

These results are confirmed by a Kruskal Wallis analysis where all probes are considered [χ^2=39.64 (westward firing cells), χ^2=43.72 (eastward firing cells), χ^2=82.3 (all cells), all $p<10^{-15}$ and df=3]. The associated Bonferroni corrected multicomparison [at 99% significance] reveals significant differences between eastward and westward moving treadmill probes, but no differences between different speeds probes.

Furthermore, when specifically considering only cells common to both slow and fast data sets, the same result was obtained [matched sample Wilcoxon sing rank test (two tailed), eastward cells: ef vs. es p=0.15, (69 cells); wf vs. ws p=0.10, (72 cells); westward cells: ef vs. es p=0.68, (72 cells); wf vs. ws p=0.0009, (76 cells)].

<div align="center">***</div>

Table 6.14 Matched cells SIGN RANK DELTA PROBE SHIFT P-VALUES (two tailed)

WESTWARD CELLS

Probe type	ef	es
wf	0.12 (63 cells)	0.04 (74 cells)
ws	0.52 (76 cells)	0.72 (76 cells)

EASTWARD CELLS

Probe type	ef	es
wf	0.05 (61 cells)	0.07 (71 cells)
ws	3.8×10^{-4} (63 cells)	0.007 (77 cells)

When considering only cells that were common to both sets [*e.g.* eastward cells that were included in both the ef and wf dataset], the same results hold as shown by matched sample Wilcoxon sign rank tests.

<div align="center">***</div>

Figure 6.1: Linear relationships between field's location on the track and probe shift

Delta probe shift relative to the field's centroid in the prior baseline for each probe type (row) and cell direction of firing (column). The green curve is the least squares linear fit, which is affected by outliers. Red curve is the absolute distance robust fit. Note that for eastward firing cells the rat moves left to right and for westward firing cells the rat moves right to left. Shifts with the treadmill are positive for the ef and es probes and negative for the wf and ws probes. The x-axis indicates the centroid of the field in the baseline prior to each probe, measured in bins. The y-axis shows the delta probe shift, measured in bins.

Figure 6.2 Quadratic relationships between field's location on the track and probe shift

Delta probe shift relative to the field's centroid in the prior baseline for each probe type (row) and cell direction of firing (column). The green curve is the least squares quadratic fit, which is affected by outliers. Red curve is the absolute distance robust fit. Note that for eastward firing cells the rat moves left to right and for westward firing cells the rat moves right to left. Shifts with the treadmill are depicted by convex curves for eastward moving treadmill probes and concave curves for westward moving treadmill probes. The x-axis indicates the centroid of the field in the baseline prior to each probe, measured in bins. The y-axis shows the delta probe shift, measured in bins.

Figure 6.3 No relationships between field's location on the track and baselines shift

Delta baselines shift relative to the field's centroid in the prior baseline for each probe type (row) and cell direction of firing (column). Note that for eastward firing cells the rat moves left to right and for westward firing cells the rat moves right to left. The x-axis indicates the centroid of the field in the baseline prior to each probe, measured in bins. The y-axis shows the delta baselines shift, measured in bins.
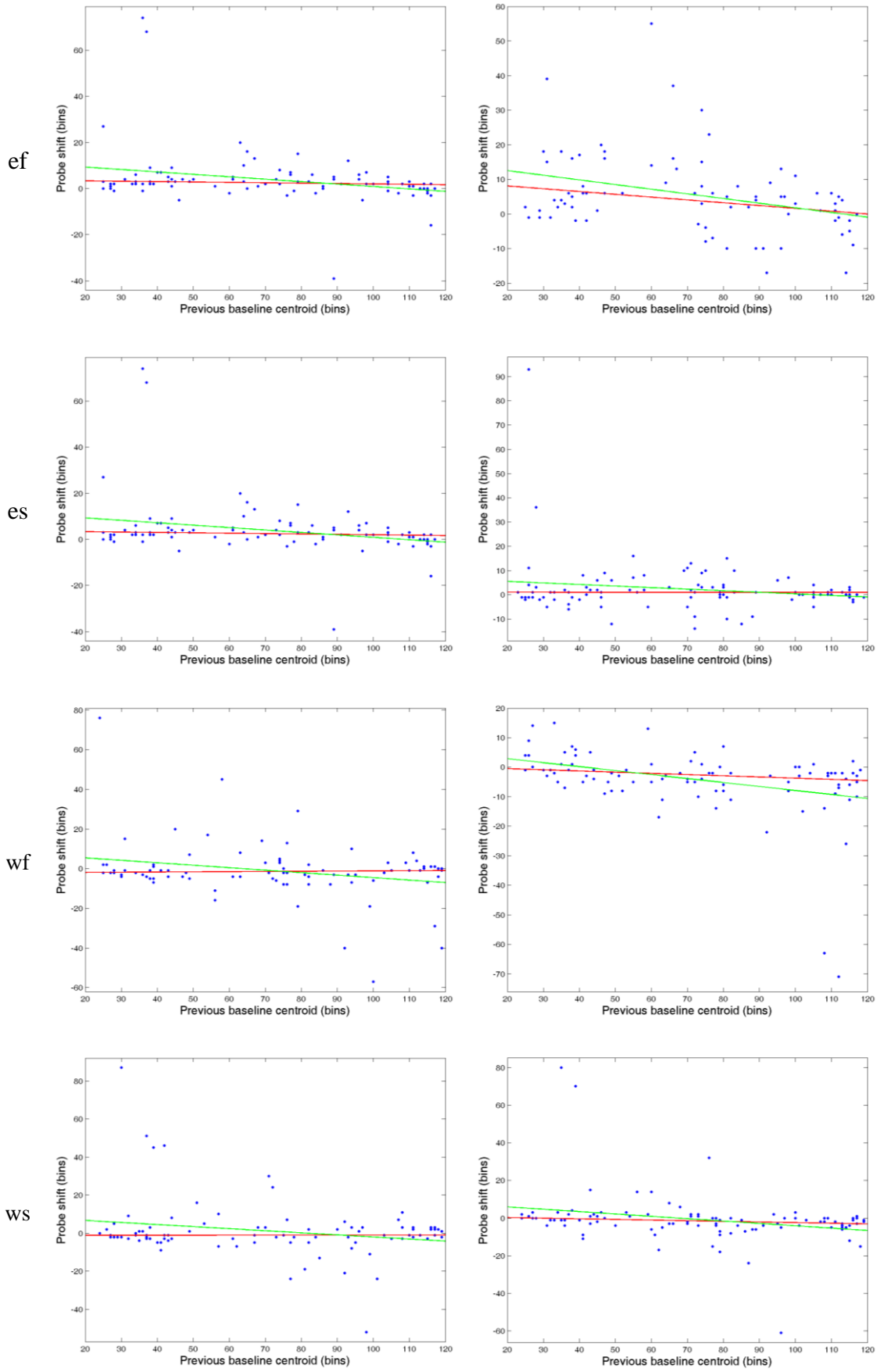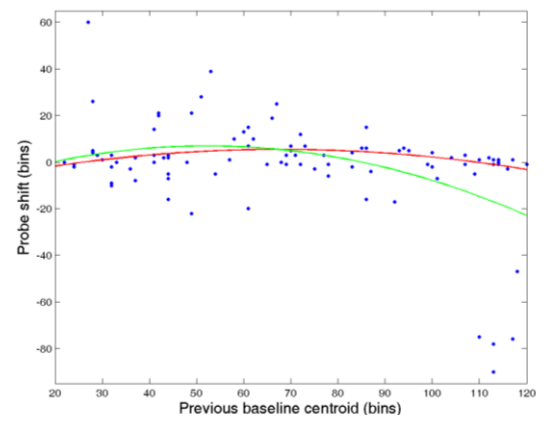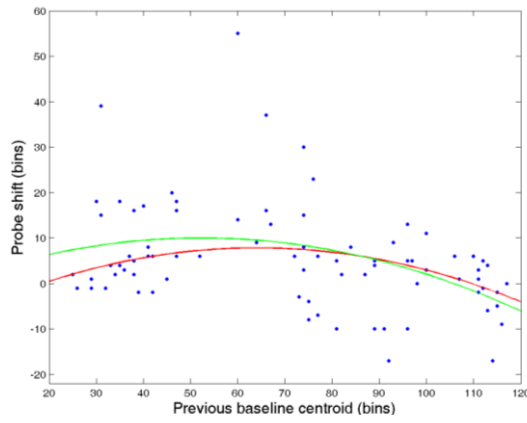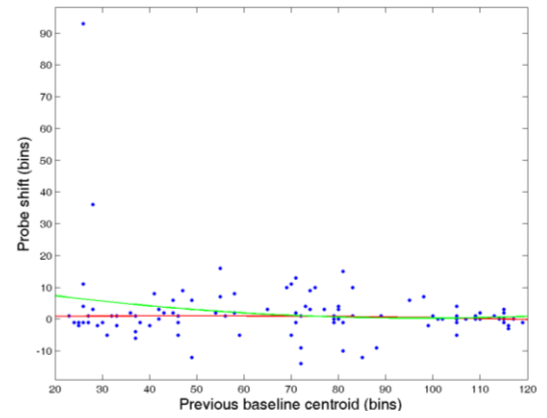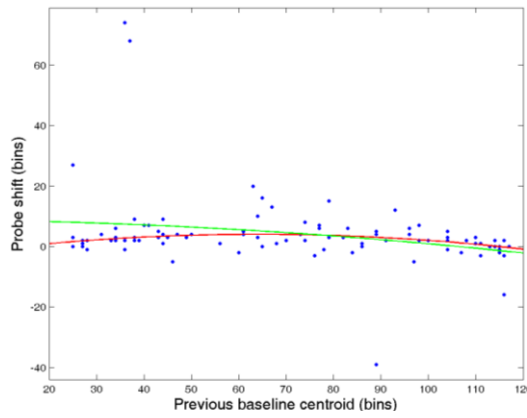
EASTWARD CELLS   WESTWARD CELLS

ef

es

wf

ws

6.2 EASTWARD CELLS   WESTWARD CELLS

ef

es

wf
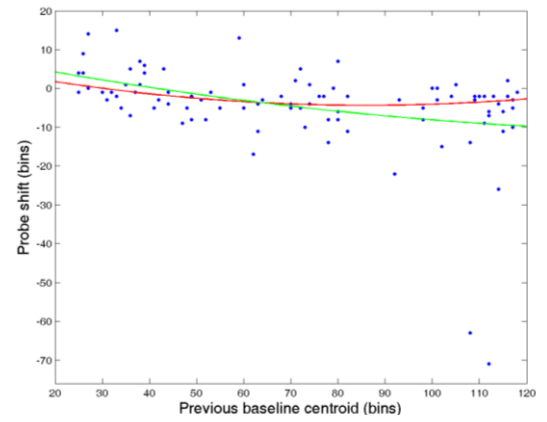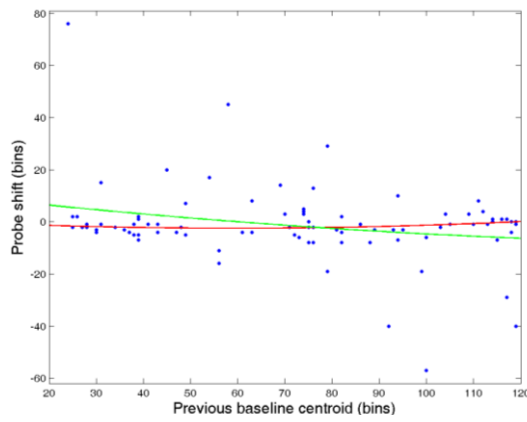
ws
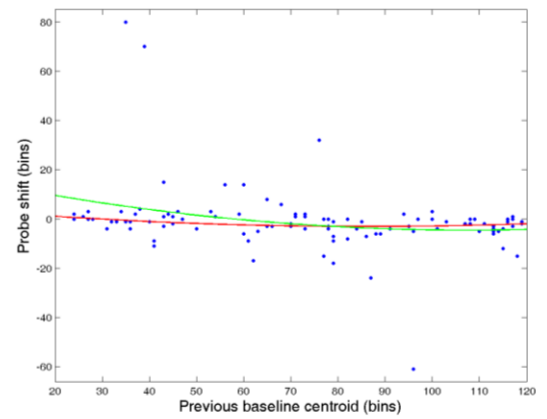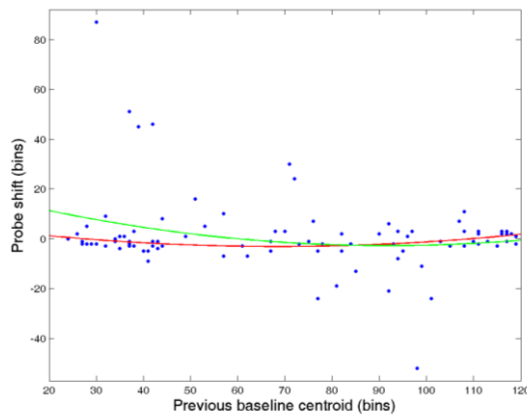
6.3 EASTWARD CELLS   WESTWARD CELLS

ef
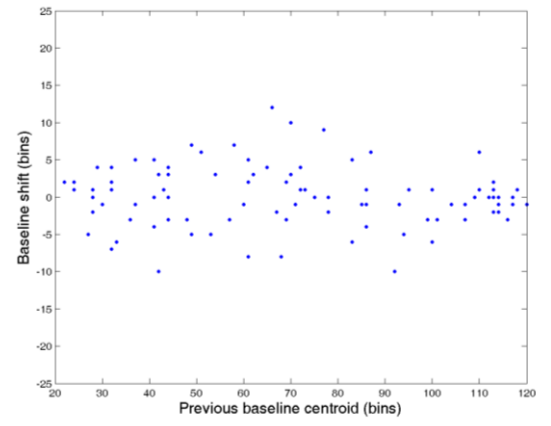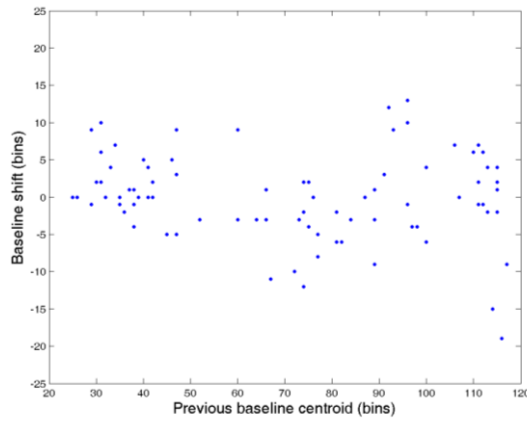
es
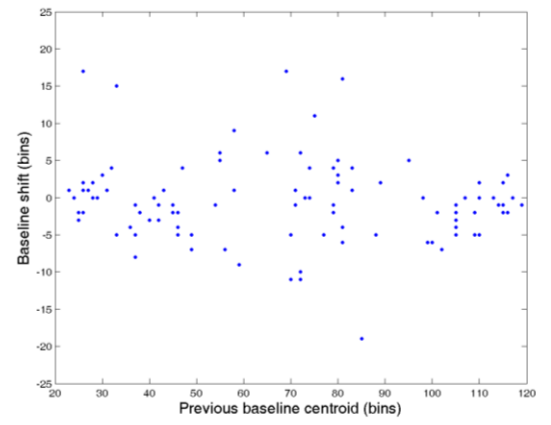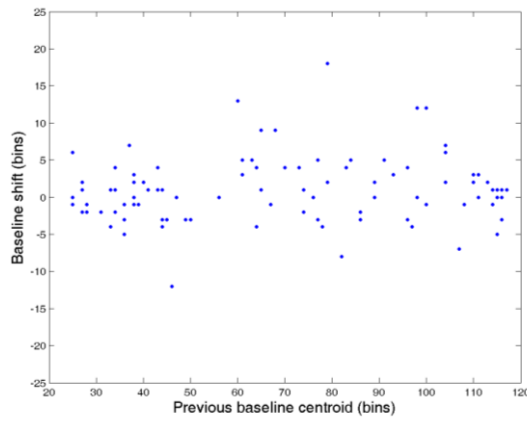
wf
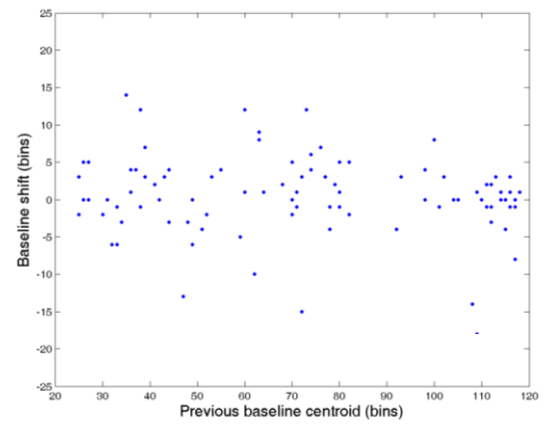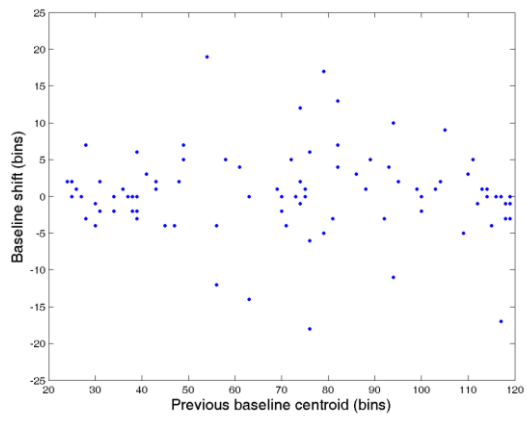
ws
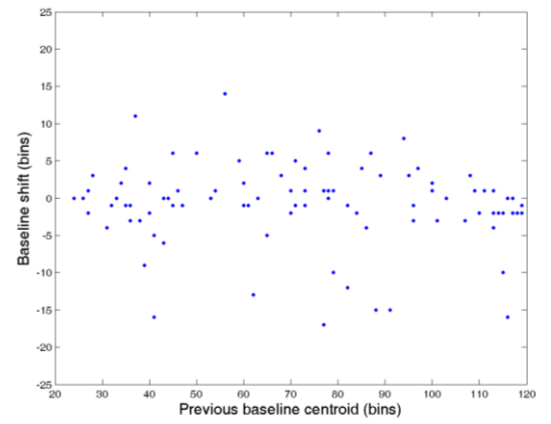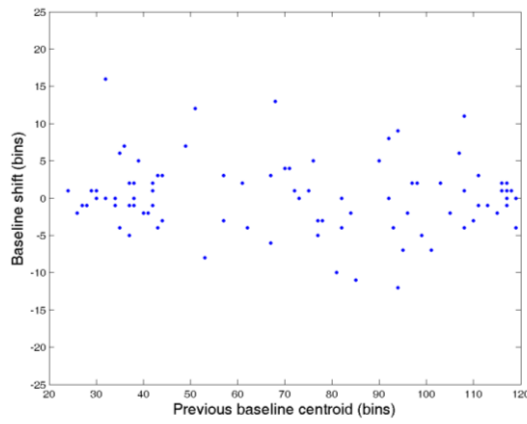
Table 6.15 RANKSUM DELTA PROBE SHIFT COMPARING THE THREE SECTIONS OF THE LINEAR TRACK

WESTWARD CELLS P_INI/P_SHUFFLE

% shuffles with RANSKSUM statistic better than original data

	Middle vs. Start	Middle vs. End	Beginning vs. End	Median Start/ No fields	Median Middle/ No fields	Median End/ No fields
ef	**0.003/0.001**	0.32/0.16	0.07/0.96	-1 (28)	3.5 (32)	1 (33)
es	**0.04/0.02**	0.18/0.09	0.76/0.62	0 (29)	2 (34)	1 (36)
wf	0.24/0.87	**0.03/0.01**	**0.006/10^{-4}**	-3 (33)	-4 (30)	-1 (31)
ws	0.48/0.76	**0.07/0.03**	**0.001/$7x10^{-4}$**	-2.5 (34)	-2.5 (36)	0 (30)

EASTWARD CELLS P_INI/P_SHUFFLE

% shuffles with RANSKSUM statistic better than original data

	Middle vs. Start	Middle vs. End	Beginning vs. End	Median Start/ No fields	Median Middle/ No fields	Median End/ No fields
ef	0.95/0.47	**0.006/0.002**	**$7x10^{-4}$/$4x10^{-4}$**	6 (30)	7 (22)	0.5 (30)
es	0.98/0.48	**0.03/0.01**	**0.007/0.004**	3 (36)	3 (26)	2 (32)
wf	0.98/0.48	0.31/0.84	0.57/0.71	-2 (29)	-2 (29)	-1 (30)
ws	0.30/0.15	0.66/0.33	0.91/0.45	-1 (37)	-2 (22)	-1 (33)

Note that initial p-values are two tailed while final p-values [obtained using the same shuffling procedure as for the quadratic fits, but with 10000 shuffles] are one tailed. Also note that start/end are relative to the rat's direction of movement [*i.e.* for the rat moving eastward the start is the west end of the track and for the rat moving westward it is the east end of the track]. The last three columns in each table indicate the median value of the shift in each track division as well as the number of cells included in each set, in brackets.

Figure 6.4 The two data plotting modes for eastward firing cells in the es,wf and ws probes.

Prior baseline centroid (x-axis) vs. probe centroid (y-axis) for the original data (column 1) and the reconstructed data (column 2). Red lines indicate the no shift location. Note that in column 1 the red line is consistent with cells that are bound to an environment frame of reference, while in column2 the red line is consistent with cell relying 100% on path integration. Note that the rat is moving from left to right.
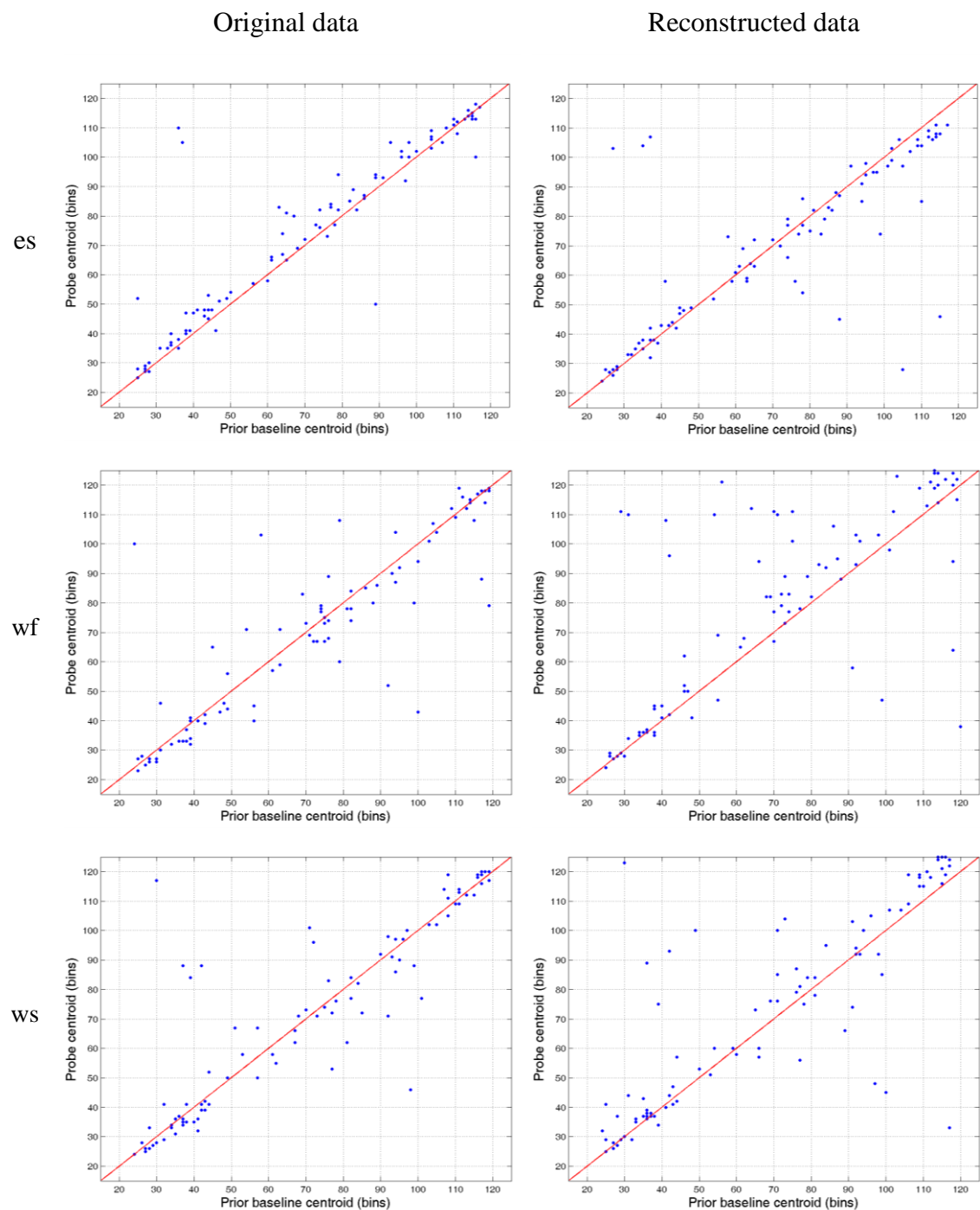
Figure 6.5 The two data plotting modes for westward firing cells in the ef, es and ws probes.

Prior baseline centroid (x-axis) vs. probe centroid (y-axis) for the original data (column 1) and the reconstructed data (column 2). Red lines indicate the no shift location. Note that in column 1 the red line is consistent with cells that are bound to an environment frame of reference, while in column2 the red line is consistent with cell relying 100% on path integration. Note that the rat is moving from right to left.
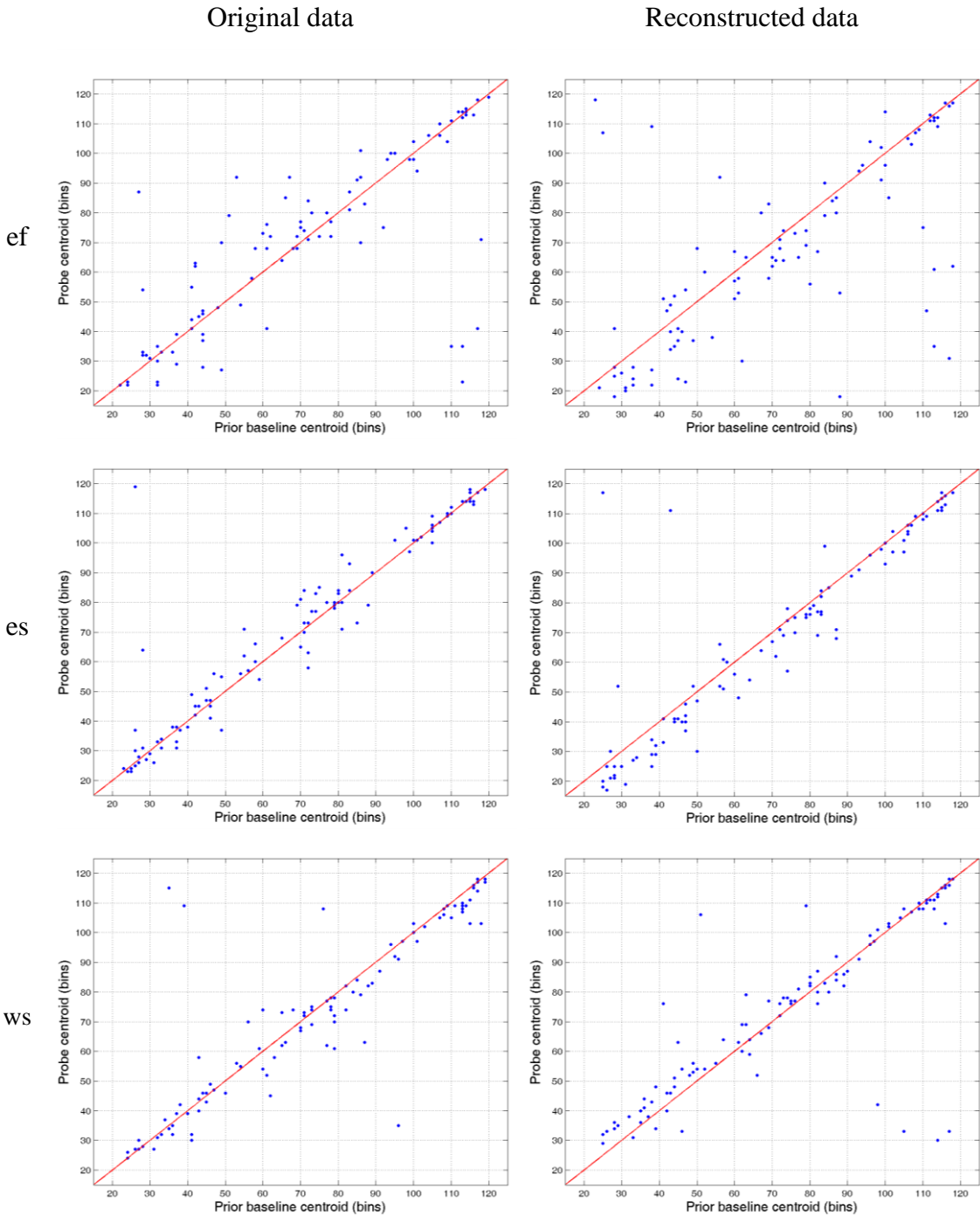
Table 6.16 FIELD SIZE CHANGES ACROSS TRIALS

ALL CELLS

Probe type	ef	es	wf	ws
No of fields	175	193	182	192
Median delta probe (in bins)	1	0	2	1.5
Mean delta probe (in bins)	1.49	0.98	2.41	2.37
St. dev. delta probe (in bins)	18.20	11.80	15.70	14.63
Median delta baselines (in bins)	-1	-1	-1	0
Mean delta baselines (in bins)	-1.12	0.05	-1.86	1.66
St. dev. delta baselines (in bins)	11.09	10.93	11.74	11.74

WESTWARD CELLS

Probe type	ef	es	wf	ws
No of fields	93	99	94	100
Median delta probe (in bins)	1	1	2	2
Mean delta probe (in bins)	0.78	1.91	2.73	1.78
St. dev. delta probe (in bins)	15.39	13.18	12.51	13.54
Median delta baselines (in bins)	0	-1	-1	0
Mean delta baselines (in bins)	-1.53	0.80	-1.24	1.66
St. dev. delta baselines (in bins)	9.50	11.76	10.65	12.96

EASTWARD CELLS

Probe type	ef	es	wf	ws
No of fields	82	94	88	92
Median delta probe (in bins)	2	0	2	1
Mean delta probe (in bins)	2.26	0.02	2.06	3.02
St. dev. delta probe (in bins)	21.00	10.12	18.58	15.78
Median delta baselines (in bins)	-1	-1	-1	0
Mean delta baselines (in bins)	-0.66	-04.7	-2.51	1.66
St. dev delta baselines (in bins)	12.71	9.98	12.83	10.32

Table 6.17 SIGN RANK 0 MEDIAN FIELD SIZE CHANGES

DELTA BASELINE P-VALUES (two tailed)

Probe type	ef	es	wf	ws
All cells	0.17	0.28	0.02	0.32
Westward cells	0.23	0.85	0.11	0.60
Eastward cells	0.49	0.18	0.07	0.37

DELTA PROBE P-VALUES (two tailed)

Probe type	ef	es	wf	ws
All cells	0.29	0.36	0.014	0.015
Westward cells	0.72	0.21	0.03	0.06
Eastward cells	0.26	0.99	0.25	0.11

The change in-field size across baselines or from prior baseline to probe was not significantly different from 0.

<center>***</center>

Table 6.18 RANKSUM DELTA BASELINES FIELD SIZE

ALL CELLS P-VALUES (two tailed)

Probe type	ef	es	wf	ws
ef	-	0.73	0.60	0.08
es	-	-	0.45	0.11
wf	-	-	-	0.02

WESTWARD CELLS P-VALUES (two tailed)

Probe type	ef	es	wf	ws
ef	-	0.55	0.82	0.23
es	-	-	0.47	0.54
wf	-	-	-	0.16

EASTWARD CELLS P-VALUES (two tailed)

Probe type	ef	es	wf	ws
ef	-	0.91	0.61	0.20
es	-	-	0.70	0.09
wf	-	-	-	0.055

There was no difference in field size changes across baselines as quantified by a ranksum tests, namely fields were similarly distorted between successive baselines, irrespective of intervening probe [except ws for all cells and eastward cells].

<div align="center">***</div>

Table 6.19 RANKSUM DELTA PROBE FIELD SIZE

ALL CELLS P-VALUES (two tailed)

Probe type	ef	es	wf	ws
ef	-	0.68	0.49	0.50
es	-	-	0.16	0.19
wf	-	-	-	0.96

WESTWARD CELLS P-VALUES (two tailed)

Probe type	ef	es	wf	ws
ef	-	0.70	0.22	0.40
es	-	-	0.28	0.54
wf	-	-	-	0.61

EASTWARD CELLS P-VALUES (two tailed)

Probe type	ef	es	wf	ws
ef	-	0.33	0.83	0.92
es	-	-	0.37	0.21
wf	-	-	-	0.76

Moreover, there was no difference in field size change from baseline to probe [ranksum test], irrespective of probe type. Thus, all probes resulted in similar responses in field size change.

Table 6.20 PRECESSION SLOPE

WESTWARD CELLS

Probe type	ef	es	wf	ws	dk
No of fields	93	99	94	100	53
Median prior baseline (in deg/cm)	-3.171	-2.751	-3.192	-3.045	-2.478
Mean prior baseline (in deg/cm)	-4.032	-3.675	-3.57	-3.99	-3.129
St. dev. prior baseline (in deg/cm)	3.591	3.003	2.898	3.948	2.73
Median probe (in deg/cm)	-2.31	-2.94	-1.764	-2.142	-1.911
Mean probe (in deg/cm)	-3.864	-4.032	-2.835	-3.129	-3.969
St. dev. probe (in deg/cm)	5.922	4.473	3.486	3.192	6.09

EASTWARD CELLS

Probe type	ef	es	wf	ws	dk
No of fields	82	94	88	92	49
Median prior baseline (in deg/cm)	-2.352	-2.961	-2.835	-3.087	-1.617
Mean prior baseline (in deg/cm)	-3.108	-3.444	-3.675	-3.696	-2.814
St. dev. prior baseline (in deg/cm)	2.898	3.108	3.633	3.36	3.906
Median probe (in deg/cm)	-1.344	-2.121	-2.646	-2.94	-1.323
Mean probe (in deg/cm)	-2.331	-2.982	-3.192	-3.591	-1.806
St. dev. probe (in deg/cm)	2.478	3.213	3.15	4.494	1.764

***

Table 6.21 PRECESSION AMOUNT

WESTWARD CELLS

Probe type	ef	es	wf	ws	dk
Median prior baseline (in deg)	201.87	173.84	167.21	173.71	174.55
Mean prior baseline (in deg)	189.64	169.88	165.39	170.84	163.33
St. dev. prior baseline (in deg)	111.21	103.31	108.04	105.44	107.19
Median probe (in deg)	124.94	171.67	114.04	142.43	99.16
Mean probe (in deg)	137.14	167.50	138.60	146.43	127.90
St. dev. probe (in deg)	113.74	108.68	109.21	108.64	114.23

EASTWARD CELLS

Probe type	ef	es	wf	ws	dk
Median prior baseline (in deg)	164.47	162.50	149.86	178.87	131.11
Mean prior baseline (in deg)	158.83	174.52	159.58	172.15	146.54
St. dev. prior baseline (in deg)	116.20	122.43	117.72	121.39	118.77
Median probe (in deg)	78.50	142.73	159.69	110.42	99.42
Mean probe (in deg)	118.791	146.10	154.08	143.23	126.20
St. dev. probe (in deg)	118.04	117.72	121.12	121.80	115.18

***

Table 6.22 PHASE-POSITION CORRELATION

WESTWARD CELLS

Probe type	ef	es	wf	ws	dk
Median prior baseline (R)	-0.55	-0.51	-0.50	-0.54	-0.52
Mean prior baseline (R)	-0.48	-0.45	-0.43	-0.46	-0.44
St. dev. prior baseline (R)	0.25	0.25	0.26	0.26	0.27
Median probe (R)	-0.40	-0.50	-0.40	-0.43	-0.37
Mean probe (R)	-0.33	-0.42	-0.35	-0.38	-0.34
St. dev. probe (R)	0.28	0.25	0.27	0.26	0.32

EASTWARD CELLS

Probe type	ef	es	wf	ws	dk
Median prior baseline (R)	-0.44	-0.48	-0.48	-0.54	-0.42
Mean prior baseline (R)	-0.39	-0.42	-0.41	-0.43	-0.37
St. dev. prior baseline (R)	0.28	0.31	0.29	0.30	0.28
Median probe (R)	-0.24	-0.40	-0.42	-0.34	-0.33
Mean probe (R)	-0.29	-0.34	-0.37	-0.34	-0.34
St. dev. probe (R)	0.29	0.30	0.28	0.32	0.28

***

6.3 Phase precession analysis

No differences were found, at the population level, in terms of precession slope, amount or phase-position correlation across successive baselines or from prior baseline to probes.

When considering each individual dataset, there is a strong correlation for all precession measures across successive baselines [SLOPE: R=0.45-0.8, p $<10^{-5}$; AMOUNT: R=0.3-0.65, p$<10^{-4}$; PHASE-POSITION CORRELATION: R=0.3-0.6, p<0.001]. Precession measures for moving treadmill probes also correlated significantly with prior baselines ones [SLOPE: R= 0.3-0.7; AMOUNT: R=0.25-0.65, PHASE-POSITION CORRELATION: R=0.2-0.5, all p<0.01]. Interestingly, the only non-significant correlations between probe and prior baseline measures were for darkness probes [p>0.35 for all measures].

When considering all prior and subsequent baselines and grouping by intervening probe type and preferred direction of firing, a Kruskall Wallis analysis yielded no significant differences [SLOPE: p=0.26, χ^2=22.54, df=19; AMOUNT: p=0.61, χ^2=16.63, df=19; PHASE-POSITION CORRELATION: p=0.27, χ^2=22.2, df=19]. Thus, all the baselines are similar.

The results for matched sample Wilcoxon sign rank test [not shown] comparing the delta baselines versus delta probe were all not significant, indicating no differences in any precession measure across trials. This was confirmed by a Kruskal Wallis analysis, whose results are detailed below.

For the <u>slope of precession</u>, Kruskal Wallis yielded p=0.002, χ^2= 26.17, df=9 (westward firing cells), p=0.07, χ^2= 15.77, df=9 (eastward firing cells), p=0.0002, χ^2=31.96, df=9 (all cells). A Bonferroni corrected multicomparison [at 95% significance] revealed no differences for the eastward or westward firing cells. When considering all cells, the change in baselines across the wf probe (delta baselines wf) was significantly different from the probe to previous baseline change for the ef and ws probes.

For <u>the amount of precession</u>, the Kruskal Wallis results were: p=1.9x10^{-5}, χ^2=37.76, df=9 (westward firing cells), p=0.18, χ^2=12.55, df=9 (eastward firing cells), p=0.0001, χ^2=33.09, df=9 (all cells). A Bonferroni corrected multicomparison [at 95% significance] revealed that the significant difference in both the westware cells and the all cells case was due to the ef probe (*i.e.* delta probe ef) which exhibited shallower median precession than the es and wf baselines (delta baselines es/wf).

For <u>the phase-position correlation</u>, the Kruskal Wallis results were: p=3.1x10^{-5}, χ^2=36.57, df=9 (westward firing cells), p=0.21, χ^2=12.08, df=9 (eastward firing cells), p=1.8x10^{-5}, χ^2=33.09, df=9 (all cells). A Bonferroni corrected multicomparison [at 95% significance] picked up exactly the same differences as in the amount of precession case.

In summary, the changes from prior baseline to probe are not significantly different from the changes across corresponding successive baselines. There appears to be a difference induced by a single probe (ef for westward firing cells). However, this is not against its adjacent baselines, but other baselines in general. This difference generates significant p-values for the Kruskal Wallis analysis, but these cannot be interpreted as evidence that precession is different in probes.

Changes in precession slope across successive baselines and from probes to the prior baseline correlate with changes in field size, at individual data set level [successive baselines: R=0.2-0.35, p<0.01; probe to prior baseline: R=0.2-0.45, p<0.01].

<p align="center">***</p>

Table 6.23 PERCENTAGE OF QUIESCENT CELLS

Probe type	ef	es	wf	ws	dk
WESTWARD CELLS % quiescent cells & (absolute field numbers excluded/included)	9.71 (10/93)	1.98 (2/99)	10.48 (11/94)	3.85 (4/100)	37.65 (33/53)
EASTWARD CELLS % quiescent cells & (absolute field numbers excluded/included)	18.81 (19/82)	2.08 (2/94)	7.37 (7/88)	5.15 (5/92)	40.24 (32/49)

More cells were quiescent during darkness probes that in any other moving treadmill probe. The percentages above were obtained by adding excluded (*i.e.* quiescent) + included cells and expressing excluded as a percentage of total number of cells for each probe. Adding excluded (*i.e.* quiescent) + included cells and expressing excluded as a percentage of total number of cells, 37.65% of the east cells and 40.24% of the west cells were quiescent during darkness, as opposed to 6.53% and 8.48% respectively during moving treadmill probes.

<center>***</center>

Table 6.24 SHIFT FOR CELLS THAT FIRE BOTH DURING DARKNESS AND MOVING TREADMILL PROBES

WESTWARD CELLS

Probe type	ef	es	wf	ws
Number of fields	43	39	43	40
Median of delta baselines (in bins)	0	-1	0	0
Mean of delta baselines (in bins)	0.49	-1.59	1.07	-1.05
St. dev. of delta baselines (in bins)	4.16	4.61	6.05	5.82
Median of delta probe (in bins)	2	0	-2	-1
Mean of delta probe (in bins)	2	1.13	-4.26	2.85
St. dev. of delta probe (in bins)	18.15	7.80	15.07	17.62
P-value sign rank test (one tailed)	0.05	0.004	0.6×10^{-4}	0.48

EASTWARD CELLS

Probe type	ef	es	wf	ws
Number of fields	41	43	39	40
Median of delta baselines (in bins)	-1	1	0	1
Mean of delta baselines (in bins)	-1.34	1.42	-0.87	1.17
St. dev. of delta baselines (in bins)	6.28	4.67	6.85	5.09
Median of delta probe (in bins)	5	2	-2	-1
Mean of delta probe (in bins)	5.10	5.67	-4.79	0.82
St. dev. of delta probe (in bins)	10.09	15.54	11.63	12.18
P-value sign rank test (one tailed)	2.3×10^{-5}	0.03	0.01	0.06

7 References

Agster KL, Burwell RD (2009) Cortical efferents of the perirhinal, postrhinal, and entorhinal cortices of the rat, *Hippocampus*, 19:1159-86

Ahissar E (2008) And motion changes it all, *Nat Neurosci*, 11:1369-70

Alyan S, Jander R (1994) Short-range homing in the house mouse, Mus musculus: Stages in the learning of directions, *Anim Behav*, 48:285-98

Amaral DG, Lavenex P (2007), in The Hippocampus Book (eds Anderson P, Morris R, Amaral D, Bliss T, O'Keefe J), 37-114, (*Oxford University Press,* Oxford, 2007)

Amaral DG, Witter MP (1995) in The Rat Nervous System 2nd edn (ed Paxinos, G), pp 444, (*Elsevier Academic Press*, San Diego, 2004)

Andres KH, von Düring M, Veh RW (1999) Subnuclear organization of the rat habenular complexes, *J Comp Neurol*, 407:130-50

Battaglia FP, Sutherland GR, McNaughton BL (2004) Local sensory cues and place cell directionality: Additional evidence of prospective coding in the hippocampus, *J Neurosci,* 24:4541–50

Best PJ, White AM, Minai A (2001) Spatial processing in the brain: the activity of hippocampal place cells, *Annu Rev Neurosci*, 24:459-86

Blair HT, Sharp PE (1996) Visual and vestibular influences on head-direction cells in the anterior thalamus of the rat, *Behav Neurosci*, 110:643-60

Bland BH, Bird J, Jackson J, Natsume K (2006) Medial septal modulation of the ascending brainstem hippocampal synchronizing pathways in the freely moving rat, *Hippocampus*, 16:11-9

Bland BH, Jackson J, Derrie-Gillespie D, Azad T, Rickhi A, Abriam J (2006) Amplitude, frequency, and phase analysis of hippocampal theta during sensorimotor processing in a jump avoidance task, *Hippocampus*, 16:673-81

Bland BH, Oddie SD (1998) Anatomical, electrophysiological and pharmacological studies of ascending brainstem hippocampal synchronizing pathways, *Neurosci Biobehav Rev*, 22:259-73

Bland BH, Oddie SD (2001) Theta band oscillation and synchrony in the hippocampal formation and associated structures: the case for its role in sensorimotor integration, *Behav Brain Res*, 127:119-36

Bostock E, Muller RU, Kubie JL (1991) Experience-dependent modifications of hippocampal place cell firing, *Hippocampus*, 1:193-205

Bures J, Fenton AA, Kaminsky Y, Rossier J, Sacchetti B, Zinyuk L (1997) Dissociation of exteroceptive and idiothetic orientation cues: effect on hippocampal place cells and place navigation, *Philos Trans R Soc Lond B Biol Sci*, 352:1515-24

Burwell RD, Amaral DG (1998) Cortical afferents of the perirhinal, postrhinal, and entorhinal cortices of the rat, *J Comp Neurol*, 398:179-205

Buzsáki G (1996) The hippocampo-neocortical dialogue, *Cereb Cortex*, 6:81-92

Buzsáki G (2002) Theta oscillations in the hippocampus, *Neuron*, 33:325-40

Buzsáki G (2005) Theta rhythm of navigation: link between path integration and landmark navigation, episodic and semantic memory, *Hippocampus*, 15:827-40

Buzsáki G, Draguhn A (2004) Neuronal oscillations in cortical networks, *Science*, 304:1926-9

Celio MR (1990) Calbindin D-28k and parvalbumin in the rat nervous system, *Neruoscience*, 35:375-475

Cheng S, Frank LM (2008) New experiences enhance coordinated neural activity in the hippocampus, *Neuron*, 57:303-13

Cho J, Sharp PE (2001) Head direction, place, and movement correlates for cells in the rat retrosplenial cortex, *Behav Neurosci*, 115:3-25

Clark BJ and Taube JS (2009) Deficits in landmark navigation and path integration after lesions of the interpeduncular nucleus, *Behav Neurosci*, 123:490-503

Clark BJ, Sarma A, Taube JS (2009) Head direction cell instability in the anterior dorsal thalamus after lesions of the interpeduncular nucleus, *J Neurosci*, 29:493-507

Crapse TB, Sommer MA (2008) Corollary discharge circuits in the primate brain, *Curr Opin Neurobiol*, 18:552-7

Cressant A, Muller RU, Poucet B (1997) Failure of centrally placed objects to control the firing fields of hippocampal place cells, *J Neurosci*, 17:2531-42

Cressant A, Muller RU, Poucet B (1999) Further study of the control of place cell firing by intra-apparatus objects, *Hippocampus*, 9:423-31

Cressant A, Muller RU, Poucet B (2002) Remapping of place cell firing patterns after maze rotations, Exp *Brain Res*, 143:470-9

Csicsvari J, Hirase H, Czurkó A, Mamiya A, Buzsáki G (1999) Fast network oscillations in the hippocampal CA1 region of the behaving rat, *J Neurosci*, 19:RC20

Csicsvari J, Hirase H, Mamiya A, Buzsáki G (2000) Ensemble patterns of hippocampal CA3-CA1 neurons during sharp wave-associated population events, *Neuron*, 28:585-94

Csicsvari J, O'Neill J, Allen K, Senior T (2007) Place-selective firing contributes to the reverse-order reactivation of CA1 pyramidal cells during sharp waves in open-field exploration, *Eur J Neurosci*, 26:704-16

Czurkó A, Hirase H, Csicsvari J, Buzsáki G (1999) Sustained activation of hippocampal pyramidal cells by 'space clamping' in a running wheel, *Eur J Neurosci*, 11:344-52

Davidson TJ, Kloosterman F, Wilson AW (2009), Hippocampal replay of extended experience, *Neuron*, 63:497-507

Davoodi FG, Motamedi F, Naghdi N, Akbari E (2009) Effect of reversible inactivation of the reuniens nucleus on spatial learning and memory in rats using Morris water maze task, *Behav Brain Res*, 198 :130-5

Dayawansa S, Kobayashi T, Hori E, Umeno K, Tazumi T, Ono T, Nishijo H (2006) Conjunctive effects of reward and behavioral episodes on hippocampal place-differential neurons of rats on a mobile treadmill, *Hippocampus*, 16:586-95

Diba K, Buzsáki G (2007) Forward and reverse hippocampal place-cell sequences during ripples, *Nat Neurosci*, 10:1241-2

Dickinson MH, Farley CT, Full RJ, Koehl MA, Kram R, Lehman S (2000) How animals move: an integrative view, *Science*, 288:100-6

Dominici N, Dati E, Nico D, Cappellini G, Ivanenko YP, Lacquaniti F (2009) Changes in the limb kinematics and walking-distance estimation after shank elongation: evidence for a locomotor body schema?, *J Neurophysiol*, 101:1419-29

Ego-Stengel V, Wilson MA (2007) Spatial selectivity and theta phase precession in CA1 interneurons, *Hippocampus*, 17:161-74

Etienne AS, Jeffery KJ (2004) Path integration in mammals, *Hippocampus*, 14:180-92

Etienne AS, Lambert SJ, Reverdin B, Teroni E (1993), Learning to recalibrate the role of dead reckoning and visual cues in spatial navigation, *Anim Learn & Behav,* 21:266-80

Etienne AS, Maurer R, Séguinot V (1996) Path integration in mammals and its interaction with visual landmarks, *J Exp Biol*, 199:201-9

Fenton AA, Csizmadia G, Muller RU (2000) Conjoint control of hippocampal place cell firing by two visual stimuli: I The effects of moving the stimuli on firing field positions, *J Gen Physiol*,116:191-210

Fenton AA, Kao HY, Neymotin SA, Olypher A, Vayntrub Y, Lytton WW, Ludvig N (2008) Unmasking the CA1 ensemble place code by exposures to small and large

environments: more place cells and multiple, irregularly arranged, and expanded place fields in the larger space, *J Neurosci*, 28:11250-62

Fenton AA, Muller RU (1998) Place cell discharge is extremely variable during individual passes of the rat through the firing field, *Proc Natl Acad Sci USA,* 95:3182-87

Fisher NI, (1993) Statistical analysis of circular data, (*Cambridge University Press*, Cambridge, 1993)

Foster DJ, Wilson MA (2006) Reverse replay of behavioural sequences in hippocampal place cells during the awake state, *Nature*, 440:680-3

Foster TC, Castro CA, McNaughton BL (1989) Spatial selectivity of rat hippocampal neurons: dependence on preparedness for movement, *Science,* 244:1580–1582

Frank LM, Brown EN, Wilson MA (2000), Trajectory Encoding in the Hippocampus and Entorhinal Cortex, *Neuron*, 27:169-178

Freund TF, Buzsáki G (1996) Interneurons of the hippocampus, *Hippocampus*, 6:347-470

Fuhs MC, Vanrhoads SR, Casale AE, McNaughton B, Touretzky DS (2005) Influence of path integration versus environmental orientation on place cell remapping between visually identical environments, *J Neurophysiol*, 94:2603-16

Furtak SC, Wei SM, Agster KL, Burwell RD (2007) Functional neuroanatomy of the parahippocampal region in the rat: the perirhinal and postrhinal cortices, *Hippocampus*, 17:709-22

Gavrilov VV, Wiener SI, Berthoz A (1998) Discharge correlates of hippocampal complex spike neurons in behaving rats passively displaced on a mobile robot, *Hippocampus*, 8:475-90

Geisler C, Robbe D, Zugaro M, Sirota A, Buzsáki G (2007) Hippocampal place cell assemblies are speed-controlled oscillators, *Proc Natl Acad Sci USA*, 104:8149-54

Gerfen CR (2004) in The Rat Nervous System 3rd edn (ed Paxinos, G), 455-508 (*Elsevier Academic Press*, San Diego, 2004)

Goodridge JP, Taube JS (1995) Preferential use of the landmark navigational system by head direction cells in rats, *Behav Neurosci,* 109:49-61

Gothard KM, Hoffman KL, Battaglia FP, McNaughton BL (2001) Dentate gyrus and ca1 ensemble activity during spatial reference frame shifts in the presence and absence of visual input, *J Neurosci*, 21:7284-92

Gothard KM, Skaggs WE, McNaughton BL (1996a) Dynamics of mismatch correction in the hippocampal ensemble code for space: interaction between path integration and environmental cues, *J Neurosci,* 16:8027–40

Gothard KM, Skaggs WE, Moore KM, McNaughton BL (1996b) Binding of hippocampal CA1 neural activity to multiple reference frames in a landmark-based navigation task, *J Neurosci*, 16:823-35

Goulding M (2009) Circuits controlling vertebrate locomotion: moving in a new direction, *Nat Rev Neurosci*, 10:507-18

Groenewegen HJ and Witter MP (2004) in The Rat Nervous System 3rd edn (ed Paxinos, G), 407-53 (*Elsevier Academic Press*, San Diego, 2004)

Hafting T, Fyhn M, Molden S, Moser MB, Moser E (2005) Microstructure of a spatial map in the entorhinal cortex, *Nature,* 436:801–6

Hallworth NE, Bland BH (2004) Basal ganglia--hippocampal interactions support the role of the hippocampal formation in sensorimotor integration, *Exp Neurol*, 188:430-43

Harker KT, Whishaw IQ (2004) A reaffirmation of the retrosplenial contribution to rodent navigation: reviewing the influences of lesion, strain, and task, *Neurosci Biobehav Rev*, 28:485-96

Harris KD, Henze DA, Csicsvari J, Hirase H, Buzsáki G (2000) Accuracy of tetrode spike separation as determined by simultaneous intracellular and extracellular measurements, *J Neurophysiol*, 84 :401-14

Harris KD, Henze DA, Hirase H, Leinekugel X, Dragoi G, Czurkó A, Buzsáki G (2002) Spike train dynamics predicts theta-related phase precession in hippocampal pyramidal cells, *Nature*, 417:738-41

Harris KD, Hirase H, Leinekugel X, Henze DA, Buzsáki G (2001) Temporal interaction between single spikes and complex spike bursts in hippocampal pyramidal cells, *Neuron,* 32:141-9

Henze DA, Borhegyi Z, Csicsvari J, Mamiya A, Harris KD, Buzsáki G (2000) Intracellular features predicted by extracellular recordings in the hippocampus in vivo, *J Neurophysiol*, 84:390-400

Hetherington PA, Shapiro ML (1997) Hippocampal place fields are altered by the removal of single visual cues in a distance-dependent manner, *Behav Neurosci*, 111:20-34

Hill B, Best P (1981) Effects of deafness and blindness on the spatial correlates of hippocampal unit activity in the rat, *Exp Neurol,* 74:204-17

Hirase H, Czurkó A, Csicsvari J, Buzsáki G (1999) Firing rate and theta-phase coding by hippocampal pyramidal neurons during 'space clamping', *Eur J Neurosci*, 11:4373-80

Hok V, Lenck-Santini PP, Roux S, Save E, Muller RU, Poucet B (2007) Goal-related activity in hippocampal place cells, *J Neurosci*, 27:472-82

Horii A, Russell NA, Smith PF, Darlington CL, Bilkey DK (2004) Vestibular influences on CA1 neurons in the rat hippocampus: an electrophysiological study in vivo, *Exp Brain Res,*155:245-50

Horii A, Takeda N, Mochizuki T, Okakura-Mochizuki K, Yamamoto Y, Yamatodani A (1994) Effects of vestibular stimulation on acetylcholine release from rat hippocampus: an in vivo microdialysis study, *J Neurophysiol*, 72:605-11

Huxter JR, Burgess N, O'Keefe J (2003) Independent rate and temporal coding in hippocampal pyramidal cells, *Nature,* 425:828-32

Huxter JR, Senior TJ, Allen K, Csicsvari J (2008) Theta phase-specific codes for two-dimensional position, trajectory and heading in the hippocampus, *Nat Neurosci*, 11:587-94

Jahn K, Wagner J, Deutschländer A, Kalla R, Hüfner K, Stephan T, Strupp M, Brandt T (2009) Human hippocampal activation during stance and locomotion: fMRI study on healthy, blind, and vestibular-loss subjects, *Ann NY Acad Sci*, 1164:229-35

Jeewajee A, Lever C, Burton S, O'Keefe J, Burgess N (2008) Environmental novelty is signaled by reduction of the hippocampal theta frequency, *Hippocampus*, 18:340-8

Jeffery KJ (1998) Learning of landmark stability and instability by hippocampal place cells, *Neuropharmacology*, 37:677-87

Jeffery KJ, Donnett JG, Burgess N, O'Keefe JM (1997) Directional control of hippocampal place fields, *Exp Brain Res*, 117:131-42

Jeffery KJ, O'Keefe JM (1999) Learned interaction of visual and idiothetic cues in the control of place field orientation, *Exp Brain Res*, 127:151-61

Jones BF, Witter MP (2007) Cingulate cortex projections to the parahippocampal region and hippocampal formation in the rat, *Hippocampus*, 17:957-76

Jordan LM (1998) Initiation of locomotion in mammals, *Ann NY Acad Sci*, 860:83-93

Kerr KM, Agster KL, Furtak SC, Burwell RD (2007) Functional neuroanatomy of the parahippocampal region: the lateral and medial entorhinal areas, *Hippocampus*, 17:697-708

Kiehn O (2006) Locomotor circuits in the mammalian spinal cord, *Annu Rev Neurosci*, 29:279-306

Klausberger T, Somogyi P (2008) Neuronal diversity and temporal dynamics: the unity of hippocampal circuit operations, *Science*, 321:53-7

Knierim JJ (2002) Dynamic interactions between local surface cues, distal landmarks, and intrinsic circuitry in hippocampal place cells, *J Neurosci*, 22:6254-64

Knierim JJ, Kudrimoti HS, McNaughton BL (1995) Place cells, head direction cells, and the learning of landmark stability, *J Neurosci*, 15:1648-59

Knierim JJ, Kudrimoti HS, McNaughton BL (1998) Interactions between idiothetic cues and external landmarks in the control of place cells and head direction cells, *J Neurophysiol*, 80:425-46

Knierim JJ, McNaughton BL (2001) Hippocampal place-cell firing during movement in three-dimensional space, *J Neurophysiol*, 85:105-16

Knierim JJ, Rao G (2003) Distal landmarks and hippocampal place cells: effects of relative translation versus rotation, *Hippocampus*, 13:604-17

Krout KE, Belzer RE, Loewy AD (2002) Brainstem projections to midline and intralaminar thalamic nuclei of the rat, *J Comp Neurol*, 448:53-101

Kubie JL, Fenton AA (2009) Heading-vector navigation based on head-direction cells and path integration, *Hippocampus*, 19:456-79

Lavenex P, Schenk F (1995) Influence of local environmental olfactory cues on place learning in rats, *Physiol Behav*, 58:1059-66

Lavenex P, Schenk F (1998) Olfactory traces and spatial learning in rats, *Anim Behav*, 56:1129-36

Lecourtier L, Kelly PH (2007) A conductor hidden in the orchestra? Role of the habenular complex in monoamine transmission and cognition, *Neurosci Biobehav Rev*, 31:658-72

Lee AK, Wilson MA (2002) Memory of sequential experience in the hippocampus during slow wave sleep, *Neuron*, 36:1183-94

Lee I, Knierim JJ (2007) The relationship between the field-shifting phenomenon and representational coherence of place cells in CA1 and CA3 in a cue-altered environment, *Learn Mem*, 14:807-15

Lenck-Santini PP, Muller RU, Save E, Poucet B (2002) Relationships between place cell firing fields and navigational decisions by rats, *J Neurosci*, 22:9035-47

Leutgeb JK, Leutgeb S, Moser MB, Moser EI (2007) Pattern separation in the dentate gyrus and CA3 of the hippocampus, *Science,* 315:961–6

Lever C, Wills T, Cacucci F, Burgess N, O'Keefe J (2002) Long-term plasticity in hippocampal place-cell representation of environmental geometry, *Nature*, 416: 90-4

Louie K, Wilson MA (2001) Temporally structured replay of awake hippocampal ensemble activity during rapid eye movement sleep, *Neuron*, 29:145-56

Lu X, Bilkey DK (2009) The velocity-related firing property of hippocampal place cells is dependent on self-movement, *Hippocampus,* [Epub ahead of print DOI: 101002/hipo20666]

Lubenov EV, Siapas AG (2009) Hippocampal theta oscillations are travelling waves, *Nature*, 459:534-9

Maaswinkel H, Whishaw IQ (1999) Homing with locale, taxon, and dead reckoning strategies by foraging rats: sensory hierarchy in spatial navigation, *Behav Brain Res*, 99:143-52

Markus EJ, Barnes CA, McNaughton BL, Gladden VL, Skaggs WE (1994) Spatial information content and reliability of hippocampal CA1 neurons: effects of visual input, *Hippocampus,* 4:410-21

Markus EJ, Qin YL, Leonard B, Skaggs WE, McNaughton BL, Barnes CA (1995) Interactions between location and task affect the spatial and directional firing of hippocampal neurons, *J Neurosci,* 15:7079-94

Marlinski V, McCrea RA (2009) Self-motion signals in vestibular nuclei neurons projecting to the thalamus in the alert squirrel monkey, *J Neurophysiol*, 101:1730-41

Matthews BL, Ryu JH, Bockaneck C (1989) Vestibular contribution to spatial orientation Evidence of vestibular navigation in an animal model, *Acta Otolaryngol Suppl*, 468:149-54

Maurer AP, Cowen SL, Burke SN, Barnes CA, McNaughton BL (2006) Phase precession in hippocampal interneurons showing strong functional coupling to individual pyramidal cells, *J Neurosci*, 26:13485-92

Maurer AP, McNaughton BL (2007) Network and intrinsic cellular mechanisms underlying theta phase precession of hippocampal neurons, *Trends Neurosci*, 30:325-33

Maurer AP, Vanrhoads SR, Sutherland GR, Lipa P, McNaughton BL (2005) Self-motion and the origin of differential spatial scaling along the septo-temporal axis of the hippocampus, *Hippocampus*, 15:841-52

McNaughton BL, Barnes CA, Gerrard JL, Gothard K, Jung MW, Knierim JJ, Kudrimoti H, Qin Y, Skaggs WE, Suster M, Weaver KL (1996) Deciphering the hippocampal polyglot: the hippocampus as a path integration system, *J Exp Biol*, 199:173-85

McNaughton BL, Barnes CA, O'Keefe J (1983) The contributions of position, direction, and velocity to single unit activity in the hippocampus of freely-moving rats, *Exp Brain Res*, 52:41-9

McNaughton BL, Battaglia FP, Jensen O, Moser EI, Moser MB (2006) Path integration and the neural basis of the 'cognitive map', *Nat Rev Neurosci*, 7:663-78

Mehta MR, Barnes CA, McNaughton BL (1997) Experience-dependent, asymmetric expansion of hippocampal place fields *Proc Natl Acad Sci USA*, 94: 8918–21

Mehta MR, Lee AK, Wilson MA (2002) Role of experience and oscillations in transforming a rate code into a temporal code, Nature, 417:741-6

Mehta MR, Quirk MC, Wilson MA (2000) Experience-dependent, asymmetric shape of hippocampal receptive fields, *Neuron*, 25:707-15

Merrill EG, Ainsworth A (1972) Glass-coated platinum-plated tungsten microelectrodes, Med & Biol Eng, 10:662-72

Mittelstaedt H (2000) Triple-loop model of path control by head direction and place cells, *Biol Cybern*, 83:261-70

Mittelstaedt ML, Mittelstaedt H (1980) Homing by path integration in a mammal, *Naturwissenschaften*, 67:566-7

Mittelstaedt ML, Mittelstaedt H (2001) Idiothetic navigation in humans: estimation of path length, Exp *Brain Res*, 139:318-32

Montgomery SM, Betancur MI, Buzsáki G (2009) Behavior-dependent coordination of multiple theta dipoles in the hippocampus, *J Neurosci*, 29:1381-94

Muller RU, Bostock E, Taube JS, Kubie JL (1994) On the directional firing properties of hippocampal place cells, *J Neurosci*, 14:7235-51

Muller RU, Kubie JL (1987) The effects of changes in the environment on the spatial firing of hippocampal complex-spike cells, *J Neurosci*, 7:1951-68

Muller RU, Kubie JL, Ranck JB Jr (1987) Spatial firing patterns of hippocampal complex spike cells in a fixed environment *J Neurosci*, 7:1935–50

Murray EA, Bussey TJ, Sasida LM (2007) Visual perception and memory: A new view of medial temporal lobe function in primates and rodents, *Annu Rev Neruosci*, 30:99-122

Nádasdy Z, Hirase H, Czurkó A, Csicsvari J, Buzsáki G (1999) Replay and time compression of recurring spike sequences in the hippocampus, *J Neurosci*, 19:9497-507

Nitz D (2009) Parietal cortex, navigation, and the construction of arbitrary reference frames for spatial information, *Neurobiol Learn Mem*, 91:179-85

O'Keefe J (2007) in The Hippocampus Book (eds Anderson P, Morris R, Amaral D, Bliss T, O'Keefe J), 475-548 (*Oxford University Press,* Oxford, 2007)

O'Keefe J, Burgess N (1996) Geometric determinants of the place fields of hippocampal neurons, *Nature*, 381:425-8

O'Keefe J, Conway DH (1978) Hippocampal place units in the freely moving rat: why they fire where they fire, *Exp Brain Res*, 31:573-90

O'Keefe J, Dostrovsky J (1971) The hippocampus as a spatial map Preliminary evidence from unit activity in the freely moving rat, *Brain Res*, 34:171-5

O'Keefe J, Nadel L (1978) The hippocampus as a cognitive map, (*Oxford University Press,* Oxford, 1978)

O'Keefe J, Recce ML (1993) Phase relationship between hippocampal place units and the LFP theta rhythm, *Hippocampus*, 3:317–30

O'Keefe, J (1976) Place units in the hippocampus of the freely moving rat, *Exp Neurol,* 51:78–109

Olypher AV, Lánský P, Fenton AA (2002) Properties of the extra-positional signal in hippocampal place cell discharge derived from the overdispersion in location-specific firing, *Neuroscience*, 111:553-66

O'Neill J, Senior T, Csicsvari J (2006) Place-selective firing of CA1 pyramidal cells during sharp wave/ripple network patterns in exploratory behavior, *Neuron*, 49:143-55

O'Neill J, Senior TJ, Allen K, Huxter JR, Csicsvari J (2008) Reactivation of experience-dependent cell assembly patterns in the hippocampus, *Nat Neurosci*, 11:209-15

Palomero-Gallagher N and Zilles K (2004) in The Rat Nervous System 3rd edn (ed Paxinos, G), 729-57 (*Elsevier Academic Press*, San Diego, 2004)

Pan WX, McNaughton N (2004) The supramammillary area: its organization, functions and relationship to the hippocampus, *Prog Neurobiol*, 74:127-66

Paz-Villagrán V, Lenck-Santini PP, Save E, Poucet B (2002), Properties of place cell firing after damage to the visual cortex, *Eur J Neurosci,* 16:771-6

Paz-Villagrán V, Save E, Poucet B (2004) Independent coding of connected environments by place cells, *Eur J Neurosci*, 20:1379-90

Paz-Villagrán V, Save E, Poucet B (2006) Spatial discrimination of visually similar environments by hippocampal place cells in the presence of remote recalibrating landmarks, *Eur J Neurosc*, 23:187-95

Poucet B, Lenck-Santini PP, Paz-Villagrán V, Save E (2003) Place cells, neocortex and spatial navigation: a short review, *J Physiol Paris*, 97:537-46

Puryear CB, King M, Mizumori SJ (2006) Specific changes in hippocampal spatial codes predict spatial working memory performance, *Behav Brain Res*, 169:168-75

Quirk GJ, Muller RU, Kubie JL (1990) The firing of hippocampal place cells in the dark depends on the rat's recent experience, *J Neurosci*, 10:2008–17

Ranck JB Jr (1973) Studies on single neurons in dorsal hippocampal formation and septum in unrestrained rats I Behavioral correlates and firing repertoires, *Exp Neurol*, 41:461-531

Ranck JB Jr (1984) Head-direction cells in the deep cell layers of the dorsal presubiculum in freely moving rats, *Soc Neurosci Abstr*, 10:599

Redish AD, Rosenzweig ES, Bohanick JD, McNaughton BL, Barnes CA (2000) Dynamics of hippocampal ensemble activity realignment: time versus space, *J Neurosci*, 20:9298-309

Renaudineau S, Poucet B, Save E (2007) Flexible use of proximal objects and distal cues by hippocampal place cells, *Hippocampus*, 17:381-95

Risold PY (2004) in The Rat Nervous System 3rd edn (ed Paxinos, G), 605-32 (*Elsevier Academic Press*, San Diego, 2004)

Rosenzweig ES, Redish AD, McNaughton BL, Barnes CA (2003) Hippocampal map realignment and spatial learning, *Nat Neurosci*, 6:609-15

Rossier J, Haeberli C, Schenk F (2000) Auditory cues support place navigation in rats when associated with a visual cue, *Behav Brain Res*, 117:209-14

Rossier J, Schenk F (2003) Olfactory and/or visual cues for spatial navigation through ontogeny: olfactory cues enable the use of visual cues, *Behav Neurosci*, 117:412-25

Rossignol S, Dubuc R, Gossard JP (2006) Dynamic sensorimotor interactions in locomotion, *Physiol Rev*, 86:89-154

Rotenberg A, Muller RU (1997) Variable place-cell coupling to a continuously viewed stimulus: evidence that the hippocampus acts as a perceptual system, *Philos Trans R Soc Lond B Biol Sci*, 352:1505-13

Russell NA, Horii A, Smith PF, Darlington CL, Bilkey DK (2003) Long-term effects of permanent vestibular lesions on hippocampal spatial firing, *J Neurosci*, 23:6490-8

Russell NA, Horii A, Smith PF, Darlington CL, Bilkey DK (2006) Lesions of the vestibular system disrupt hippocampal theta rhythm in the rat, *J Neurophysiol*, 96:4-14

Sargolini F, Fyhn M, Hafting T, McNaughton BL, Witter MP, Moser MB, Moser EI (2006) Conjunctive representation of position, direction, and velocity in entorhinal cortex, *Science*, 312:758-62

Save E, Cressant A, Thinus-Blanc C, Poucet B (1998) Spatial firing of hippocampal place cells in blind rats, *J Neurosci*, 18:1818-26

Save E, Nerad L, Poucet B (2000) Contribution of multiple sensory information to place field stability in hippocampal place cells, *Hippocampus*, 10:64-76

Schmidt R, Diba K, Leibold C, Schmitz D, Buzsáki G, Kempter R (2009) Single-trial phase precession in the hippocampus, *J Neurosci*, 29:13232-41

Shapiro ML, Tanila H, Eichenbaum H (1997) Cues that hippocampal place cells encode: dynamic and hierarchical representation of local and distal stimuli, *Hippocampus*, 7:624-42

Sharp PE, Blair HT, Etkin D, Tzanetos DB (1995) Influences of vestibular and visual motion information on the spatial firing patterns of hippocampal place cells, *J Neurosci*, 15:173-89

Sharp PE, Turner-Williams S, Tuttle S (2006) Movement-related correlates of single cell activity in the interpeduncular nucleus and habenula of the rat during a pellet-chasing task, *Behav Brain Res*, 166:55-70

Shibata H, Kondo S, Naito J (2004) Organization of retrosplenial cortical projections to the anterior cingulate, motor, and prefrontal cortices in the rat, *Neurosci Res*, 49:1-11

Shiroyama T, Kayahara T, Yasui Y, Nomura J, Nakano K (1999) Projections of the vestibular nuclei to the thalamus in the rat: a Phaseolus vulgaris leucoagglutinin study, *J Comp Neurol*, 407:318-32

Siegel JJ, Neunuebel JP, Knierim JJ (2008) Dominance of the proximal coordinate frame in determining the locations of hippocampal place cell activity during navigation, *J Neurophysiol*, 99:60-76

Sirota A, Buzsáki G (2005) Interaction between neocortical and hippocampal networks via slow oscillations, *Thalamus Relat Syst*, 3:245-59

Skaggs WE, McNaughton BL (1998) Spatial firing properties of hippocampal CA1 populations in an environment containing two visually identical regions, *J Neurosci*, 18:8455-66

Skaggs WE, McNaughton BL, Gothard KM, Markus EJ (1993) in Advances in Neural Information Processing Systems (eds Hanson SJ, Cowan JD, Giles CL), 1030−7 (*Morgan-Kaufman*, San Mateo, 1993)

Skaggs WE, McNaughton BL, Wilson MA, Barnes CA (1996) Theta phase precession in hippocampal neuronal populations and the compression of temporal sequences, *Hippocampus*, 6:149-72

Smith PF (1997) Vestibular-hippocampal interactions, *Hippocampus*, 7:465-71

Smith PF, Darlington CL, Zheng Y (2010) Move it or lose it--is stimulation of the vestibular system necessary for normal spatial memory?, *Hippocampus*, 20:36-43

Sommer MA, Wurtz RH (2008) Brain circuits for the internal monitoring of movements, *Annu Rev Neurosci*, 31:317-38

Song EY, Kim YB, Kim YH, Jung MW (2005) Role of active movement in place-specific firing of hippocampal neurons, *Hippocampus*, 15:8-17

Stackman RW, Clark AS, Taube JS (2002) Hippocampal spatial representations require vestibular input, *Hippocampus*, 12:291-303

Stackman RW, Golob EJ, Bassett JP, Taube JS (2003) Passive transport disrupts directional path integration by rat head direction cells, *J Neurophysiol*, 90:2862-74

Tanila H (1999) Hippocampal place cells can develop distinct representations of two visually identical environments, *Hippocampus*, 9:235-46

Tanila H, Shapiro ML, Eichenbaum H (1997) Discordance of spatial representation in ensembles of hippocampal place cells, *Hippocampus*, 7: 613-23

Taube JS (2007) The head direction signal: origins and sensory-motor integration, *Annu Rev Neurosci*, 30:181-207

Taube JS, Muller RU, Ranck JB Jr (1990) Head-direction cells recorded from the postsubiculum in freely moving rats. I. Description and quantitative analysis, *J Neurosci*; 10:420-35

Terrazas A, Krause M, Lipa P, Gothard KM, Barnes CA, McNaughton BL (2005) Self-motion and the hippocampal spatial metric, *J Neurosci*, 25:8085–96

Teruel-Martí V, Cervera-Ferri A, Nuñez A, Valverde-Navarro AA, Olucha-Bordonau FE, Ruiz-Torner A (2008) Anatomical evidence for a ponto-septal pathway via the nucleus incertus in the rat, *Brain Res*, 1218:87-96

Thompson LT, Best PJ (1989) Place cells and silent cells in the hippocampus of freely-behaving rats, *J Neurosci*, 9:2382-90

Thompson LT, Best PJ (1990) Long-term stability of the place-field activity of single units recorded from the dorsal hippocampus of freely behaving rats, *Brain Res*, 509:299-308

Van der Werf YD, Witter MP, Groenewegen HJ (2002) The intralaminar and midline nuclei of the thalamus: Anatomical and functional evidence for participation in processes of arousal and awareness, *Brain Res Brain Res Rev*, 39:107-40

van Strien NM, Cappaert NL, Witter MP (2009) The anatomy of memory: an interactive overview of the parahippocampal-hippocampal network, *Nat Rev Neurosci*, 10: 272-82

Vann SD, Aggleton JP, Maguire EA (2009) What does the retrosplenial cortex do?, *Nat Rev Neurosci*, 10:792-802

Vertes RP, Hoover WB, Do Valle AC, Sherman A, Rodriguez JJ (2006) Efferent projections of reuniens and rhomboid nuclei of the thalamus in the rat, *J Comp Neurol*, 499:768-96

Vertes RP, Hoover WB, Szigeti-Buck K, Leranth C (2007) Nucleus reuniens of the midline thalamus: link between the medial prefrontal cortex and the hippocampus, *Brain Res Bull*, 71:601-9

Vertes RP, Kocsis B (1997) Brainstem-diencephalo-septohippocampal systems controlling the theta rhythm of the hippocampus, *Neuroscience*, 81:893-926

Vidal PP and Sans A (2004) in The Rat Nervous System 3rd edn (ed Paxinos, G), 965-96 (*Elsevier Academic Press*, San Diego, 2004)

Wallace DG, Gorny B, Whishaw IQ (2002) Rats can track odors, other rats, and themselves: implications for the study of spatial behavior, *Behav Brain Res,* 1131:185-92

Wallace DG, Hines DJ, Whishaw IQ (2002) Quantification of a single exploratory trip reveals hippocampal formation mediated dead reckoning, *J Neurosci Methods*, 113:131-45

Wallace DG, Martin MM, Winter SS (2008) Fractionating dead reckoning: role of the compass, odometer, logbook, and home base establishment in spatial orientation, Naturwissenschaften, 95:1011-26

Whishaw IQ, Vanderwolf CH *(1973)* Hippocampal LFP and behavior: Changes in amplitude and frequency of RSA (theta rhythm) associated with spontaneous and learned movement patterns in rats and cats, *Behav Biol*, 8:461-84

Whitlock JR, Sutherland RJ, Witter MP, Moser MB, Moser EI (2008) Navigating from hippocampus to parietal cortex, *Proc Natl Acad Sci USA*, 105:14755-62

Wiener SI (1996) Spatial, behavioral and sensory correlates of hippocampal CA1 complex spike cell activity: implications for information processing functions, *Prog Neurobiol*, 49:335-61

Wiener SI, Berthoz A, Zugaro MB (2002) Multisensory processing in the elaboration of place and head direction responses by limbic system neurons, *Brain Res Cogn Brain Res*, 14:75-90

Wiener SI, Korshunov VA, Garcia R, Berthoz A (1995) Inertial, substratal and landmark cue control of hippocampal CA1 place cell activity, *Eur J Neurosci*, 7:2206-19

Wiener SI, Paul CA, Eichenbaum H (1989) Spatial and behavioral correlates of hippocampal neuronal activity, *J Neurosci*, 9:2737-63

Wills TJ, Lever C, Cacucci F, Burgess N, O'Keefe J (2005) Attractor dynamics in the hippocampal representation of the local environment, *Science*, 308:873-6

Wilson MA, McNaughton BL (1993) Dynamics of the hippocampal ensemble code for space, *Science*, 261:1055-8

Wilson MA, McNaughton BL (1994) Reactivation of hippocampal ensemble memories during sleep, *Science*, 265:676-9

Witter MP (2006) Connections of the subiculum in the rat: Topography in relation to columnar and laminar organization, *Behav Brain Res*, 174:251-64

Witter MP, Amaral DG (2004) in The Rat Nervous System 3rd edn (ed Paxinos, G), 635–704 (*Elsevier Academic Press*, San Diego, 2004)

Witter MP, Naber PA, van Haeften T, Machielsen WC, Rombouts SA, Barkhof F, Scheltens P, Lopes da Silva FH (2000) Cortico-hippocampal communication by way of parallel parahippocampal-subicular pathways, *Hippocampus*, 10:398-410

Wittlinger M, Wehner R, Wolf H (2006) The ant odometer: stepping on stilts and stumps, *Science*, 312:1965-7

Wood ER, Dudchenko PA, Robitsek RJ, Eichenbaum H (2000) Hippocampal neurons encode information about different types of memory episodes occurring in the same location, *Neuron*, 27: 623-33

Yamaguchi Y, Aota Y, McNaughton BL, Lipa P (2002) Bimodality of theta phase precession in hippocampal place cells in freely running rats, *J Neurophys*, 87:2629-42

Zheng Y, Horii A, Appleton I, Darlington CL, Smith PF (2001) Damage to the vestibular inner ear causes long-term changes in neuronal nitric oxide synthase expression in the rat hippocampus, *Neuroscience*, 105:1-5

Zinyuk L, Kubik S, Kaminsky Y, Fenton AA, Bures J (2000) Understanding hippocampal activity by using purposeful behavior: place navigation induces place cell discharge in both task-relevant and task-irrelevant spatial reference frames, *Proc Natl Acad Sci USA*, 97:3771-6

Zugaro MB, Berthoz A, Wiener SI (2002) Peak firing rates of rat anterodorsal thalamic head direction cells are higher during faster passive rotations, *Hippocampus*, 12:481-6

Zugaro MB, Monconduit L, Buzsáki G (2005) Spike phase precession persists after transient intrahippocampal perturbation, *Nat Neurosci*, 8:67-71

Zugaro MB, Tabuchi E, Fouquier C, Berthoz A, Wiener SI (2001) Active locomotion increases peak firing rates of anterodorsal thalamic head direction cells, *J Neurophysiol*, 86:692-702

Zugaro MB, Tabuchi E, Wiener SI (2000) Influence of conflicting visual, inertial and substratal cues on head direction cell activity, *Exp Brain Res*, 133:198-208